**OsloMet – Oslo Metropolitan University**

**Department of Civil Engineering & Energy Technology**
**Section of Civil Engineering**

## Master Program in Structural Engineering & Building Technology

# MASTER THESIS

| TITLE OF REPORT | DATE 25.05.2022 |
|---|---|
| Numerical analysis of the Vattedal bridge strengthened with UHPC overlays | PAGES / ATTACHMENTS 99 / 5 |
| AUTHOR(S) Mats Lanner and Bjørnar Degnes | SUPERVISOR(S) Katalin Vertes Mahdi Kioumarsi |

| IN COLLABORATION WITH | CONTACT PERSON |
|---|---|
| Norwegian Public Roads Administration and Vestland County Municipality | Jorunn Hillestad Sekse |

SUMMARY / SYNOPSIS

This master thesis addresses how ultra-high performance concrete strengthening can affect the structural response of a single-span concrete bridge in Vattedal, Tysnes.

Several FE-models with different UHPC configurations are analyzed in Abaqus and compared to the reference bridge. Model updating was carried out by performing operational modal analysis on the obtained data from frequency measurements.

The presented results compare the different UHPC configurations in terms of force-displacement curves and crack development.

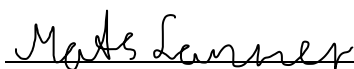| KEYWORDS |
|---|
| ULTRA-HIGH PERFORMANCE CONCRETE |
| NUMERICAL ANALYSIS |
| STRENGTHENING |

# Foreword

This master thesis is written at Oslo Metropolitan University in the spring of 2022 as a part the master program Structural Engineering and Building Technology at the Department of Civil Engineering and Energy Technology. The thesis has a scope of 30 credits and is conducted in the fourth and last semester.

The main goal of the thesis is to compare different strengthening configurations with ultra-high performance concrete on the Vattedal Bridge. It addresses how to apply the material in different ways and how to simulate the structural response of concrete using finite element software. In addition, modal updating is carried out to validate the FE-model.

The presented work results from good cooperation and mutual engagement on the topic, where most of the communication has taken place via zoom. The supervisors offered good problem statements throughout the process, allowing us to continuously challenge ourselves. We also appreciated being able to travel to Tysnes to carry out the bridge inspection, which put a whole new dimension to the study. Therefore, the master's thesis has been a very educational end to the study for both of us.

OsloMet, Oslo 25.05.2022

Mats Lanner                                          Bjørnar Degnes

# Abstract

The background for the work presented in this thesis is based on a proposal from the Norwegian Public Roads Administration to look at the possibility of strengthening the Vattedal bridge at Tysnes. The bridge is classified as BkT8, but due to high traffic loads it has been decided to classify it as BK10/60, and therefore it has a demand for strengthening. The main purpose was therefore to compare different strengthening configurations with ultra-high performance concrete on this bridge.

The following objectives set the foundation for the study:

- To study how concrete bridges can be strengthened with ultra-high performance concrete.
- To investigate how different UHPC configurations affect the structural response of the Vattedal bridge.
- To validate the FEM models through operational modal analysis and model updating.

To compare the effect of different UHPC configurations on flexural capacity, a 3D finite element model was developed and updated by local frequency measurements for each of the different cases. The bridge models were validated thorough operational modal analysis to get a more realistic approach to how the bridge behaved. A bridge inspection was therefore carried out in collaboration with Vestland County Municipality, where accelerograph sensors from OMAway were installed to extract modal behavior.

The results from the measurements were later extracted in Unquake OMAway and the FE-model was updated based on the measured natural frequencies, which provided a more realistic model. The different strengthening configurations were analyzed in Abaqus and compared with the original bridge when the model was updated. Three cases of UHPC configurations were compared. UHPC was applied on top of the bridge deck and in the tension zone. The last case was implemented with a larger UHPC thickness to check if this had any effect. The results present force-displacement curves and crack development for the different cases.

# Table of content

# List of Figures

# List of Tables

# Abbreviations

| | | |
|---|---|---|
| UHPC | – | Ultra-high performance concrete |
| UHPFRC | – | Ultra-high performance fiber reinforced concrete |
| CDP | – | Concrete damage plasticity |
| RPC | – | Reactive powder concrete |
| SVV | – | Statens Vegvesen / Norwegian Public Roads Administration |
| FDD | – | Frequency domain decomposition |
| FFT | – | Fast fourier transform |
| FHWA | – | Federal highway administration (USA) |
| FRP | – | Fiber reinforced polymer |
| CFRP | – | Carbon fiber reinforced polymer |
| RC | – | Reinforced concrete |
| FEM | – | Finite element method |
| FE | – | Finite element |
| OMA | – | Operational modal analysis |
| BkT8 | – | Bridge classification with maximum truck load of 40 tons |
| Bk10/60 | – | Special classification from Bk10 (50 tons) with maximum truck load of 60 tons |

# 1 Introduction

In recent years, there has been an increased focus on optimizing various structures regarding design, environmental emissions, and costs. It is a well-known challenge that combining all factors without one thing exceeding the other is demanding, especially with today's high requirements and standards. More research into making the most out of the resources that have already been utilized will therefore contribute to establish a new and more sustainable course for the industry we know today as a major contributor to increased greenhouse gas emissions. To realize this, it is necessary to acquire a thorough understanding of restoration and strengthening of existing buildings and other structures.

As a result of many years of exposure to the Nordic environment many historic structures, and specially bridges, along Norway's coast established in the postwar period now require extensive care and repair. During the twentieth century, the country's infrastructure underwent a major upgrade, and there was a need for rapid and effective solutions in many regions. Structures were not often planned to survive for 100 or even 50 years at the time, as they are now. As a result of new technology, today's solutions are also far more reliable and predictable than older structures. Quality was not a major priority at the time, but when these structures meet today's strict requirements and standards, new issues emerge that must be addressed, especially when it comes to bridge constructions. The consequences of many years of exposure to traffic loads and other environmental stresses can have undesirable outcomes. Therefore, it is important that existing bridges are examined and maintained on a regular basis, which again can lead to high costs.

In recent decades, several innovative technologies for restoring old concrete structures have been developed. Research and application have lately gained traction in the strengthening of existing concrete bridges and other concrete structures. Methods such as polymer and steel wrapping, are widely used to strengthen concrete columns and covers, but the use of concrete wrapping has also received increased attention. This approach presents issues in terms of strength and protection, as well as other downsides. As a result, having a stronger type of concrete that is more resistant to environmental stressors and that can deliver more predictable strength properties will be of high advantage. As a result, ultra-high performance concrete (UHPC) was created to perfectly match these requirements. UHPC is a more durable

form of concrete that may be employed in whole structures as well as in a variety of strengthening applications. Because of its excellent qualities, the material shows promising outcomes for structural rehabilitation and strengthening of damaged structures. It may be used on columns, decks, beams, bridge components, and a variety of other structural elements.

The purpose of this thesis is directed to existing concrete bridges that need to be strengthened. In this regard, a bridge case was assigned in collaboration with the Norwegian Public Roads Administration and Vestland County Municipality, which possessed the necessary prerequisites to fulfill the study. The Vattedal Bridge is a concrete bridge in the municipality of Vestland. There have previously been challenges associated with corrosion and peeling, and the bridge has been repaired by applying new layers of concrete over the damaged areas. Therefore, it is desirable to find a long-term strengthening solution in the future. The potential of employing carbon fiber sheets has been examined in the past, but without success. Figure 1 illustrates the condition of the bridge at the time the inspection was carried out.



*Figure 1 - The Vattedal bridge in Vestland County Municipality*

To investigate UHPC as strengthening method of the Vattedal bridge, a finite element analysis was carried out where different methods for applying the UHPC were investigated, modelled, and compared. In the procedure, the finite element method software Abaqus was used for modeling and analysis. The attention of the analysis was focused on the stress distribution,

displacement, and crack formation for a static load case. Due to the complexity of the concrete and the unpredictable behavior of it, an essential aspect of the study is also to investigate the possibilities for modelling composites with brittle behavior. It`s discovered that there is presently limited selections of conventional material models and parameters for non-linear finite element analyses of concrete.

Model updating was performed on the bridge to analyze the model as realistic as possible. This comprises updating the parameters in the model to approach reality in the best possible way. Sensors from Unquake were installed on the bridge to monitor the frequencies. The results from this assessment were then used to do operational modal analysis, OMA.

## 1.1 Aim and scope

The following objectives set the foundation for the study:

- To study how concrete bridges can be strengthened with ultra-high performance concrete.
- To investigate how different UHPC configurations affect the structural response of the Vattedal bridge.
- To validate the FEM models through operational modal analysis and model updating.

The scope of the thesis includes determining and comparing different strengthening configurations with UHPC for the Vattedal Bridge. The goal is to be able to distinguish between different strengthening approaches in terms of flexural behavior and crack development. Also, an important part is to validate the model through model updating. This part is not only for the purpose of getting a more realistic model, but it was also a goal to obtain a more thorough understanding of this type of procedure for use on other types of structures in the future.

## 1.2 Limitations

Some limitations must be considered, and some problems occurred in the procedure. First, the results in this thesis are only based on FE-modelling and not on experimental testing. This decrease the validity of the results since they are only based on model predictions with model updating.

The study does not draw any further conclusion about whether the bridge can be classified as Bk10/60 due to time limitations and the desired focus area of the study. The results strictly focus on predicting how much the bridge can be strengthened with UHPC, and how significant increase in capacity the different strengthening cases can provide compared to the original bridge.

Problems occurred during the modal measurements. Some of the sensors did not have the right sampling rates, meaning that they could not be used in further analysis. Also, some of the sensors had non-working SD-card which could not be predicted before the results were transferred to a computer. Out of 6 sensors, only two worked properly and could be used for further analysis. This is not an optimal amount of sensor for measuring natural frequencies, but there was still possible to extract some modal parameters and to move the model parameters in Abaqus towards the experimental ones, to a certain extent.

Initially, it was not planned to perform modal analysis. But after discussion with the supervisors, this became the preferred way to validate the FE- model. It turned out that the process of getting familiar with the equipment and understanding how it worked was greater than first assumed. In addition, the equipment didn't work as desired, and therefore it took longer than expected to extract decent results. This shifted the planned progress and gave shorter time for the remaining Abaqus analyses.

## 1.3   Thesis structure

To get an overview of how the study is structured and what is included in each chapter, a brief summary of the content is described in this chapter.

**Chapter 2** – The literature review is presented after the introduction chapter. Here, the framework and overview of existing research on the topic is described. General trends, keywords, countries represented, and a short overview of in-depth reviewed studies are included.

**Chapter 3** – Ultra-high performance concrete addresses general information, composition, mechanical properties, and application of UHPC, among other things. The applications of UHPC in bridge engineering are especially explained. To get a broader and realistic

understanding of what UHPC can be used for, examples are included where the material is implemented in larger constructions.

**Chapter 4** – Strengthening is about general strengthening methods and a brief explanation of how these work. Further, the strengthening of UHPC is described, and last, the use of UHPC for strengthening bridges is considered.

**Chapter 5** – Method describes the research question, the strategy, and the Vattedal bridge case in-depth.

**Chapter 6** – FEM analysis includes a description of FEM analysis on concrete structures, an explanation of different material models, including the CDP model used in this study, and the development of Abaqus models. This chapter finishes with the workflow in Abaqus and the modal updating of the model.

**Chapter 7** – Results and discussion present and compares the findings for different strengthening approaches. This includes force-displacement curves, deformations, and crack development.

**Chapter 8** – Conclusion and future work concludes the study and explains the possibilities of future work.

**Attachment A** – 12-1185 Vattedal – Initial drawings

**Attachment B** – Concrete damage plasticity parameters for normal concrete

**Attachment C** – Concrete damage plasticity parameters for UHPC

**Attachment D** – Rebar drawings from SVV

# 2 Literature review

The primary purpose of the literature review was to provide a framework and a good overview of the existing research on the topic as well as to map the research activity over the last decade. The topic was chosen based on an interest in learning more about ultra-high performance concrete, especially when it comes to it`s potential for strengthening and rehabilitation. In order to narrow the selection of studies down to a smaller sample, a review using the search engine Scopus was conducted. It should be noted that the literature review also included studies that were not found in Scopus. Other search engines like Research Gate and Google scholar were also used to identify relevant studies. In this section, the study sample from Scopus is presented.

The mapping of recent research activity gave a good base for further in-depth reviews and provided a general understanding of the subject. The approach was also helpful in narrowing down the topic. This review can also help introduce a new topic with limited background knowledge and offer a good overview for future researchers when selecting a study approach. The following chapter is shortly presenting the general trends observed from the existing research on UHPC and which research was most valuable for the purpose of this thesis.

## 2.1 General trends observed

Figure 2 shows the years in which the gathered research was published. The chart shows that the number of research published has been steadily increasing since 2016 till now. Because of the advancement of new technologies, particularly in the area of optimizing construction materials and components, this is an expected outcome. UHPC is increasingly used in these cases, especially in bridge engineering. The majority of the research was published in 2021, with 2020 and 2019 following closely after.
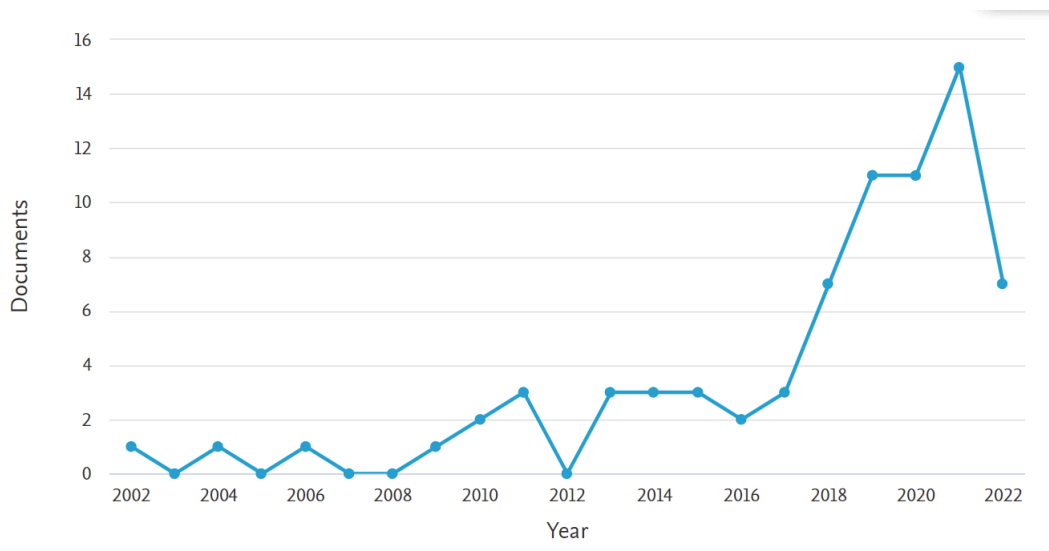
*Figure 2 - Publications by year after 2002*

A summary of the research locations is another interesting observation. This is primarily related to the 1st author's geographic location. Figure 3 gives the publications by country from the year 2002 to the present. With 18 and 29 publications, respectively, the United States and China are the leading countries regarding the number of published research. As a result, these countries are responsible for 63.5 % of the collected research.
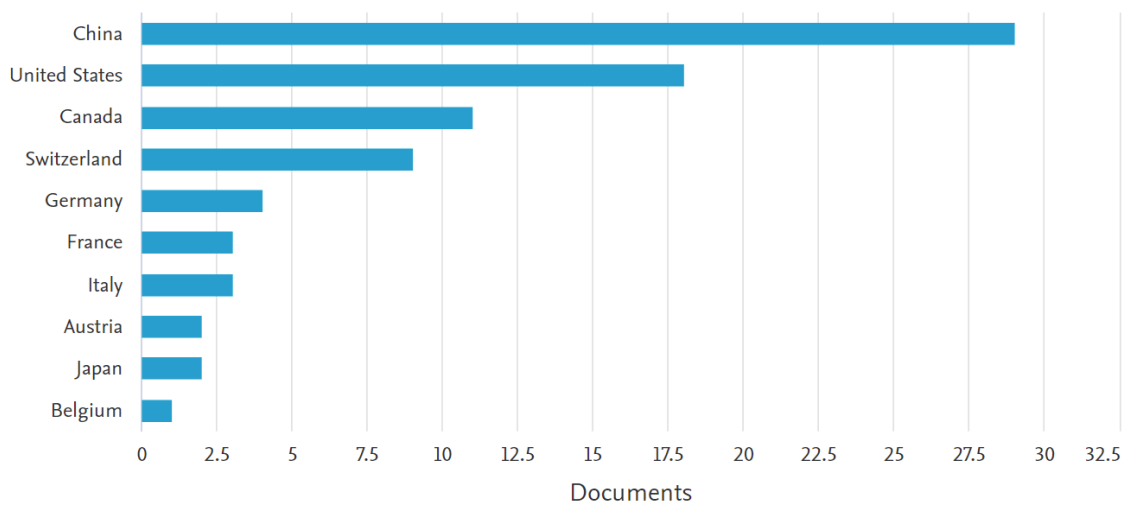


*Figure 3 - Publications country after 2002*

The most often used keywords in the sample are shown in Figure 4. The color scheme describes in which year the different keyword is most common. It also explains the relationship between the different terms, allowing viewers to get a sense of where UHPC is most typically applied. The keywords attached to the largest circles in the figure are also the most common in the sample of studies. It can be seen from the figure that most publications

with UHPC have been in the recent years. Bridge, bridge deck, strengthening, ultra-high performance concrete and maintenance are the most used keywords. Ultra-high performance concrete is represented with three different words and are therefore the most used keyword if these are merged together. In addition, the shortenings uhpfrc and uhpc are also represented.
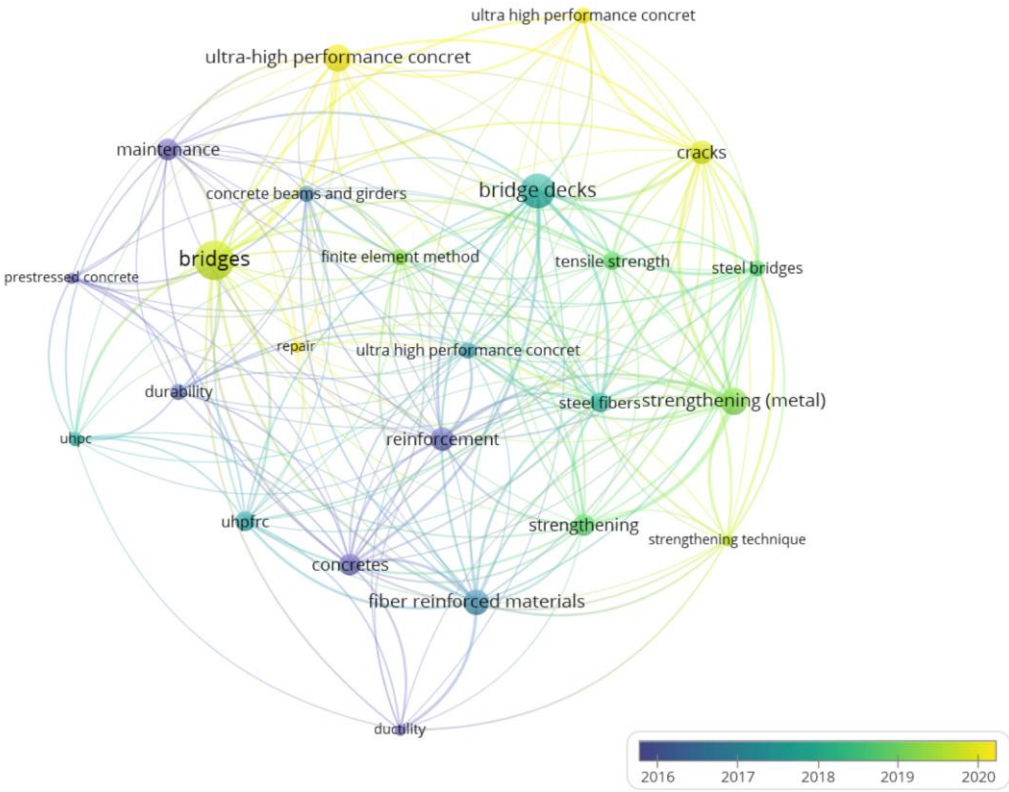


*Figure 4 - Keyword word cloud*

### 2.1.1 In-depth reviewed studies

Some research on using UHPC to strengthen existing structures has been presented in the literature. The research was found to be helpful for getting a better understanding of the subject. Important studies from the sample have been briefly described in this section. Some of the presented studies were reviewed in previous semesters.

Brühwiler et al. [1] investigated the effect of using ultra-high performance fiber reinforced concrete (UHPFRC) as rehabilitation on a short-span bridge in Switzerland. This was the very first application where the material was used to strengthen an existing bridge in the country. The study was found helpful as the bridge in Switzerland provides similar geometry as the Vattedal bridge.

Zhu et al. [2] looked at the effectiveness of different strengthening configurations with UHPC on a reinforced concrete beam. In the study, they developed analytical and numerical models in order to simulate structural response and evaluate cracks and the ultimate capacity of the strengthened beams. The study concludes that UHPC can be used to increase flexural capacity of reinforced concrete beams.

Koo et al. [3] investigated the strengthening effect of concrete column jacketing with UHPC. Their study evaluated different strengthening configurations with UHPC, and the overlay thicknesses were compared through experimental testing. The findings showed that the UHPFRC jacketing method significantly impacted the test columns.

Shafieifar et al. [4] did a study were both UHPC and normal-strength concrete were subjected to several compression and tensile tests. To predict the behavior of the UHPC compared to the conventional concrete, a validated finite element model utilizing the concrete damage plasticity model (CDP) was also looked into. Therefore, this research was especially interesting to learn more about the method and to see the strength differences between UHPC and conventional concrete. The CDP model is later utilized in this study.

Esfahani et al. [5] simplified the concrete damage plasticity model and specified the values in tabular form in order to simulate concrete behavior. Their findings included softening/hardening rules, damage parameters, and other parameters for the concrete damage plasticity model. They presented their findings for concrete grades B20, B30, B40 and B40 in different tables. Their results were utilized in this study to model the behavior of concrete.

Hashim et al. [6] developed a damage plasticity model for ultra-high performance fiber reinforced concrete (UHPFRC) for different concrete mix designs. The mixes were compared based on the outcomes from uniaxial compression and tensile tests. The research obtained different model parameters for UHPC and were utilized in this study to model the behavior of the material.

# 3   Ultra-high performance concrete

In the 19th century, modern concrete was introduced. During the 20th century, it was substantially developed as a key component for most construction and building activities. It has therefore become one of the most widely used building materials worldwide. Fiber reinforced concrete (FRC) and High-performance concrete (HPC) were introduced in the 1970s and 1980s. This type of concrete typically had a 50 to 120 MPa compressive strength, with improved durability properties. This got a lot of attention, and since then, researchers have continued to investigate how to utilize and improve the fiber-reinforced concrete and develop the concrete even more. By the turn of this century, an incredible technological breakthrough was achieved by utilizing ultra-high performance concrete technology, recognized by UHPC. This new technology allowed for remarkable levels of quality that were previously unimaginable. The expression UHPC, or ultra-high-performance concrete was first used in the early 90s. Then it specified a concrete material with compressive strength of more than 120 MPa and with increased durability. In the years after 2000, the term UHPC is also referred to as ultra-high performance fiber-reinforced concrete (UHPFRC) as well. This is because most of the UHPC mixes includes fibers [7-9].

Ultra-high performance concrete is a kind of concrete that has higher compression- and tensile strength, as well as reduced permeability, and increased ductility and durability. Fibers are commonly used in UHPC to increase the mix's tensile strength [8, 10]. The utilization of fine aggregates is another characteristic of UHPC. As a result, the resultant concrete is substantially denser than regular concrete, which has a significant impact on the strength qualities. This makes UHPC suitable for a large variety of applications.

Regular concrete has a typical compressive strength of 20 – 40 Mpa. UHPC on the other hand, has significantly higher compressive strength. There are different definitions of how strong the concrete must be, to be defined as UHPC. Usually, it must have a minimum specified compressive strength of 120 MPa, but some guidelines suggests that the minimum should be 150 MPa. The typical range of UHPC is therefore from 120 – 200 MPa [8, 11]. The fibers contribute to an increase of the tensile strength, flexural stiffness, and makes it more ductile. The most common fiber types in UHPC are steel, plastic, glass, or a combination [8, 12].

Scientists and constructors that have worked with UHPC have concluded that there are lots of benefits of using UHPC instead of normal concrete, and some of the benefits are distinguishable [8, 12]. It can give the structure an improved speed of construction and a simplified construction technique. Some of the reasons are that a smaller amount of concrete is required, because of the ability to make the structures slimmer and thinner. It also improves the durability, reduces out of service, maintenance, and complexity, as well as extended service life. The structures require less upkeep and have a much longer service life [12]. In fact, some developers claim that UHPC can have a life expectancy of over 300 years, which is four times more than most structures currently built [13].

These benefits are mainly the reasons why UHPC is a preferred material among architects and contractors. It allows the architects to design slim, complex, and special structures. Contractors can be able to build these structures with the use of concrete, which is not possible with normal concrete. They can also save time, money, and speed of construction. Also, the structure can have a longer expected service life.

The most common use of concrete is cast-in-place concrete. UHPC on the other hand is frequently used as precast elements, and this is also the preferred construction technique. The reason for this is that it is very sensitive to the concreting and mixing process, the fiber execution, as well as the mix composition and climatic boundary conditions. UHPC is therefore more dependent on the practical execution than normal concrete. In addition, UHPC is far more brittle than regular concrete. However, it can be made more ductile by adding the proper fibers [14]. To achieve the best possible result, the utilization of the fibers has to be done correctly. It is critical that the fibers are distributed and oriented properly. Avoid lumps and accumulations since they can generate weak spots in the concrete. As a result, the order in which the fibers are added to the mix is critical for the overall performance of UHPC structures.

## 3.1  Composition

UHPC can also be considered as more sustainable than normal concrete. The use of cement is higher in UHPC, and the use of fine aggregates can therefore be reduced, while coarse aggregates is not used at all. The amount of concrete required in a structure can be reduced

drastically, and therefore it will require less cement and aggregates in total. As mentioned, the use of fibers will increase the tensile strength, which will make the structure's tensile capacity higher, and the need for rebars will decrease. In that way, it is also possible to save reinforcing steel [15]. The recyclability is also better than normal concrete. It can be recycled several times, and at last, it can be used as filling in construction sites and as road base. This is possible because some of the cement is not being hydrated during the hardening. The rest is therefore available for reuse [15].

High-quality cement is one of the essential ingredients for creating UHPC. Compared to normal concrete, UHPC is known to have a substantially lower water-binder ratio. This value is usually less than 0,2 by weight of cement, which can be considered low compared to other concrete mixtures. With this amount of water, the resulting concrete is considerably denser, resulting in higher compressive strength and permeability. The mixture is also supplemented with other cementitious materials and finer aggregates. Superplasticizer and steel fibers are the last ingredients added to the mix. The idea is to remove coarse aggregates and replace them with finer ones, to promote homogeneity. Compared to typical composites, this will result in a more uniform stress distribution when an element is loaded. Combining all of the abovementioned elements will eventually result in the desired packing density of the mix [8, 16]. Figure 5 illustrates an example of the distribution of the different materials in the UHPC mixture compared to conventional concrete.
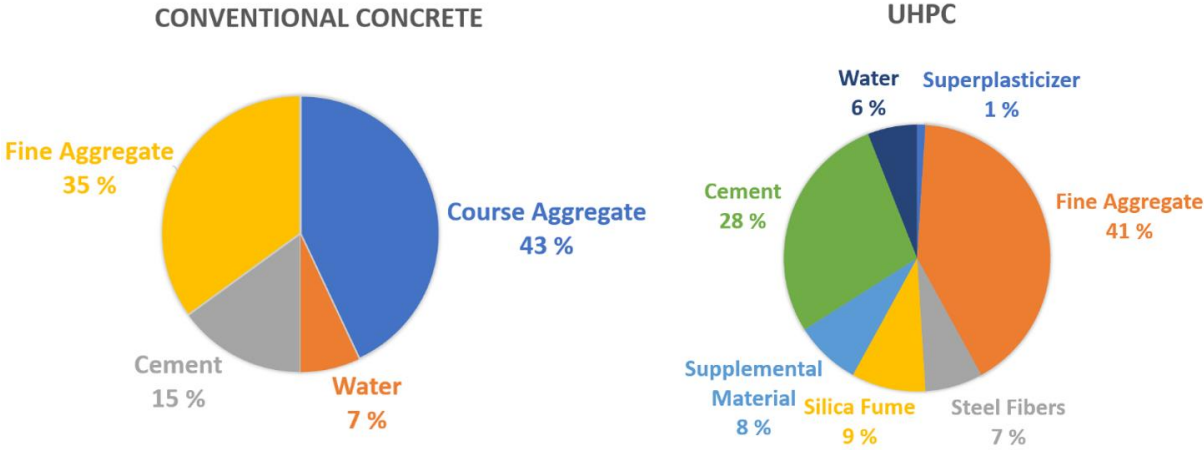


*Figure 5 - Typical distribution of materials in the UHPC mix compared to conventional concrete [17]*

Furthermore, the steel fibers added to the mixture have different tensile stress than the concrete, which effectively reduces the formation of concrete cracks. To reduce the amount of water and enhance the strength of the concrete, a restricted amount of effective superplasticizer is applied and the dose must be carefully managed to avoid the rate of concrete setting slowing down too much [18]. Supplementary cementitious materials are alternatives to ordinary Portland cement and can bind the aggregates the same way. These materials are by-products of other industries, and they are often treated as garbage and ends up in landfills [19].

### 3.1.1 Microstructure and fibers

The very low water/binder ratio is essential for UHPC's dense microstructure and great strength. As a result, the matrix contains almost no capillaries and is diffusion resistant. Another property that contributes to the high strength of UHPC is that it is made up of numerous mixed components in such a manner that the particles are packed very densely together [20].

The brittle behavior of concrete is widely known to augment when the strength increases. This is also noticeable with UHPC. The disadvantage this causes, may be efficiently offset by adding fibers, which result in a significant increase in post-peak compression and tension behavior. This can results in a more favorable reaction in general and better warnings when failure is about to occur [20]. Adding steel fibers to the concrete mix will increase the fracture toughness, tensile- and compressive strength, ductility, and energy absorption capacity of the UHPC matrix, although their effectiveness varies depending on the kind of fiber used [9].

Steel fibers are particularly well incorporated into the fine-grained UHPC matrix's microstructure, which is dense, solid, and uniform. As a result, it is possible for high stresses to be transferred in favorable conditions. The scenario occurs if sufficient well-oriented steel fibers are available in the concrete matrix. Steel fibers do not have a significant influence on the compressive strength. On the other hand, the tensile strength of a UHPC mix containing steel fibers is normally in the range of 15-20 MPa, which is nearly twice as high as the tensile strength of UHPC without steel fibers [21].

When it comes to ductility, the fibers will have a large impact. When the concrete starts rupturing, the friction between the fibers and the concrete matrix will overcome so that the

structure is able to perform better when exposed to dynamic loading. Short, thin fibers with a diameter of 0,20 mm and a length of 9–17 mm produced from high-strength steel with a tensile strength of 2000 N/mm$^2$ have shown to be the best alternative, also considering workability [20].

## 3.2  Mechanical properties

Research indicates that UHPC shows significant improvement when it comes to mechanical properties compared to normal strength concrete. These properties make the material suitable in a large variety of structures and structural components.

### 3.2.1  Behavior in compression

UHPC is usually characterized by having a compressive strength larger than 120 MPa, but 150 MPa is normally desirable [22]. Shafieifar et al. [4] concluded that the compressive strength of the conventional UHPC used in their study was three to four times higher than normal-strength concrete. The substantial mechanical friction force between steel fibers and the concrete matrix preserved the cylinders and cubes intact even after failure during the compression tests conducted in the study. The control sample of normal strength concrete on the other hand, fractured into big concrete fragments after failure. This result indicates that UHPC can promote high compressive strength while at the same time preserving acceptable flexibility.

The compressive strength of UHPC can be measured in a laboratory, the same way as for normal concrete. Usually, a cube or cylindrical specimen of UHPC is used for the test. This means that the compressive strength of a particular composition must be tested to determine its exact strength. Mathematically, the compressive strength cannot be calculated. Of course, some prescriptions can guarantee a specific strength because the composition has been quality-checked and frequently tested, so that the assumed strength has become somewhat standardized [8].

### 3.2.2  Behavior in tension

Despite the fact that non-reinforced concrete is not normally built to withstand direct tension, and tensile strength is largely ignored in construction design, tensile strength is used to predict the cracking during load impact. UHPC, on the other hand, has a much higher tensile strength

than normal-strength concrete, implying that it can maintain tensile strength even after the first cracks appears. As a result, determining the tensile strength of UHPC is critical in the design process [4].

It is hard to predict an accurate tensile strength for UHPC. This is because it highly depends on the fibers. The amount of steel fibers and the type of fibers used in the concrete matrix is important regarding the behavior in tension. Proper distribution and orientation are essential for optimal performance. Lumps and accumulations are therefore important factors that needs to be avoided. This is mainly the reason that the tensile strength is often assumed to be a conservative value. To get an estimated value of the tensile strength, the following formula developed by Graybeal et al. [23] can be used. This formula calculates the tensile strength from a ratio of the compressive strength.

$$f_t = 0,65 * \sqrt{f_c} \qquad\qquad\qquad \text{(Eq.1)}$$

The tensile strength of UHPFRC is typically 5% of the compressive strength, which relates to approximately 6-10 Mpa depending on the composition and the fibers utilized [24].

### 3.2.3  Modulus of elasticity

UHPC has a higher modulus of elasticity than regular concrete with the same aggregate type. The aggregate type and paste volume fraction have an impact on the magnitude of the effect [8, 25]. When it comes to modeling reinforced concrete structures in general, the modulus of elasticity is a significant design parameter. This characteristic directly relates to the shortening of concrete components due to compressive stress, creep, and shrinkage. Due to concrete shortening between columns, beams, and walls, internal stresses in reinforced concrete buildings are redistributed. To get the most accurate value for the modulus of elasticity, it can be found using laboratory tests, but normally it is estimated from the given compressive strength. The modulus of elasticity depends on different factors, such as the fibers, the concrete mix, and the amount of fine aggregates. UHPC premixes can give a modulus of elasticity as high as 50 to 60 GPa [8, 26]. Normally, the value is lower than this.

### 3.2.4  Poisson's ratio

The Poisson's ratio is defined as "the deformation in the material in a direction perpendicular to the direction of the force", according to Beyadi et al. [27]. It can be expressed by the negative of the lateral strain divided by the axial strain. It can therefore be found through tests

in a laboratory. Through uniaxial compression tests, it is possible to find both the lateral and the axial deformations [27]. The Federal Highway Administration in USA have made a list of 7 different Poisson's ratios for UHPC. These values are gathered from different researchers, and they are all close to 0,2. Therefore 0,2 is the most commonly used value for UHPC [24].

### 3.2.5  Stress-strain relation

Constitutive material models are used in engineering design to compute the relation between stresses and strains within a particular cross section. This relation can then be utilized to calculate the moment capacity of the section. Prior to attaining peak compressive stress, the stress-strain behavior of UHPC is essentially linear up to about 50% of this value, according to Haber et al. [28]. The compressive stress-strain response softens after the peak, resulting in a non-linear response.

## 3.3  Durability properties

One of the main objectives of utilizing UHPC is to improve the durability properties of the structure.  An ideal concrete mix should last a long period without significantly deteriorating in quality. Concrete constructions are frequently exposed to environmental impacts and might thus be subjected to harsh circumstances that cannot be avoided. Water penetration, chemical assaults, steel reinforcement corrosion, alkali-silica reactions, carbonation, and freeze-thaw attacks are examples of these situations. When concrete structures are subjected to a severe environment for a long period of time, the expenses of rehabilitation and maintenance may drastically increase. The permeability of the concrete matrix is the key to avoiding structural degradation owing to such durability challenges. If the concrete is less porous, it will last considerably longer. Because of the dense microstructure of UHPC, it shows higher resistance against chloride ingress than conventional concrete. This property makes it possible to use less concrete for the same durability, and thus, costs can be reduced. The new UHPC technologies will enable the development of concrete with outstanding durability, extending the service life of structures and allowing them to withstand harsh environments much more than they were previously able to [9].

The dense microstructure of UHPC also makes it more resistant against corrosion. According to Birkedal et al. [29], ultra-high performance concrete has a significantly increased resistance

against corrosion. They found out that UHPC beams have nearly ten times as good resistance as beams made of normal SV-40 concrete. The SV-40 is a standard concrete that corresponds to durability class MF40 and has a compressive strength of 45 MPa.

## 3.4  General application

Especially in Europe, North America, and Japan, the application of UHPC has gradually expanded over the recent years [8, 16]. The material is suitable for a wide range of infrastructures, including bridges and quay structures. The unique mechanical properties of the material allow it to be applied in structures with a high degree of complexity, such as connections and areas where redesign for optimization is a priority [8, 30]. In terms of chloride ion permeability resistance, carbon resistance, and wear-resisting performance, UHPC clearly outperforms conventional concrete. As a result, it has a wide range of possible applications in a variety of environments. The engineering applications of UHPC, on the other hand, are still in the early stages of development. Continued research is required to improve and stabilize the material characteristics [18]. When it comes to building components, UHPC has mostly been used for cladding and roof components for buildings with slender and aesthetic architecture. The possibilities of using UHPC in other construction areas such as prefabricating piles and substructures are also being investigated.

The Runway at Haneda Airport in Tokyo is a good example of how UHPC can be utilized in a large-scale project. The goal of this project was to reduce project expenses while also attempting to improve the structure's quality. The project is an excellent example of how to meet stringent durability requirements while also saving significant money by decreasing the structure's weight through the use of UHPC. Figure 6 illustrates the new airport that was forced to be built offshore due to a shortage of land area. The project ran from 2007 to 2010, and the platform had a total area of 200 000 $m^2$ with UHPC [31].
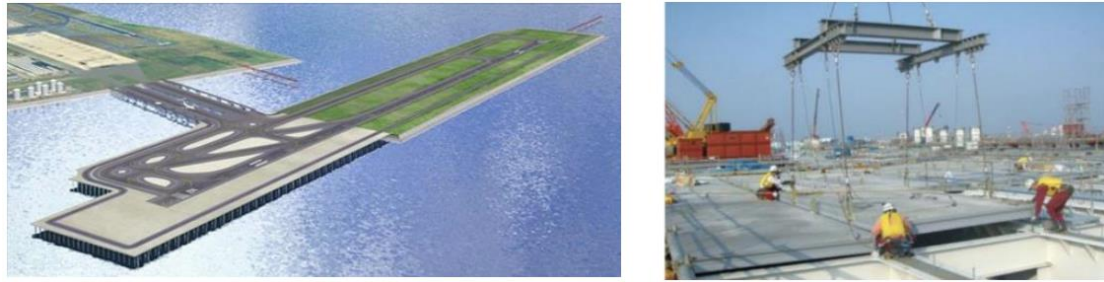
*Figure 6 - L: The new runway at Haneda airport, where the left side is built with UHPC elements supported by steel piles. R: Placing the prefabricated UHPC elements at site [31]*

The St. Elizabeths east gateway pavilion, illustrated in Figure 7, is another structure built with UHPC. This is a quite different structure and another way of using UHPC than at the Haneda Airport. Because of the good material properties, it is possible to make slim, complex structures like this pavilion in concrete. It has a unique form, long spans, and just a thin concrete layer as deck. The pavilion looks like it is floating above the ground because of the long spans. It is used for dining, events and markets, and it is one of the first steps in developing the St. Elizabeths east campus [32].



*Figure 7 - St. Elizabeths east gateway pavilion [32]*

## 3.5   Application of UHPC in bridge engineering

The exceptional mechanical properties of UHPC makes it ideal for considering traditional design methods for a wide range of bridges and bridge components. Research has shown that UHPC is very suitable for structures with complex geometry where traditional solutions are

not adequate. Numerous studies have investigated the possibility of applying UHPC on bridges. This have resulted in an increase of UHPC applications, and many new UHPC bridges being built all over the world [8, 16]. UHPC can be used in various components and structures in a bridge. Bridge girders, decks, beams, and prefabricated elements are some of the most common areas of use. To get an overview of how it can be used, USA will be taken as example.

USA is one of the countries where UHPC is most widespread. Since the US FHWA (Federal highway administration) started using UHPC in 2006, it has been utilized in multiple projects. In USA, the most common structures built or repaired with UHPC are bridges. FHWA decided to start mapping the application of UHPC to get an overview, and to see the development. Researchers at FHWA then made an interactive map that illustrates where UHPC is used in the years from 2006 to 2020. The website also shows how UHPC is applied. For instance, it is possible to filter by location, and whether it is prefabricated elements, bridge deck overlays or repair. 2021 or 2022 is not mapped yet, so in reality there are more bridges than presented [33]. The map is displayed at Figure 8.



*Figure 8 - Map showing bridges employing UHPC by year [33]*

The map above shows that there are most UHPC bridges at the east coast of the US, and least in the middle and south-west. The different colored dots represent the year the bridges were built or repaired. UHPC as construction material in concrete bridges are gradually increasing and is used more in the later years. This is well illustrated in Figure 9. The figure shows the number of bridges and in which year it was built or used. From 2014 to 2018 the use of UHPC augmented significantly. It went from 10 bridges a year, to almost 70 bridges a year. Since the use has increased to 7 times as many bridges over a period of 4 years, it is possible to imagine

that the use will only increase in the future as well. Especially if the rest of the country implements UHPC like the north-east coast.
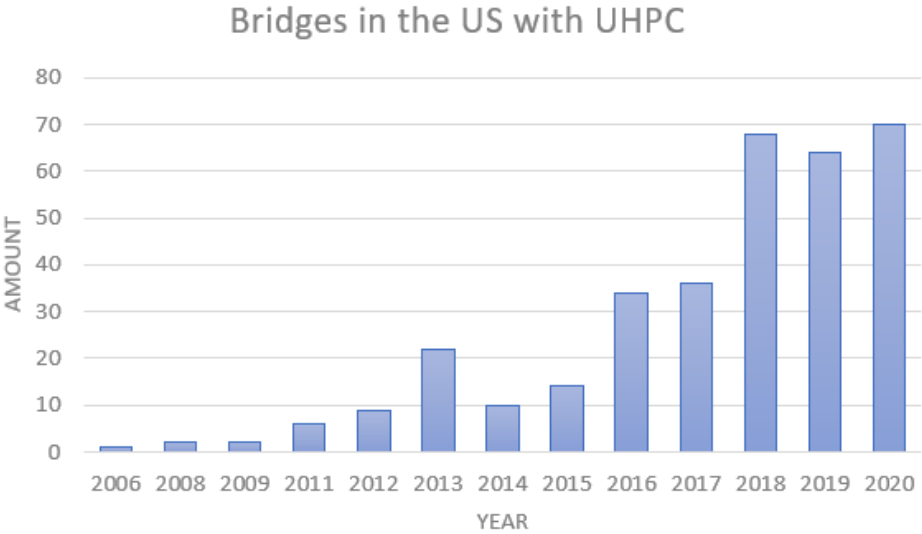


*Figure 9 - Bridges in the US where UHPC is used is used*

The use of UHPC in USA is assumed to reflect other parts of the world as well, such as Europe. The use of UHPC in Europe is therefore assumed to have the same increase in bridge application, but also for other structures such as buildings, dams etc.

Figure 10 illustrates the world's first UHPC pedestrian bridge. It was built in Sherbrooke, Quebec, Canada in 1997, signifying the initial application of UHPC in bridge engineering. Aside from the use of ultra-high strength material, the Sherbrooke Footbridge incorporates a number of other milestones, including concrete confinement, the absence of steel bar reinforcement, and pioneering approaches in precast/prestressed concrete design and finishing. The bridge is made out of a post-tensioned open-web space truss with no traditional steel reinforcement. It was made of reactive powder concrete (RPC), a cement-based substance proportioned with sand, cement, very fine silica fume and quartz powders. Fine steel fibers were also added, resulting in increased ductility. In the top and bottom chord members, the RPC had a compressive strength of 200 MPa. The UHPC deck had a thickness of 3 cm [34].

*Figure 10 - Canada Sherbrooke Overpass [34]*

In 2001, FHWA launched the UHPC research program. Since then, the group has undertaken several research projects and continues to promote UHPC applications in bridge engineering in the United States. The Mars Hill bridge in Iowa, shown in Figure 11 was the first UHPC bridge ever built in North America, and it was the result of five years of collaborative research. This bridge earned a PCA (Portland Cement Association) concrete bridge award in 2006 for its numerous unique characteristics. This includes a decreased amount of structural reinforcing steel, a basic appearance, and the use of longer and thinner beams. The bridge is a high-grade, single span, simply supported bridge with a width of 8 m and a span length of 33,5 m [18].



*Figure 11 - The American Mars Hill Bridge [18]*

# 4 Strengthening of structures

Structures that are subjected to a severe environment, aging, increased loading, fatigue, or corrosion may require extensive maintenance and repair over time. These factors have a significant effect on the frequency and size of cracks, which can lead to severe structural damage. As a result, structural strengthening has been an important topic in civil engineering in recent decades since many structures built in the 1970s, 1980s, and 1990s need to be restored to meet today's standards [8].

## 4.1 Existing strengthening methods

When strengthening existing structures, wrapping with polymer, steel, and concrete are three of the most frequent rehabilitation procedures currently in use. These approaches attempt to increase structural performance, stiffness, and ductility, but they are reliant on the addition of new structural parts, and the procedures contain a large number of technical specifications that may cause problems in the practical application. The disadvantages of adopting the mentioned approaches are their complexity of installation, high costs, and unpredictability in structural integrity [8, 35].

### 4.1.1 Steel jacketing

In some cases, columns in buildings or infrastructures need to be strengthened due to deterioration caused by corrosion, settlement damages, or construction errors. A commonly used method for increasing the axial strength of reinforced concrete columns is steel jacketing. However, corrosion resistance is a concern with this type of jacketing [36]. RC columns can also be covered in steel jackets to improve their fundamental strength capacity. Steel jacketing offers protection against environmental damage and inhibits shell concrete degradation, which is the primary cause of bond failure and buckling of longitudinal bars [37]. A disadvantage when it comes to steel jacketing is that the method is usually time-consuming and labor-intensive. However, steel jacketing is often less expensive compared to other methods in terms of material costs and has a simple and direct load transmission mechanism [38]. Figure 12 illustrates two different RC column models with various steel jacket configurations.
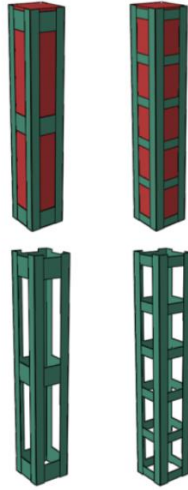
*Figure 12 - Different steel jacket configurations for concrete columns [39]*

### 4.1.2 Concrete jacketing

Strengthening existing concrete columns with additional reinforced concrete jacketing has the ability to increase column strength and stiffness in a more equally distributed manner. In contrast to conventional approaches that use steel or polymer wrapping, RC jacketing enhances the structure's durability and eliminates the need for additional fire protection. Also, no special equipment is required for this rehabilitation procedure. Because of these considerations, RC jacketing is a great option for structural repair and rehabilitation [40].

However, the traditional technique of using reinforced concrete jacketing is unlikely to remain an effective jacketing method due to several disadvantages. This includes an increase in required space for the strengthened structure, significant increased dead load, relatively long construction time, and practical issues related to bonding between existing columns and additional concrete paste [41].

### 4.1.3 Fiber reinforced polymer jacketing (FRP)

Fiber reinforced polymer jacketing (FRP) is another method used for increasing the axial strength of reinforced concrete columns. The technique is relatively new and compared to steel and concrete, FRP jacketing may provide extremely efficient confinement due to high-strength carbon fiber with a high modulus of elasticity. FRP also has the benefit of being lightweight and rust-free. The disadvantage of FRP jacketing may be that it is more costly than steel or concrete jacketing [37].

The advantages of employing FRP to strengthen existing concrete columns over other techniques are often related to ease and speed of installation, less labor, the original geometry will not be very affected, structural integrity, and a high strength-to-weight ratio. However, it has several drawbacks. Due to early debonding, the effective use of externally bonded FRP is only 30-35 %. Furthermore, FRP can be very expensive and has poor qualities when subjected to heat or moisture. Epoxy resins are used to adhere FRP to the outside of the column [38].

## 4.2    Strengthening with UHPC

More study in the use of UHPC overlays as a strengthening approach is important to implement the method to become a preferred procedure. This can lead to an improved and simplified process of strengthening existing concrete structures. An ideal scenario from a structural perspective would be to increase the structural capacity to the appropriate level while also lowering assembly related costs. In order to achieve this, it is necessary to simplify and standardize the process. When compared to other existing strengthening and rehabilitation approaches, UHPC has a lot of potential in terms of simplicity and cost optimization. It has been demonstrated through research that applying UHPC as an extra overlaying element to existing concrete components may significantly increase the flexural capacity of the initial structural elements [8, 42]. Under certain conditions, the enhanced structure with fiber-based cementitious materials offers a huge potential for significantly enhanced ductility. The effect of the fibers when UHPC is cracked is the biggest reason for the improved ductility. The fibers will be exposed to friction due to the contact surfaces that occur before the material begins to crack. After the cracking process has initiated, the fibers will continue to share the external forces, slowing down and reducing the cracking development [8, 43].

Because of UHPC's unique qualities, it can be used to repair reinforced concrete structures which have been subjected to poor maintenance and have had their capacity reduced due to adverse environmental conditions. It is possible to extend the service life of a structure and strengthen its load-bearing properties by adding UHPC to it. It can also be applied at individual structural parts that are particularly exposed.  UHPC has primarily been utilized to improve existing structures that have needed to be reinforced due to changes in load

circumstances or where the concrete has been damaged. For bridges, this can be accomplished by applying a layer of UHPC on surfaces that is prone to corrosion. This may be the top of the bridge deck, the underside, or the bridge girder, for instance. For other structures, such as beams, it can be done by increasing the cross-section of the beam, or strictly some of the exposed sides [8, 44].

### 4.2.1 Beams

Existing RC beams exposed to harsh environmental conditions may have the need to be strengthened due to deterioration or load changes. Because of its high compressive and tensile strength, UHPC is a suitable material for rehabilitation and capacity improvement of existing concrete structures. Existing research has looked into the effect of adding an additional layer of UHPC to existing reinforced concrete beams, and the results have been promising in terms of flexural and torsional performance. Studies have also illustrated the great potential of adding UHPC to RC beams for deflection and crack development [8, 42]. Zhu et al. [2] investigated different strengthening configurations in terms of the location of the UHPC layer added to the RC beam. Four different configurations, shown in Figure 13, were presented in the study.
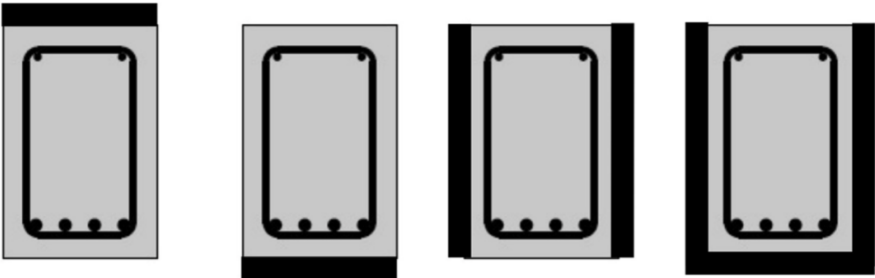


*Figure 13 - UHPC strengthening cases on RC beams [2]*

According to experimental findings, the study concluded that UHPC might be utilized to improve the flexural strength of RC beams or slabs. The improved strength of the strengthened beams varied from 0% to 400%. The greatest considerable improvement in flexural capacity was observed for beams strengthened at the tensile side with reinforced UHPC [2]. In the configuration where the UHPC layer was placed at the bottom and both sides of the beam, the flexural capacity increased the most.

### 4.2.2 Columns

Because of its high strength, UHPC can provide a stronger reinforcing impact on RC columns than standard concrete jacketing. Because of the tiny grains and fluidity of UHPC, a significantly thinner strengthening layer may be used to provide the same strength as traditional approaches. As a result, the problem of a large amount of required concrete area is significantly reduced.

Koo et al. [3] investigated the strengthening effect of UHPC jacketing on concrete columns with different thicknesses. Four identical concrete columns were made in order to compare different jacketing sizes. One column (R0) was left unstrengthened after casting and curing for two weeks, and the three other columns were jacketed with UHPFRC in various ways. The first specimen (R3) was reinforced with a 30 mm jacket, the second (R5) with a 50 mm jacket, and the third (R5S) was reinforced with a 50 mm jacket and additional stirrups within the UHPC. The four different test columns with belonging cross sections are illustrated in Figure 14.
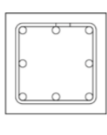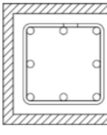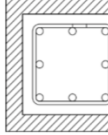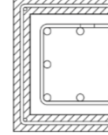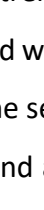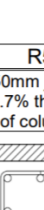


*Figure 14 - UHPC strengthening cases on RC columns [3]*

To replicate seismic stresses applied to building or bridge columns, the experiment was carried out using a cyclic load test setup. According to the results of the experiment, the UHPFRC jacketing method has a strong strengthening impact on the test columns. According to their findings, a UHPC jacket of 10 % column thickness (30 mm) increased the shear strength by over 70 %. Case R5, with a jacketing of 16.7 % column thickness (50 mm), and no additional reinforcement increased the shear strength by over 127 %. In the last case R5S, where additional reinforcement was added to the UHPC increased the shear strength by over 133 %.

If necessary, more strength might be achievable by adding transverse reinforcement. In real-world applications, the concrete jacket would be critical in shifting the failure mode from pure shear to a flexural yielding behavior and thereby improving column ductility. If high strength is required without an unnecessary increase in column size, UHPFRC jacketing might be a reasonable alternative as an RC column repair procedure [3].

### 4.2.3 Bond strength

As mentioned, the properties of UHPC make it suitable as an overlay in a variety of scenarios, such as for repairing and strengthening existing concrete bridges. However, a strong mechanical interaction between the extra UHPC layer and the underlying hardened conventional concrete is required for this application. Because UHPC is typically cast alongside standard-strength concrete, the bond strength between the two composites is critical for achieving the best potential usage. The bond between two composite materials is known to be affected by numerous factors such as substrate surface conditions, curing process and the age of the bond. Predicting the bond between the UHPC and the substrate concrete can therefore be a challenging aspect when it comes to modelling using finite element software [8, 45].

Although the properties of UHPC show good compatibility in the use of strengthening existing concrete structures, specific studies are necessary to determine the resulting compatibility of the structure when UHPC is added as an overlay to existing concrete. The bond between the two materials must be assessed in order to determine the strength of the total system consisting of both materials. The thickness of the repairing layer also plays an important role when it comes to performance. The repairing layer should be optimized to reduce the applied dead load, but at the same time maintain adequate capacity [8, 46].

Valikhani et al. [47] investigated experimentally the bond strength between UHPC and substrate made out of conventional concrete with different surface preparations. Thirty specimens were examined with various surface preparations, such as roughness, mechanical connectors, and bonding agents. The study addresses the effect that the surface roughness has on the bonding strength between two composites. The research concluded that using a bonding agent and mechanical connectors for rough surfaces between concrete and UHPC has a substantial impact on the interface's bond strength. According to the findings, the combination of a rough surface created by sandblasting and mechanical connections

significantly influences the structural capacity. The findings are very relevant for use in bigger projects, such as bridge repair or strengthening with UHPC or concrete in general.

## 4.3    Strengthening of bridges with UHPC

As presented in chapter 3.5, the use of UHPC on bridges in the US has significantly increased the latest years. The exceptional mechanical properties of the material and the ability to make the bridges slim, and to build complex components can be some of the reasons. As shown in the former chapters regarding beams and columns, UHPC is very applicable for strengthening these types of elements. Both of them are often included when a bridge is being repaired or strengthened. Therefore, it is very relevant to implement the use of UHPC for bridge strengthening. It can include strengthening a bridge girder, column, deck, or even all three simultaneously.

The interactive map made by the US FHWA is shown once again in Figure 15 underneath. This time, the map only displays the bridges in the US that were repaired or strengthened using UHPC from the years 2006 to 2020. The use of UHPC for repair or strengthening is almost limited to the East coast, especially the North-East.
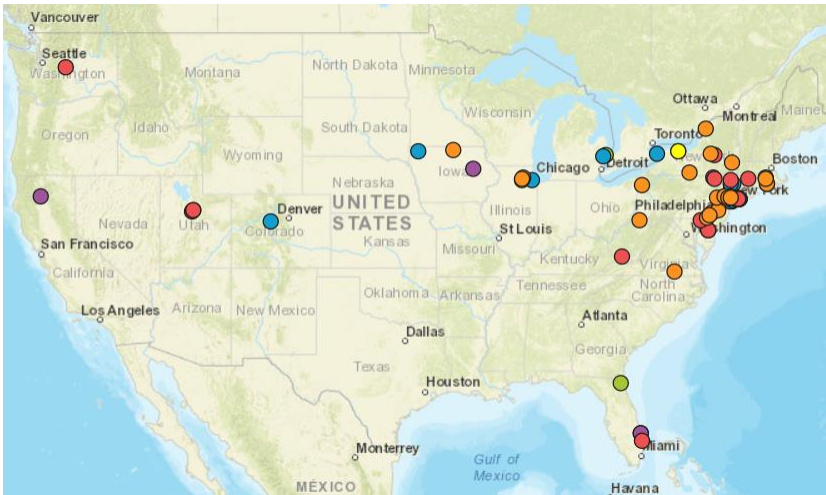


*Figure 15 - Map showing bridges repaired/strengthened with UHPC in USA [33]*

In Figure 16, the number of bridges repaired and/or strengthened with UHPC is displayed as a chart. The same trend as for UHPC in general, can be seen. It is especially in the 3-4 latest years that the use of UHPC has been used for this purpose in the US.
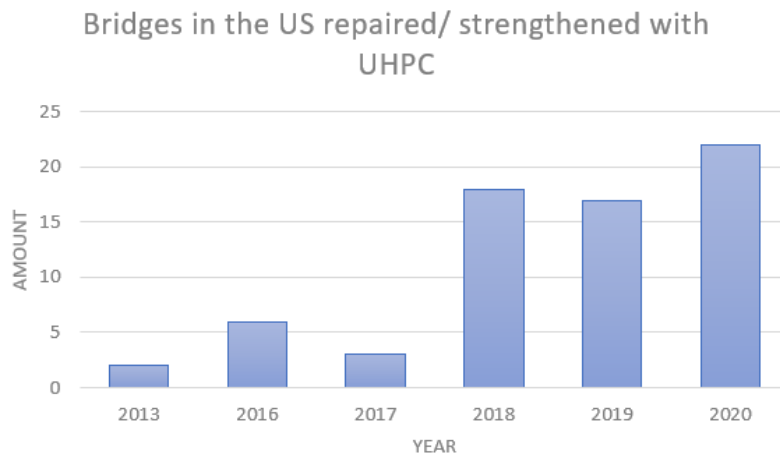
*Figure 16 - Strengthening or repair of bridges using UHPC in USA*

The Commodore Barry Bridge in Philadelphia, illustrated in Figure 17, was one bridge that was strengthened with UHPC. This bridge was built from 1969 to 1974 and is a cantilever bridge connecting Pennsylvania and New Jersey [48]. Due to age, wear and tear, and poor condition of the bridge, it was necessary to repair the bridge deck in 2020. UHPC were then used to repair and strengthen the bridge. The use of UHPC in such a case have, according to Michael Venuto from DRPA [49] the potential to reduce cost, schedules and traffic impact.

At first the old bridge deck was removed, before UHPC was applied as a new bridge deck. The process of applying the material to the roadway is illustrated to the left in Figure 17. This is the largest bridge deck overlay application of ultra-high performance concrete in USA. After the job was finished, they were able to conclude that if it is successfully performed, it can result in extending the service life of the deck with 30 years, and save up to 200 million dollars in costs [49].



*Figure 17 - L: Commodore Barry Bridge in Philadelphia [48] R: Removal of the old bridge deck [49]*

Hundreds of bridges around the world have been built or repaired using UHPC during the last decade. From simple field-cast repairs to large precast elements for long-span bridges and deck replacements on major structures, its applications have been very broad. The French became early innovators and forerunners in laying the groundwork for the use of UHPC in a large range of bridge applications. UHPC is also being utilized in Switzerland to meet substantial bridge restoration needs. Furthermore, UHPC has been adopted by the bridge industry in the United States for a variety of field-cast connectors. The use of UHPC in large restoration projects and bridge components is also being promoted through research and development initiatives [50].

## 4.3.1 Bridge decks

A challenge related to rehabilitation of structures today is actually to improve the structure, and not only repair it. In Switzerland, they tried to strengthen an existing bridge over the Morge river located near Sion, using UHPC with short fibers. The bridge had to be strengthened and widened due to increased traffic load. In this case, the existing waterproofing layer on top of the bridge deck was replaced with a thin layer of UHPC. In addition, extra reinforcement was added to both provide good protection against environmental impacts but also to make the bridge deck stronger. According to the study, this can be done without affecting the dead load of the structure. The conceptual idea in this project was to apply UHPC in the zones exposed to high mechanical and environmental loads. This is certainly relevant at the upper surface of the deck slab on bridges. The deck slab may also be subjected to higher mechanical loads when the traffic loads increases. To not apply more load to existing reinforcement and foundations, it was desirable to increase the load capacity without increasing the dead weight of the bridge [1, 51]. Figure 18 illustrates the conceptual idea of the procedure used to fix the bridge.
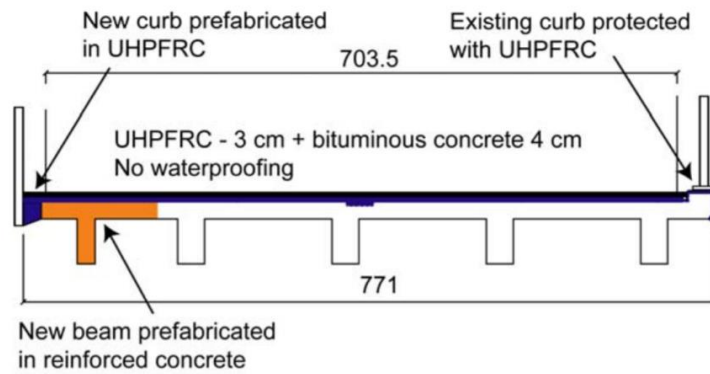
*Figure 18 - Conceptual idea of the approach that were applied on the bridge rehabilitation project in Switzerland [1]*

Three different cross-section solutions were proposed in the study, as seen in Figure 19. The alternatives were established as a starting point and were intended to be implemented based on the current state of the bridge structure.

The first cross-section (left) is a solution that is suitable if the bridge's existing load carrying capacity is sufficient. This technology will be ideally suited to defend against environmental impact and potentially provide a longer lifespan for the bridge structure when it is subjected to high environmental loads, which over time might cause corrosion in the reinforcement or other damages. The solution is therefore suitable for existing structures that are in relatively good condition.

The second cross-section (middle) represents the case where the top reinforcement layer has been subjected to corrosion and needs to be replaced. Existing concrete and reinforcement in the top-layer are therefore replaced with a layer of UHPC in addition to new reinforcement. This solution ensures both protection against environmental loads and strengthens the bridge's load-bearing capacity.

The last cross-section (right) is primarily intended to strengthen the load-bearing capacity of the structure. A layer of reinforced UHPC is added on top of the existing structure without removing the existing reinforcement. The reinforcement will act as external bonded additional reinforcement. The solution both strengthens the structure in addition to adding protection against environmental loads.
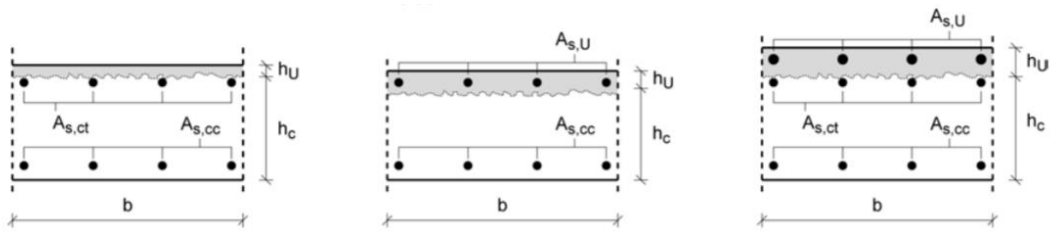
*Figure 19 - Different solutions on how to improve bridge slab decks using UHPC depending on the structures existing condition [1]*

The study concluded that the dense pore structure of UHPC will contribute to higher resistance to future chloride ingress compared to using ordinary concrete. In the project, they chose to use a solution which included replacement of the existing rebars with new reinforcement. This was necessary because of the chloride ingress that the bridge had been exposed to from the top.

Because of the excellent qualities of UHPC, they expected that when the construction was completed, the bridge would require no additional maintenance before being dismantled. They also concluded that reinforced UHPC offers a lot of potentials and opens up a lot of new possibilities for rehabilitating old structures. With deformation tests and analytical models, they were also able to conclude that the bridge showed significantly increased performance in terms of both stiffness, durability, and resistance [1, 51].

### 4.3.2 Improvements/ measures before applying UHPC

Before the UHPC can be applied, there are a lot of measures need to be done to achieve the best possible results. Some of these measures are also done for it to be possible to create a satisfactory bonding between the old and the new concrete, as mentioned in chapter 4.2.3.

Damaged and loose concrete are normal for old bridges and structures. The damaged and loose concrete should be removed before applying the UHPC [52]. It is vital to remove the loose concrete to achieve the best possible bonding. If the loose and damaged concrete doesn't get removed, it can result in a weak spot in the construction, and the UHPC does not reach its potential. In the worst case, several of these weak spots can lead to a decrease in the structural capacity, and the strengthening will have less effect. Cracks can also create weak spots in the structure, and it can lead to corrosion, alkali-silica reactions, and peeling of the concrete. It is therefore important to repair significant cracks and prevent these cracks from

reappearing. This does not only apply for the location of the strengthening. Other areas are just as important since these spots can affect the overall performance in the same way.

Corrosion is also often seen in old constructions. To prevent the corrosion from evolving within the strengthening layer of UHPC, it is essential to remove the corroded areas on the existing reinforcement. This is usually removed by sandblasting the open area [52]. Sometimes, the reinforcement needs to be exposed before the sandblasting can be done. To protect the steel from corroding in the future, it can be taken measures. There are several different ways this can be done. Epoxy coated reinforcement are one of them, and this is reinforcement with an extra protective layer of epoxy wrapped around the steel to avoid corrosion. Another measure is cathodic protection. This is basically based on the principle of turning the reinforcement passive instead of active. The rebars are connected to another metal which can act as an anode, which makes the rebars cathode. The metal applied has to corrode more easily, and zinc, magnesium and aluminum are often used. The new anode will then corrode instead of the rebars [53].

Without using any kind of binder between the concrete and the UHPC it will most certainly peel off. Therefore, epoxy is often used to create a strong bond between the two layers. It is applied all over the surface where the strengthening will take place before the new layer is applied. Like mentioned earlier, a rough, often sandblasted, surface will help to create an even stronger bond.

# 5 The Vattedal Bridge

The Vattedal bridge was chosen in collaboration with the Norwegian Public Roads Administration based on the suggestion of finding a concrete bridge with simple geometry. It is a single-span, slack-reinforced, cast-in-place plate-bridge with a span of 8 meters.

The bridge is part of the county road 5076 and runs between Lunde and Hodnanes in Tysnes municipality south of Bergen. The bridge is located in a coastal environment and close to sea level. The road is a rather small road with a small number of vehicles using the road and crossing the bridge compared to bigger roads in the area. For example, the county road 49 and the E39 passing nearby. It is mostly the locals using the road, as well as tourists, especially during the summer. Furthermore, there are also a lot of trailers and construction vehicles driving in the area.



*Figure 20 - Location of the Vattedal bridge*

### 5.1.1 Previous repair and condition

A repair of the bridge was conducted in 2007. Before this point, the concrete had started to peel in several spots, and the reinforcement had begun to corrode. The bridge was therefore in danger of decreasing capacity if no action was taken. The sections where the concrete had peeled off, as well as the nearby areas were therefore repaired. The damaged concrete covered large areas underneath the bridge, and the areas affected can be seen in Figure 21. The blue circles show the areas, and it is as much as 6 m covered in the largest area.

To our knowledge, no measures in means of corrosion were concocted before the new concrete was applied. However, after the strengthening in 2007, the bridge has again started to take damage. The red spot on the figure indicates where there is concrete peeling at the current date.
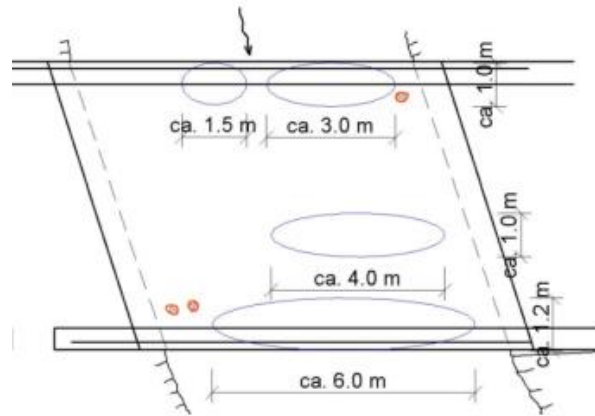


*Figure 21 - Concrete peeling repair in 2007 [52]*

Under the auspices of Vestland County Municipality, a survey of the Vattedal bridge was conducted in the autumn of 2021 [52]. Inspections revealed that the concrete on the bridge was peeling in certain local areas, corrosion had appeared, and the bridge needed to be strengthened. It was therefore decided to try to strengthen it with carbon fiber sheets. Calculations and results were provided in the report. Global analysis and assessment of carbon fiber sheets in conjunction with existing reinforcement were included in the calculations. The goal with the report was to classify the bridge as BK10/60 instead of a BKT8 like it is today. The attempt was not successful, and it was concluded that the bridge did not obtain the desirable capacity by applying carbon fiber sheets. The moment capacity had a sufficient increase, but the shear capacity did not fulfill the requirements and the bridge could therefore not be strengthened with the carbon fiber sheets.

A bridge assessment was carried out for the purpose of this thesis in collaboration with Vestland County Municipality. The main purpose of the inspection was to perform a modal assessment of the bridge. To ensure that the inspection was carried out properly, warning signs were placed out 200 m in front of the bridge to warn passing traffic, as seen in Figure 22.

*Figure 22 - Danger sign and cones at the Vattedal bridge seen from the road*

An inspection of the bridge was conducted on 15.03.2022. The bridge is considered to be in a good condition when taking the age into account. Since the repair in 2007, it has not been any large demand of repair or maintenance. Some local peeling of concrete has occurred and is also described in the report from SVV [52].

A recent photo of these spots is displayed in Figure 23. As it illustrates, some minor peeling over an area of 10-12 cm has occurred. Even though the peeling is covering a small area, it has caused corrosion to occur, which again can lead to bigger damages in the future if it does not get fixed.



*Figure 23 - Local concrete spalling where the reinforcement has started to corrode*

Vestland County Municipality took responsibility for the safety. In addition, cones were placed directly in front of the sensors so that traffic could not hit the equipment that was located at the edge of the roadway. The bridge appears to be in decent shape taking the age into consideration. Since the bridge is old, there are some minor cracks and damages to the curbs, and the concrete shows tendencies of being old. The aggregates are pretty big and are visible both on the curbs and on the underside of the bridge. This indicates that the concrete casting should have been executed better. Especially the vibration process during the cast in-place execution should have been performed better. Some local corrosion damages were detected at the bottom of the bridge deck where existing rebar was directly exposed to water splashes from the river, as well as contact with air. Where the rebar was exposed, it had a significantly decreased cross-section as a result of corrosion.

## 5.2   Bridge classifications

This chapter briefly explains the Norwegian Public Roads Administrations (SVV) different bridge classifications for traffic loads. SVV has different bridge classifications to describe what types of vehicles and loads the bridge can handle. The main classifications are Bk10, BkT8, Bk8 and Bk6. The different classifications and the respective loads in each class are displayed in Table 1. The most important load is the "Kjøretøylast" and the «Vogntoglast» which is vehicle load and trailer load respectively. Therefore, these are highlighted in the table. For a bridge to be classified as Bk10 it must withstand a trailer with a total weight of 500 kN, which corresponds to 50 tons. The classification Bk10/60 is a special classification from the normal Bk10, but with 60 tons trailer load instead of 50. For BkT8 it is 40tons [54].
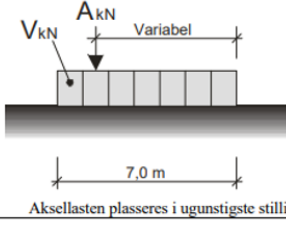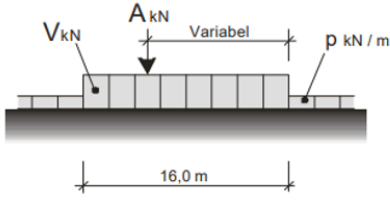
| Lasttype | Lastkonfigurasjon (∗) H kN | Bruksklasser | | | | |
|---|---|---|---|---|---|---|
| | | | Bk10 | BkT8 | Bk8 | Bk6 |
| Kjøretøylast |  7,0 m Aksellasten plasseres i ugunstigste stilling | A | 40 | 32 | 32 | 24 |
| | | V | 300 | 280 | 220 | 180 |
| Vogntoglast |  16,0 m Aksellasten plasseres i ugunstigste stilling | A | 40 | 32 | 32 | 24 |
| | | V | 500 | 400 | 320 | 280 |
| | | p | 6 | 6 | 6 | 6 |

*Table 1 - SVV bridge classifications [54]*

38

# 6  Method

## 6.1  Research statements

Several different approaches to strengthening concrete structures using UHPC were gathered throughout a literature review. The Swiss study performed by Brühwiler et al. [1], in which UHPC was applied to the top of the bridge deck, and the study conducted by Zhu et al. [2], where it was discovered that UHPC had the greatest effect when applied in the tensile zone of concrete beams, were two of the promising studies where UHPC was used for strengthening existing concrete structures. Because the Vattedal bridge shares many of the same characteristics as the bridge in Switzerland when it comes to size and span, they can be considered comparable, and thus somewhat similar results can be expected when adding UHPC as an extra layer at the top of the Vattedal bridge. It was intriguing to investigate if implementation of UHPC to the tensile zone of the bridge deck in Vattedal may produce similar outcomes as those obtained in the beam and column studies investigated. A comparison between the two approaches of applying UHPC on top, or at the tension may also be very relevant.

## 6.2  Strategy

To start the work with the thesis, it was necessary to decide for a topic. Several fields were discussed in order to find the most appropriate and interesting subject. Since the authors has previously worked with ultra-high performance concrete last semesters, and this was a topic that needed more work and investigation, it was decided to study even more in this field. To get a clear overview of the extent and the key tasks, a timeline in MS Project was conducted. A flow chart was also conducted throughout the process and was updated in the finalizing stage. The flow chart is shown in Figure 24. The flowchart is divided into 5 phases. Each of the phases has a representing color.

Phase 1 is where the topics were considered and chosen. Phase 2 is marked blue on the chart and represents the literature review of the first analysis in Abaqus. At this point, information was gathered, the theory was learned, the research question formulated, and Abaqus knowledge accumulated. This phase was the most time-consuming. The first content in the theory and method chapter are produced in this phase. Phase 3 is marked orange and

represents the cooperation with the Norwegian Public Roads Administration. This phase is parallel with phase 2, but the extent of this phase is larger towards the end. In cooperation with SVV it was decided to look into the strengthening of the Vattedal bridge, and from there, a lot of research was conducted on the bridge. Including former strengthening attempts, type of reinforcements, calculations, and classification report. At the same time, the Unquake OMAway sensors were learned how to install, operate, and read the results. This was to be able to do the bridge assessment as wanted.

After the results from the reference model in Abaqus and the results from the Unquake sensors were finalized, phase 4, marked dark green, began. This phase is where phases 2 and 3 come together and the model updating are used to combine the results from these phases. The results from the bridge assessment are used to update the reference model and move the natural frequencies toward the experimental ones. Multiple analyzes were performed in this phase, both on the reference model and the UHPC strengthened models. Theory, method, and obtained results are more or less finalized during this phase. Phase 5 is marked light green and represents the last phase of the study. This is where the thesis comes up with a conclusion and a recommendation for future work, and the thesis is finalized and delivered.
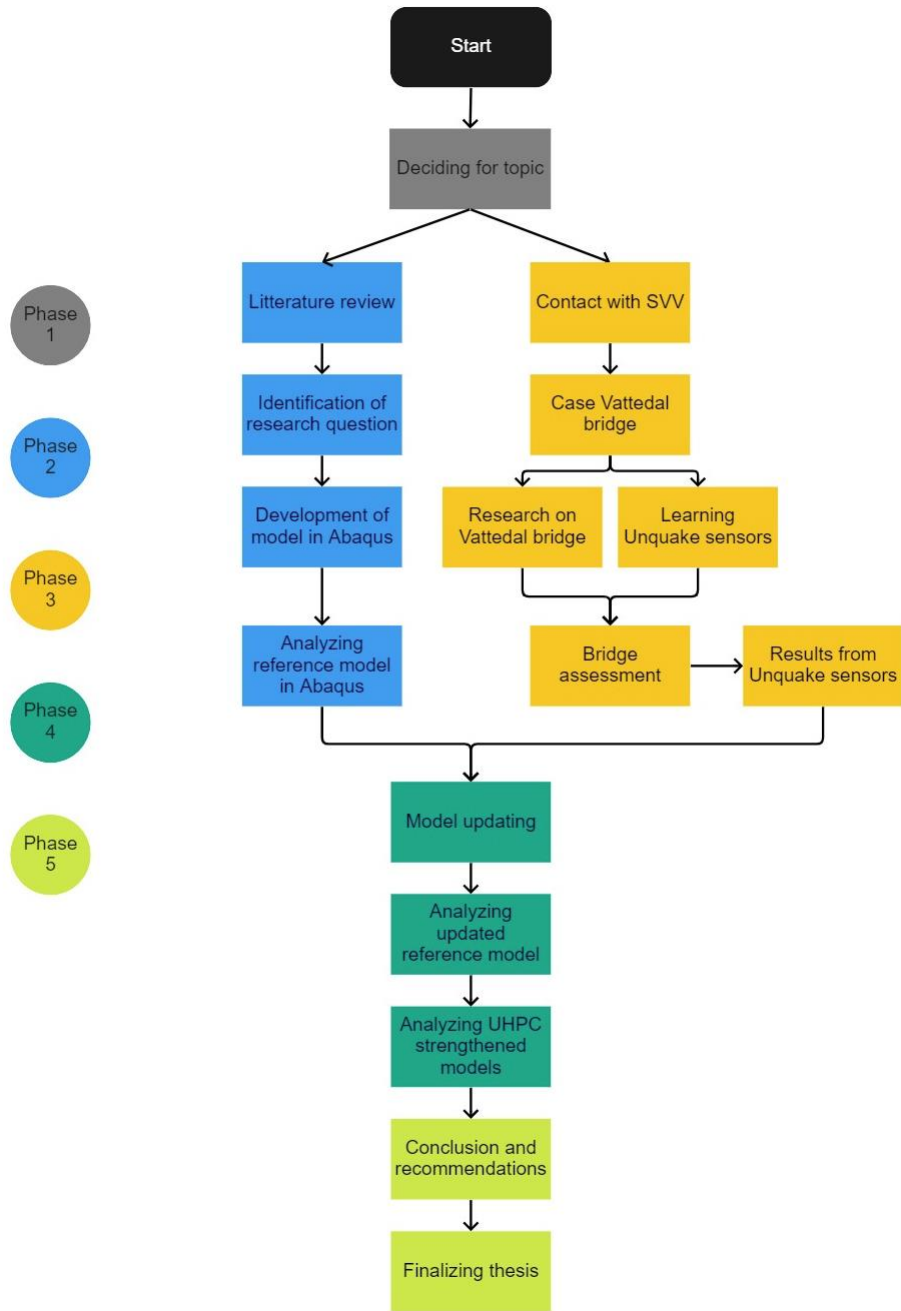
*Figure 24 - Flow chart of the thesis process*

Now for a more general description of the work in the thesis. After having a straightforward research question as a starting point, it was chosen to investigate two potential locations of UHPC on the Vattedal bridge, in addition to the initial model. An analysis of the original model was necessary to be able to compare the two cases with the current bridge and thus be able to determine how much it is possible to strengthen it with these two approaches. This model is referred to as the reference model. Both locations of UHPC were modeled and analyzed in Abaqus.

The research in this study focuses on UHPC for flexural strengthening of an existing concrete bridge. Different strengthening methods were discussed during the literature study and the experimental database was obtained based on existing compressive and tensile testing of UHPC. The public road administration provided documentation and calculations regarding the classification of the bridge and their calculations in an attempt to strengthen the bridge with carbon fiber reinforced polymer (CFRP), addressed in chapter 4.1.3. The damage degree for reinforced concrete, strengthening configuration, characteristics of UHPC layer, bonding condition, and material modelling were discussed in order to examine the effectiveness of strengthening the concrete bridge with UHPC.

An excursion to the Vattedal bridge was organized and completed in order to gain the best possible knowledge about the bridge`s current condition. During this visit, photographs were taken, a visual assessment was performed, and accelerograph sensors were installed in order to validate the FE-model with modal analysis. As a result, the project would get a much more realistic perspective.

## 6.3   Literature review

The literature review was carried out in parallel with the modeling throughout the entire project, and it provided an overview of the most important information needed to complete the study. Cooperation with The Public Road Administration was also very helpful during the whole thesis when it came to gathering existing information. A broad overview of the mechanical characteristics of UHPC, diverse applications, and available strengthening techniques were presented through the review to address the wide variety of the field.

## 6.4   Case – The Vattedal bridge

It was preferable to select an existing concrete bridge in Norway that needed to be repaired or strengthened. In collaboration with the Norwegian Public Roads Administration, it was decided that a relatively small concrete bridge with a short span and demand for strengthening was a favorable case regarding the authors` desirable research question. Therefore, it was decided that the Vattedal bridge in western Norway would be an appropriate case study.

The bridge is described as a slack-reinforced, cast-in-place plate bridge with a span of 8 meters. It has a simple geometry and is made of solid concrete. The reinforcement is taken from an old classification report from SVV, with some assumptions. The bridge has been classified as BKT8. The bridge is simply supported on a drystacked wall at each end. The foundation consists of a solid mountain underneath the drystacked wall.



*Figure 25 - The Vattedal bridge seen from both sides*

## 6.5  Validity and reliability

When considering the validity and reliability of a thesis it can be considered by asking and answering relevant questions. According to Jacobsen [55], it is especially three questions needed to be asked:

- Is the data collected reliable? In other words, can we trust the results?
- Is the result as we expected and are they reasonable?
- Are the results and what is presented the truth?

By answering these questions, it is possible to conclude whether the thesis is valid and reliable. It is often divided into internal and external validity. Where the internal validity addresses whether it is close to reality and correct and that the data is sufficient enough to conclude. While external validity addresses how it is possible to generalize the findings [55].

By focusing on what could strengthen and weaken the validity and reliability in the research process, quality and relevance is controlled throughout the thesis. Similar studies, theories, and former research have been investigated to achieve this. It is focused on research where

the author(s) have participated in the analysis, experiment, or practical execution themselves. This increases the credibility of the report and excludes sources of error that can occur when outsiders mention and addresses other researchers [55].

The reliability of the thesis depends on several factors. The process is tried to be described in a simple and understandable way so that the readers can be able to repeat the process and get the same results. It takes some effort to verify and get the same results, but it is possible if the procedure is followed.

The analysis carried out in Abaqus is aimed to be as realistic as possible to make it valid. The model is based on a given concrete type and geometry from SVV, as well as general parameters. The existing cracks, corrosion and peeling are not considered in the analysis, but would be one way to make the model more realistic. This would require more non-destructive testing and would have been very time-consuming. The plan for the thesis was to carry out model updating to update the FE- model, and then later analyze and compare different strength configurations with UHPC.

# 7 FEM analysis – Numerical analysis

Numerical modeling and computer simulations are being used to solve problems for engineers around the world. Engineers can use numerical modeling for almost any kind of problems. It can be anything from simple 2D-problems to complex 3D-problems and abstract models. Even though it is possible to solve these problems, the simulations can take a very long time. In fact, it can last for several days and even weeks. To calculate the same problem by hand calculations or with other outdated and underdeveloped methods would take an enormous amount of time [8, 56]. According to Sirois and Grilli et al. [57], numerical modelling can be defined as a *"mathematical representation of a physical (or other) behavior, based on relevant hypothesis and simplifying assumptions"*.

There are several different types of numerical modeling. In this report it is only focused on FEM – Finite element method. This is the most commonly used method in structural engineering. FEM is a way to numerically solve a complex problem. Basically, a large problem is divided into several small problems, so called finite elements. When this method is applied to a simulation, it is called an FEA – Finite element analysis. FEA creates a model that shows how the structure/ elements react and perform under the applied stress and loads [8, 58]. Several FEM software are available, but Abaqus is the software chosen and used in this study.

In structural engineering, FEA is normally used to solve displacements, stresses, buckling behavior and dynamic behavior for different structures. It can be used on whole structures, such as bridges, but also on smaller elements like single beams and columns. FEA can also be used instead of real-life experiments. This will be very time-saving and cost-effective because it is not necessary to build it in real-life, and you don't have to damage or destroy it. The development of computers is also getting better and better with time, so the process will only get faster, easier and more available in the years to come [59].

## 7.1 FEM analysis on concrete structures

FEM analysis on concrete structures is more advanced than analysis on other structural materials, such as steel. This is mainly because the concrete often consists of both concrete and steel reinforcement, and this needs to be modeled correctly to get valid results. This

challenge also applies to UHPC or fiber reinforced concrete when the fibers have to be modelled. In many FEM software, you can model the fibers to fit your structure correctly, but it is also possible to take shortcuts, such as assuming the fibers contributions when the parameter for the concrete is added. The fibers mainly contribute to the parameters regarding the tensile strength of the structure. In programs like ANSYS you can model the fibers, while it is limited options for modelling fibers in Abaqus.

## 7.2  Plastic material models

There are multiple material models to use when modeling concrete with the finite element method. A material model is an equation that relates the forces and the deformation, or in other words stresses and strains, for the specific material. Some examples of commonly used material models are Drucker-Prager, Mohr-Coulomb, and Concrete Damage Plasticity (CDP) model.  The Drucker-Prager plasticity model is designed for geological materials with pressure-dependent yield, such as concrete. For geotechnical applications, the Mohr-Coulomb failure or strength criteria can be used. It has been one of the most used design calculations for the geotechnical area.

In this study, the material model used to model concrete is the concrete damage plasticity model and it will be more thoroughly described. It is chosen based on literature study and previous experience from working with concrete in the earlier semesters. Also, the majority of the assessed studies appeared to produce good and accurate findings with the CDP model.

## 7.3  Concrete Damage Plasticity (CDP)

Both conventional concrete and UHPC may be modeled using the CDP model. The model is suitable for modeling brittle composites and is described in the remainder of this section to motivate different aspects of the constitutive theory.

It is well known that the modeling of brittle materials can be quite complex. When it comes to these materials, one of the challenges is that they function asymmetrically in the compression and tension zones. When concrete is subjected to low pressures, it becomes brittle, and the structure cracks in the tension zone and crushes in the compression zone, resulting in structural collapse. A plastic behavior can be assumed because of the reinforcing

steel inside the concrete and the steel fibers in the UHPC. The plastic damage model is a variation of classical plasticity theory in which the hardening variable is replaced with a plastic damage variable that rises only when plastic deformation occurs. This variable has a limitation value that it cannot exceed, and reaching this number represents a completely damaged structure [8, 60]. In this study, the CDP model was utilized to model both the conventional concrete and the UHPC in Abaqus.

The theory for the model is proposed by Lubliner et al. [60] and by Lee and Fenves et al. [61] and provides a general capability for the analysis of concrete structures under dynamic and cyclic loading. In the following section, the characteristic of the model given in the Abaqus theory manual is described briefly [8, 62].

### 7.3.1 Strain rate

The damaged plasticity model for concrete is based on the following strain rate:

$$\varepsilon = \varepsilon^{el} + \varepsilon^{pl} \qquad \text{(Eq.2)}$$

Where $\varepsilon$ is the total strain, $\varepsilon^{el}$ is the elastic part of the strain rate, and $\varepsilon^{pl}$ is the plastic part of the strain rate.

### 7.3.2 Stress-strain relation

Damage associated with structural failure will result in degradation in elastic stiffness. The relation between stresses and strain is therefore based on a scalar damage elasticity. A general formulation of this theory can be described as follows:

$$\sigma = (1 - d)D_0^{el} : (\varepsilon - \varepsilon^{pl}) = D^{el}(\varepsilon - \varepsilon^{pl}) \qquad \text{(Eq.3)}$$

A damage parameter $d$ is introduced to describe the scalar stiffness degradation. This value ranges between 0 and 1 where 0 means that the material is undamaged, and 1 means fully damaged. This value will be essential for the propagation of cracks in the FE-model because cracking will occur when this parameter reaches a certain value, which should be specified in the model. Also, $D_0^{el}$ is the undamaged elastic stiffness of the material and $D^{el}$ is the elastic stiffness when the material is degraded, and can also be written as:

$$D^{el} = (1 - d)D_0^{el} \qquad \text{(Eq.4)}$$

The formulation shows when the damage parameter increases, the elastic stiffness is reduced resulting in a reduction of elastic stiffness in the concrete when cracking and crushing occure.

When the damage parameter is equal to zero, the effective stress $\sigma^{eff}$ is equal to the cauchy stress $\sigma^c$. They are presented in the following equations:

$$\sigma^{eff} = D_0^{el} : (\varepsilon - \varepsilon^{pl}) \qquad \text{(Eq.5)}$$

$$\sigma^c = (1 - d)\sigma^{eff} \qquad \text{(Eq.6)}$$

The link between the effective load carrying area and the overall section area is represented by the factor (1-$d$). However, it is the effective stress area that is exposed to external loads. As a result, when damage occurs, the effective stress is more representative than the cauchy stress. Therefore, it is more convenient to define plasticity in terms of the effective stress.

### 7.3.3  Hardening

Increasing hardening factors are linked to concrete cracking and crushing in the CDP model. The variables $\varepsilon_c^{pl,h}$ and $\varepsilon_c^{pl,h}$ refer to plastic strains in tension and compression respectively and are utilized to govern the development of the yield or failure of the surface. After the material has reached plasticity, continued straining will modify the yield surface. Isotropic hardening or softening, kinematic hardening, or ideal elastic-plastic behavior can all cause this [8, 63].

### 7.3.4  Yield criteria

The plastic-damage concrete model employs a yield condition proposed by Lubliner et al. [60] as well as the modifications by Lee and Fenves et al. [61] to account for different strength evolution under tension and compression.

### 7.3.5  Compressive behavior

Uniaxial compressive behavior is frequently determined using experimental testing or constitutive models. When defining the association between the damage parameters and the compressive strength of concrete in damage plasticity models, the plastic hardening strain in compression $\varepsilon_c^{pl,h}$ has a major impact [6, 8]. This variable can be expressed as follows:

$$\varepsilon_c^{pl,h} = \varepsilon_c^{in,h} - \frac{d_c}{(1 - d_c)}\frac{\sigma_c}{E_0} \qquad \text{(Eq.7)}$$

where $E_0$ is the initial (undamaged) elastic stiffness of the material and $\varepsilon_c^{in,h}$ is the inelastic hardening strain in compression. This parameter is based on the concrete strain and the

correlation between the nominal compressive stress and the modulus of elasticity. It can be expressed as follows:

$$\varepsilon_c^{in,h} = \varepsilon_c - \frac{\sigma_c}{E_0}$$

(Eq.8)

It's called inelastic because it represents what happens to the concrete once it reaches its ultimate strength and begins to deteriorate. The Youngs modulus begins to drop at this point. Abaqus will keep tracking the concrete damage and alter the inelastic strain based on the damage to the Youngs modulus. As a result, if there is no damage to the concrete, the inelastic strain will equal the plastic strain. We'll have to specify the concrete compression damage as well if there is compression damage. The reaction of concrete to uniaxial compressive loading is shown in Figure 26.
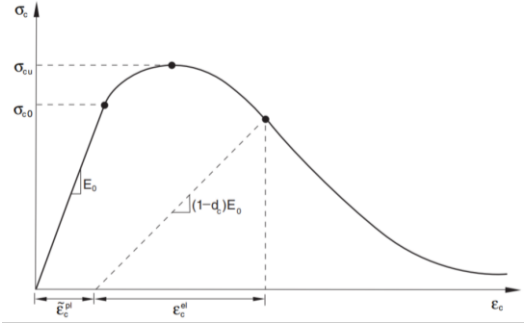


*Figure 26 - Response of concrete to uniaxial loading in compression [62]*

Cracks propagate transverse to the stress direction under uniaxial strain. As a result of the nucleation and propagation of cracks, the available load-carrying area is reduced, and the effective stress increases. The impact is less obvious under compressive stress because fractures run parallel to the loading direction. However, the effective load-carrying area also drops significantly with a large quantity of crushing.

The inelastic hardening strain in compression $\varepsilon_c^{in,h}$, which regulates the slope's unloading curve, is used to determine compression damage $d_c$ which increases for higher values of $\varepsilon_c^{in,h}$.

$$d_c = 1 - \frac{\sigma_c}{\sigma_{cu}}$$

(Eq.9)

where $\sigma_c$ is the nominal compressive strain and $\sigma_{cu}$ is the ultimate compressive strength of an unconfined cylindrical test specimen.

## 7.3.6   Tensile behavior

The reaction of concrete to uniaxial tensile loading is shown in Figure 27.
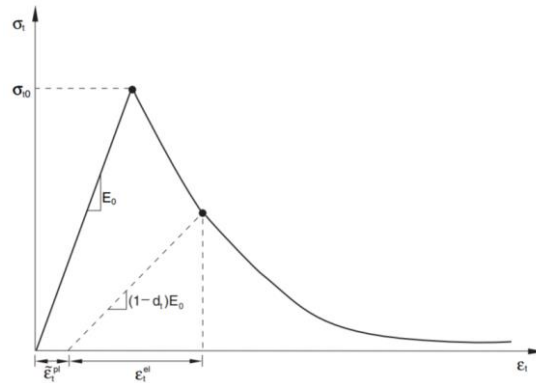


*Figure 27 - Response of concrete to uniaxial loading in tension [62]*

The plastic hardening variable related to tensile strain $\varepsilon_t^{pl,h}$ illustrated in Figure 27 and the tension damage $d_t$ can be expressed by the following two equations:

$$\varepsilon_t^{pl,h} = \varepsilon_t^{ck,h} - \frac{d_t}{(1-d_t)}\frac{\sigma_t}{E_0} \tag{Eq.10}$$

$$d_t = 1\frac{\sigma_c}{\sigma_t^0} \tag{Eq.11}$$

where $\varepsilon_t^{ck,h}$ is the hardening cracking strain.

## 7.3.7   Dilation angle and Eccentricity

The dilation angle is the angle formed by the material's internal friction. Normally, this value varies between 30 and 40 degrees. The flow potential eccentricity occurs when the hyperbolic flow potential hits its asymptote. In Figure 28, the flow potential eccentricity and the dilation angle are displayed [8, 62].
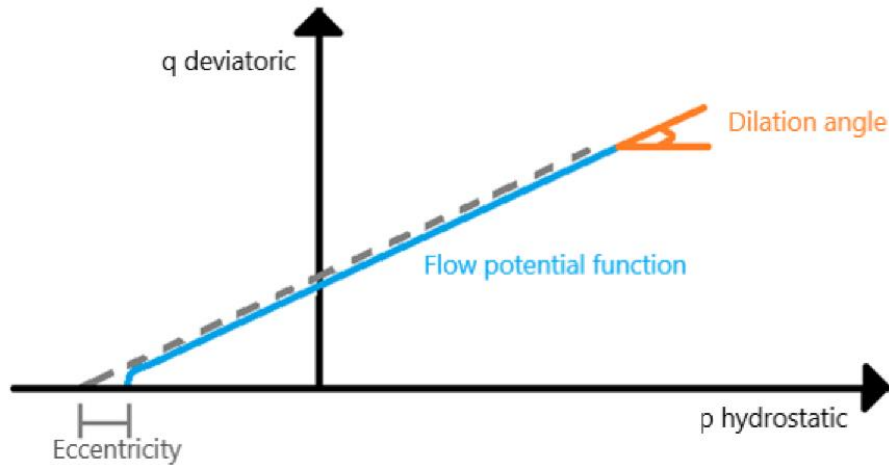
*Figure 28 - Illustration of the dilation angle and eccentricity*

### 7.3.8  Ratio of biaxial and uniaxial concrete strength and viscosity parameter

The ratio of biaxial and uniaxial concrete strength is represented by the relation $f_{b0}/f_{c0}$. 1.16 is a common value for this relationship, and this is also used in this case. This simply means that biaxially stressed concrete has a higher compressive capacity than uniaxially stressed concrete [8, 62].

The viscosity, K is the final parameter. The viscosity parameter enhances convergence performance and reduces the analysis time of reinforced concrete in numerical simulations. If you have a simple model that can be solved quickly, 0 is a good value [8, 62]. $f_{b0}/f_{c0}$ and $K$ are displayed in Figure 29. Different values of K correspond to different yield stresses in the deviatoric plane. It has a spherical form when $K_c = 1$. $K_c$ is the tensile to compressive meridian slope ratio. As a result, $K_c = q_{TM}/q_{CM}$. It basically defines the tension-compression relationship.
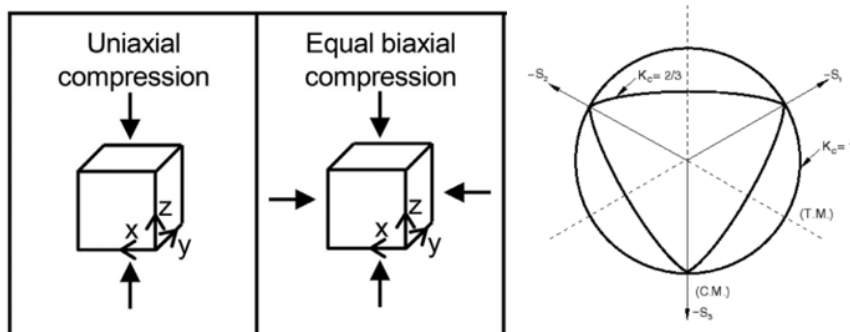


*Figure 29 - L: Ratio of biaxial and uniaxial concrete strength $f_{b0}/f_{c0}$  R: Viscosity parameter K (right) [64]*

## 7.4 Contact between surfaces

To achieve a realistic behavior, contact between the bridge deck and the supports must be considered. By incorporating the term small-sliding into Abaqus, it is possible to simulate contact behavior between two surfaces. Small sliding between two bodies relative to each other is allowed under this term, and arbitrary rotation is permitted. Modeling the interaction between two deformable bodies or one deformable and one rigid body is possible with the small-sliding capability. It is possible to use the concept in two or three dimensions. When adopting this method, one of the contact surfaces must be assigned as the "master" surface, while the other must be defined as the "slave" surface. The software then creates a constraint that prevents the slave surface nodes from penetrating the master surface. Matching meshes are also required on the contact surfaces [62].

## 7.5 Development of models in Abaqus

As previously mentioned, Abaqus is used for the analysis in this study. This software can be used for both modeling, analysis, and visualization of the component. It was first released in 1978 and had many changes and upgrades over the years. A new version has been released at the end of every year since 2000. Abaqus is popular among research institutions due to the possibility of creating its own material properties, capability, and customization [62]. When the analysis is complete, you can visualize the model with all the necessary results [8, 62].

To use the CDP model, there are several parameters that need to be determined. This includes the parameters deciding how the material behaves under certain influences, like the modulus of elasticity and Poisson's ratio. However, the CDP model also includes plasticity parameters, parameters for concrete compressive behavior, concrete compression damage, concrete tensile behavior, and concrete tension damage. These parameters are all contributing to the structural response, such as crack development, stresses/strains, and deflection.

### 7.5.1 Reference model

The reference model was modeled with normal-strength concrete, B40 and has a span length of 9 m. This model was developed before the physical bridge assessment and was only based on the geometry received from the Norwegian Public Road Administration. This implies that

the model will not be very realistic at this phase, but a quick analysis was carried out using a very coarse mesh and a small load to ensure that everything else was working properly.

The cross-section of the bridge was developed in Revit and is shown in Figure 30 underneath. The model is made with the drawings from "12-1185 Vattedal" made by the Norwegian Public Roads Administration in 1966 as reference. See attachment A for the original drawings and cross-section. The fence on top of the curbs and other accessories are not included in the cross-section because it has no impact on the analysis results.
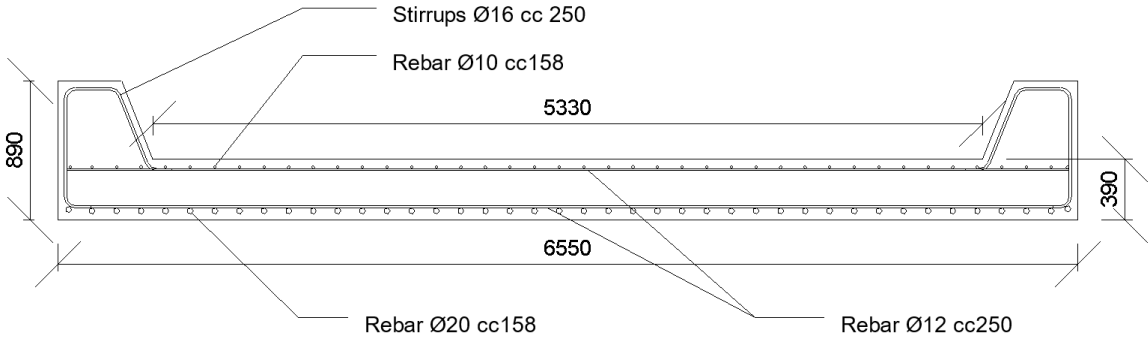


*Figure 30 - Cross-section of the bridge, developed in Revit*

A tabular presentation of the bridge dimensions is given in Table 2.

| Parameter | Value [mm] | Description |
|---|---|---|
| H | 890 | Total height, including curbs |
| $H_D$ | 390 | Height of the bridge deck |
| W | 6550 | Total width of the bridge |
| $W_D$ | 5330 | Width of the bridge deck |
| L | 9000 | Total length of the bridge |
| e | 40 | Concrete cover, including top, bottom and sides |
| S | 500 | Supports on each end of the bridge |

*Table 2 - Cross-sectional dimensions of the bridge*

The old classification report [65] mentions several cases with different thickness of the rebars, and also different concrete covers. Therefore, Ø20 mm longitudinal rebars were assumed in the bottom layer of the deck, and Ø10 mm at the top layer. Both layers have Ø12 mm rebars in the transverse direction. The curbs were reinforced with Ø16 mm stirrups as well as the bridge edges. The center distance of the rebars varies for the longitudinal, transverse and stirrups. Table 3 displays the different reinforcement in each layer, and the center-to-center distance.

| Top layer | Bottom layer | Stirrups |
|---|---|---|
| Ø10 cc158 longitudinal | Ø20 cc158 longitudinal | Ø16 cc250 curbs |
| Ø12 cc250 transverse | Ø12 cc250 transverse | Ø16 cc250 ends |

*Table 3 - Description of the reinforcement*

The concrete cover is also mentioned with different values in the classification report. For this study, a 40 mm concrete cover is assumed all over. Both in the curbs, edges, ends, top and bottom. The 3D model sketch of the Vattedal bridge with all the mentioned dimensions are illustrated in Figure 31.
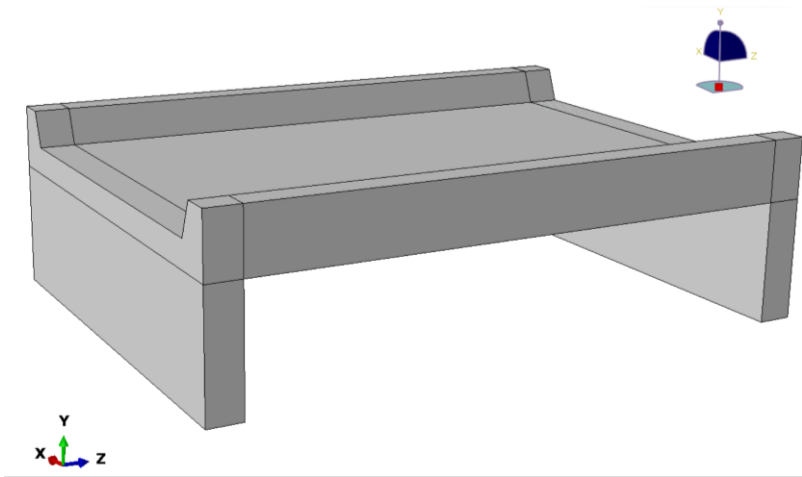


*Figure 31 - 3D model of the Vattedal bridge in Abaqus*

Due to the complexity of the concrete damage plasticity theory, the procedure has been simplified by other researchers. Therefore, a simplified concrete damage plasticity model developed by Esfahani et al. [5] was used. Their study proposes different parameters of the simplified concrete damage plasticity model, including a damage parameter, strain hardening

and softening rules, and certain other elements through experimental testing. The obtained parameters of concrete B40 are given in attachment B.  This study implements these parameters for describing the conventional concrete in the Abaqus model.

The parameters presented in attachment B plays an important role when it comes to developing a realistic behavior of concrete. The theory for the simplified damage concrete plasticity addressed in the literature review was also employed as a foundation for the reference study in which the parameters were established. The experimental findings shown in the table were validated through uniaxial tensile and compressive laboratory tests, which were then translated to a finite element model. They also validated the results by comparing empirical formulations given in previous research. The results showed a good correlation between the different approaches and results obtained in previous studies.

### 7.5.2  30 mm UHPC in the compression zone

For the first test case, a layer of UHPC was modelled as a strengthening and protective layer on the top surface of the bridge deck. The model illustrates the UHPC directly located on the existing concrete, and the overlaying asphalt is therefore not considered in the calculation.

Before developing the bridge model consisting of both the UHPC layer and the conventional concrete, the initial bridge model was copied and the additional UHPC overlay was integrated into the model as a separate part with its own unique properties. The same location of the UHPC layer was performed by Brühwiler et al. [1] with successful results. For the bridge model in this study, no additional steel reinforcement was added to the UHPC layer at the top, because there are no reports concluding that the existing reinforcement at the top layer is not sufficient. Even though there were not any rebars added, the steel fibers in the UHPC mix will contribute to tensile strength in addition to the existing rebars. Figure 32 illustrates the cross-section at the mid-span of the bridge when the UHPC layer was applied at the top.
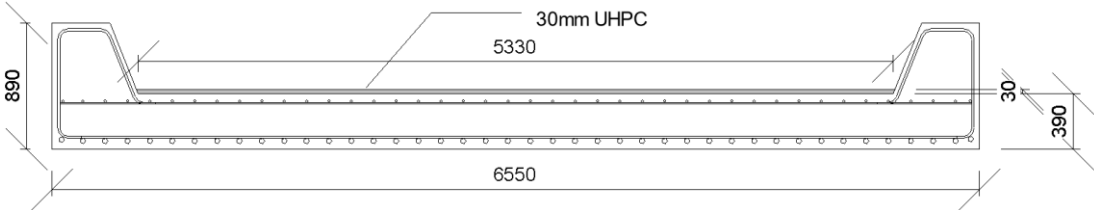


*Figure 32 - Bridge cross-section where a 30 mm UHPC overlay is applied at the top of the bridge deck*

The thickness of the UHPC overlay was set to 30 mm. This value is based on the successful outcomes obtained in the reference study, where a layer of 30 mm was applied [1]. The layer was applied over the whole upper surface like Figure 33 illustrates. The load and boundary conditions were the same as for the reference model, but in this case the load was applied on top of the UHPC layer.
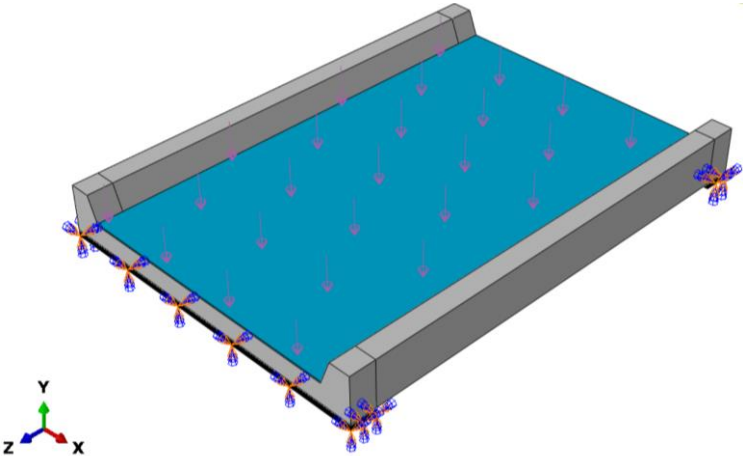


*Figure 33 - Abaqus model with 30 mm UHPC on top*

### 7.5.3  30 mm UHPC in the tensile zone

For the second test case, the UHPC layer was modelled at the underside of the bride deck. This layer was modelled at the same way as for the previous case. It was desirable to investigate if the successful strengthening of concrete beams performed by Zhu et al. [2] where the UHPC overlay was added on both sides and at the bottom of the beam, could be applied for bridges such as the one in Vattedal as well.

Because the bridge is much wider than it is thick, it was chosen to only apply the UHPC at the underside. The effect of the extension of UHPC to the sides will not have a significant improvement on the flexural strength, but it will improve the aesthetics with a UHPC layer all the way up the curbs. This will also make the bridge more corrosion-resistant because it will cover more gaps. Since the bridge already had signs of corrosion on the side edges, this could be a more suitable solution for the overall bridge performance. However, in this study, it is strictly chosen to look at the effects of UHPC as flexural strengthening. The result obtained in this project will hopefully confirm the effectiveness of the location of the overlay, and that the results are in accordance with the ones obtained in the reviewed studies.
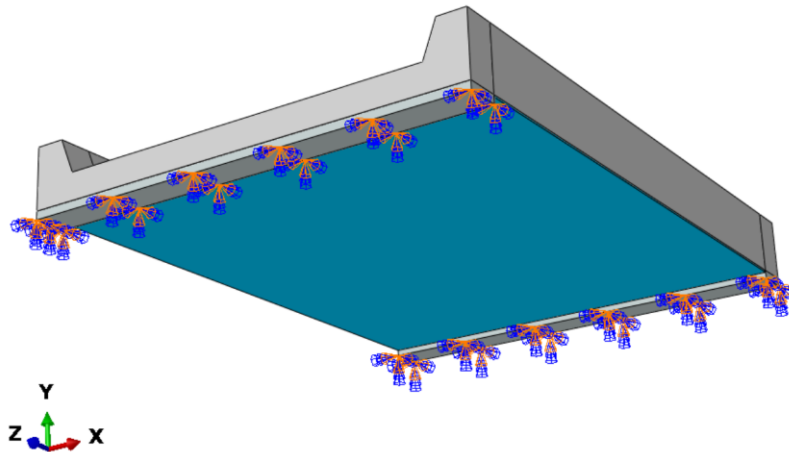
*Figure 34 - Abaqus model with 30 mm UHPC on the underside*

The UHPC layer was decided to have a thickness of 30 mm, same as for the study performed by Brühwiler et al. [1]. It will also make it more comparable to the first case (UHPC in compression zone) since the applied thickness is the same. The layer was applied over the whole bottom surface like Figure 34 illustrates.

When the UHPC is located at the tension zone of the bridge deck, it is important to get proper adhesion between the old and new concrete. Measures to secure best possible results is therefore important before applying the additional layer. Figure 35 illustrates the cross section of the bridge when it is strengthened with 30 mm UHPC in the tension zone.
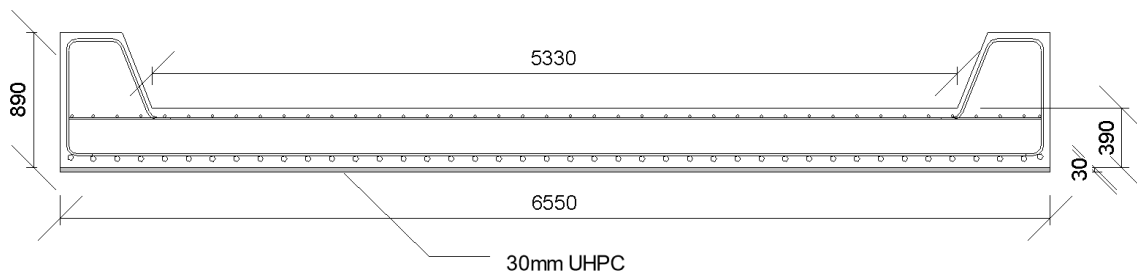


*Figure 35 - Bridge cross-section where a 30 mm UHPC overlay is applied at the underside of the bridge deck*

The reinforcement that was applied to the reference bridge model remains the same as during all the different cases. The fibers that would be included in the UHPC mix are not modelled individually or visualized in the Abaqus model, as this can be a very complex procedure. Instead, the effect of the steel fibers was considered in the UHPC material parameters. The

fibers particularly increase the tensile strength of the resulting concrete, but they also have a major influence on crack development.

The material characteristics required to simulate the UHPC were gathered from the study performed by Hashim et al. [6]. In the research, they looked at the impact of different steel fibers added to the concrete mixture with regard to the CDP theory and proposed several material parameters for UHPC. Among other types, 5D steel fibers were tested through experimental tests. This type of steel fiber has a hook on both ends and commonly has tensile strength above 2,3 MPa. The length of the fibers was 60 mm, and they had a diameter of 0,9 mm.

The input parameters used for modelling UHPC in Abaqus can be found in attachment C. This table presents all the necessary input parameters to make the model run properly with decent results, same as for the regular concrete. The concrete compression damage parameters did not show significant influence on the crack visualization compared to the tension damage parameters. This is because the bridge will take more damage in the tension zones before cracks start to develop in the compression zone. The parameters obtained in the reference study were considered as somewhat conservative for UHPC, so the results will not be as realistic as it could have been if other values were obtained. This applies especially in the case of the ultimate yield stress in concrete compressive behavior. UHPC typically has a strength of 150 MPa or more, while the reference study obtained 133,6 MPa.

### 7.5.4 50 mm UHPC in the tensile zone

To investigate if the size of the UHPC layer thickness has any effect on the flexural capacity of the bridge, a third case were implemented where the UHPC overlay on the underside was increased from 30 to 50mm. The cross-section of the case is illustrated in Figure 36.
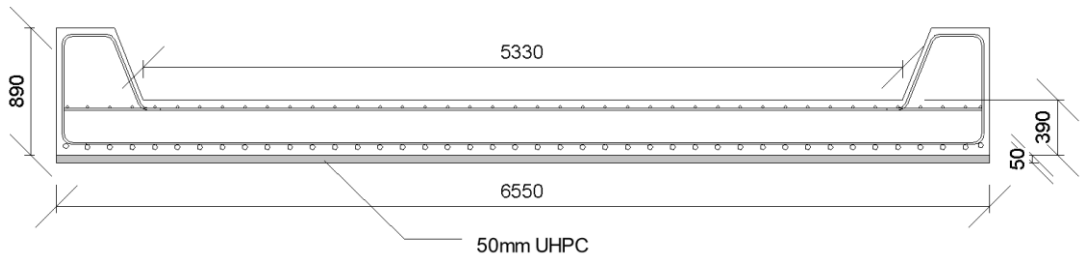


*Figure 36 - Bridge cross section where a 50 mm UHPC overlay is applied at the underside of the bridge deck*

## 7.6 Workflow in Abaqus

Some basic skills when it comes to modelling concrete structures in Abaqus were gathered from previous semester projects. However, it was highly necessary to improve the existing knowledge of Abaqus. The Abaqus theory manual and video tutorials were a helpful way to improve the skills, but the literature reviews, and support from the supervisor was also very helpful to obtain sufficient knowledge for the task. The following chapter addresses the most important steps necessary to be successful with this type of analysis in software like Abaqus.

All the different parts of the bridge, including the concrete, stirrups, and the longitudinal reinforcement, were modeled as separate parts. Using this procedure means that it will be important to achieve a good interaction between the reinforcement and the concrete. In addition, it is time-consuming to get all the bars placed correctly. The drawings provided by the Norwegian Public Roads Administration indicated how the bridge was reinforced, but some assumptions were made regarding the location of stirrups in the bridge curb.

### 7.6.1 Reinforcement

The reinforcement was modeled as 3D wire elements and both the stirrups, and the longitudinal bars were modelled as individual parts and assigned into one section each. Each bar was given a unique cross-section to make the model compared with the bridge sketches from the Norwegian Public Roads Administration.

Figure 37 illustrates how the final reinforcement looks like after all the bars have been placed correctly and with no concrete surrounding it. Because the UHPC would only be applied to the bridge deck, it was chosen to exclusively reinforce this part. This means that what occurs with the main supports isn't as significant in this case.
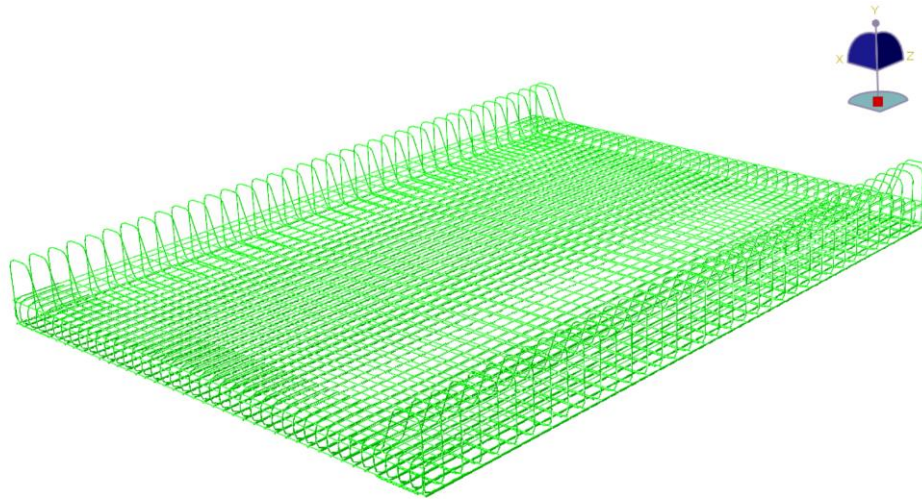
*Figure 37 - Bridge deck reinforcement from the Abaqus model*

An overview of the input parameters for the reinforcing steel used in Abaqus are given in Table 4. The steel was given a yield strength of approximately 500 MPa. A safety factor of 1,15 was also added to the yield stress for the ultimate limit state. The parameters were gathered from the general guidelines for steel reinforcement in Norway (Eurocode 2) [66]. Due to the lack of information about the current condition of the reinforcement on the Vattedal bridge, it was not looked deeply into whether the steel characteristics corresponded to reality and the validation of them, except the yield strength for undamaged steel. This means that already corroded steel was not implemented in the Abaqus model. What was considered most important in this study was that the reinforcement was considered in the analysis and that they were modelled as 3D wire elements to get a realistic behavior.

| Steel parameters | |
|---|---|
| *Elastic* | |
| Density | 7.8E-6 [kg/mm$^3$] |
| Modulus of elasticity | 210E+3 [MPa] |
| Poisson's ratio | 0.3 |
| $f_{yk}$ | 500 MPa |
| *Plastic* | |
| *Yield stress* | *Plastic strain* |
| 435 | 0 |

*Table 4 - Elastic and plastic input parameters for the reinforcing steel*

Table 5 shows the geometrical properties of the steel reinforcement in Abaqus. This includes both the longitudinal bars and stirrups in the bridge deck, and the curb stirrups.

| Rebar size | Diameter [mm] | Cross sectional area [mm$^2$] |
|:---:|:---:|:---:|
| ø10 | 10 | 78.5 |
| ø12 | 12 | 113.1 |
| ø16 | 16 | 201.1 |
| ø20 | 20 | 314.2 |

*Table 5 - Geometrical properties for the reinforcement*

### 7.6.2 Interaction

An important factor in succeeding with this type of analysis is to have the proper interaction between the reinforcement and the concrete. For this study, a constraint was added as an embedded region to obtain an adequate interaction between the reinforcing steel and the concrete. When it comes to the bond between the conventional concrete and the UHPC layer it was modelled as hard contact and the penalty method was chosen as the constraint enforcement. The contact stiffness is assumed to be linear in this case.

A tie constraint was implemented to get contact between the bridge deck and the supports. The small-sliding principle is used to model contact behavior and the part of the bridge deck resting on the supports was chosen as the master surface, while the support surface was chosen as the slave surface.

### 7.6.3 Load and boundary conditions

The load is applied as a distributed static load at the entire top surface of the bridge deck. The load has a maximum amplitude of 0,7 N/mm$^2$. A static load situation helps simplifying the modeling process and to easily simulate and compare different cases

The supports were chosen as discrete rigid. This means they cannot deform, and the reason is for the possibility to strictly look at the deformations of the bridge, not the supports. The boundary conditions were first applied as fixed on the entire surface of each end of the bridge deck without any supporters. As a result, the force needed to be increased in order to get visible fractures and appropriate deformations for comparison. After the first attempt, which was successful. The supports were added to make the bridge more realistic.

At first, the supports were modelled in full scale as fixed, but rotation was permitted in all directions. The other support was considered free, but any movements in the y and z direction were restricted. After struggling with the analysis, it was decided to reduce the size of the

supports. This helped a lot because of less elements were made in the mesh procedure. Figure 38 illustrates the model when the load and boundary conditions are added.
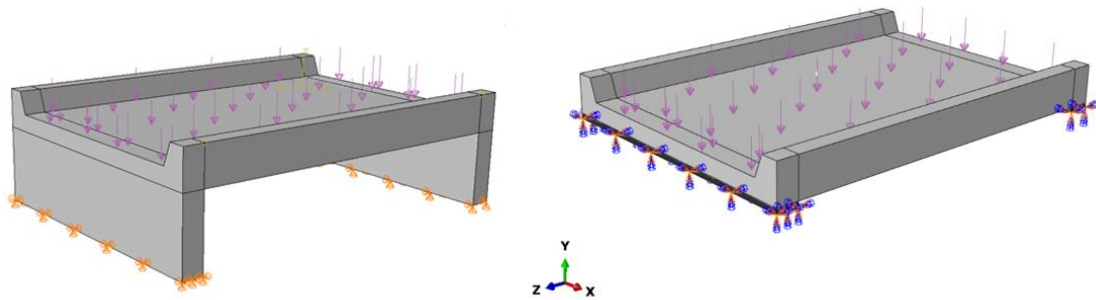


*Figure 38 - L: Reference model with full scale supports. R: Reduced supports with loads and boundary conditions*

## 7.6.4 Mesh and analysis

The mesh size plays an important role when it comes to the accuracy of the results. The size of the mesh also very often has a large impact on the analysis time. The finer the mesh is, the longer analysis time is required. Therefore, a very coarse mesh was selected in the beginning to check if everything else was running properly. This made it possible to complete the analysis in a short period of time. Changes could be made quickly, and it was possible to see if the changes were satisfying. This confirmed the model, and a finer mesh could then be selected for the final results. When choosing a finer mesh in combination with a higher load, the time of the analysis become longer. At the most, the analysis took around 7 days to complete. A fine mesh was also necessary in order to get a more precise crack visualization.

A global 8-node linear brick with reduced integration was selected as the mesh type for the entire bridge model, implying that the concrete parts all had to be assigned the same mesh size. The reason for this is that when modeling contact between the bridge deck and the supports, all components are required to be specified as independent parts. This means that the process will be simplified a lot when choosing a global mesh instead of meshing all the different parts individually. However, this will also impact the time for the analysis. Figure 39 shows the reference model when it is meshed.
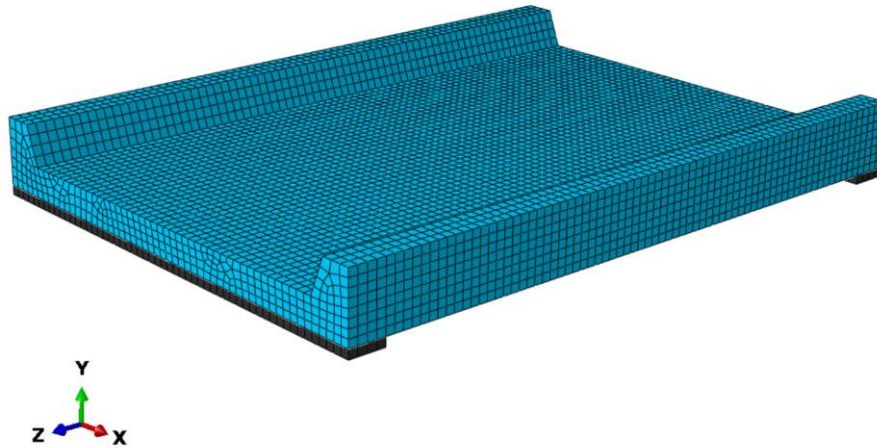
*Figure 39 - Illustration of the meshed reference model in 3D (mesh size 120)*

The number of elements and the corresponding mesh size that was created for each part is presented in Table 6. An analysis with 300 mm mesh size was first carried out at the reference model to verify that it worked properly. This was assumed to be a very coarse mesh. After trying out several mesh sizes and a mesh sensitivity analysis was conducted successfully, the appropriate mesh size was chosen to visualize the cracks in the best possible way. Both the 30 mm and the 50 mm UHPC layer obtained the same number of elements for every mesh size. The reason is that the layer is smaller than 120. It can be seen in the table that when reducing the mesh size with only 20 mm, this creates thousands of extra elements. Therefore, it was essential to find a mesh size that were fine enough to get accurate results, but at the same time optimize it to reduce time.

The reinforcement is modelled as truss element and are therefore not meshed the same way as the 3D elements. The mesh size of the reinforcement was set to 400 mm and remained the same when choosing a finer mesh for the rest of the model.

| Bridge part | Elements | Mesh size [mm] |
|---|---|---|
| Supports | 330 | 100 |
| | **220** | **120** |
| | 123 | 160 |
| | 99 | 200 |
| | 44 | 300 |
| Bridge Deck | 30420 | 100 |
| | **18825** | **120** |
| | 7840 | 160 |
| | 3588 | 200 |
| | 1550 | 300 |
| UHPC | 5280 | 100 |
| | **3685** | **120** |
| | 2050 | 160 |
| | 1320 | 200 |
| | 594 | 300 |

*Table 6 - Elements generated for each part and mesh size*

A mesh sensitivity analysis was carried out in order to find the appropriate mesh size. The analysis was executed to find the mesh that is fine enough to visualize the cracks in a sufficient way. This means that when the force-displacement curves from the different mesh sizes are closing in on each other, the results are getting more and more accurate. This can reduce the time for the analysis considerably. It is simply conducted by analyzing the bridge with a coarse mesh in the beginning, and then changing it finer and finer for each analysis until you end up with the most appropriate mesh size. Figure 40 illustrates the detail level of three mesh sizes.
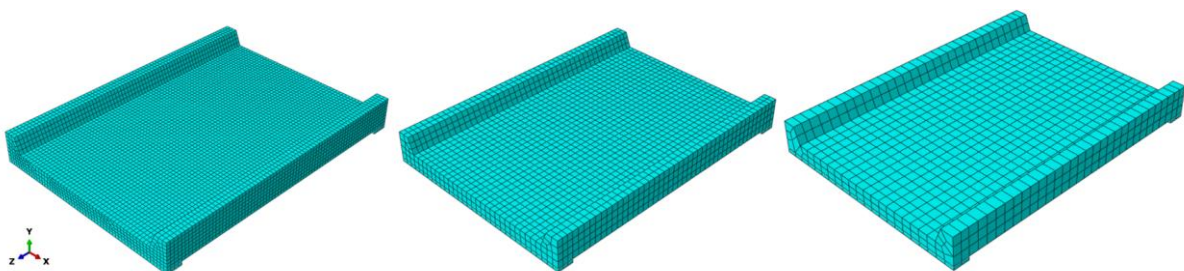


*Figure 40 - Different mesh sizes. L:120 mm, M:200 mm, R:300 mm*

The first analysis was carried out at 300 mm mesh size. It can be seen from Figure 41 that both the 300 mm and the 200 mm mesh gave the wrong behavior. It was discovered for mesh size 160 that the curve started to act different. A size of 120 mm was then chosen, and this also gave other results. At last, mesh size 100 mm were analyzed. As may be observed from Figure 41, the model with this mesh size didn't get as far as the others. This was due du the fact that this is a very fine mesh, and due to time limitations, the analysis had to be aborted. However, the graph reached far enough to see that it was very equal to 120 mm. The results were barely influenced, and the force-displacement curve were pretty much the same as for 120 mm. Therefore, a 120 mm mesh size was chosen for the rest of the analyses, since the extra 20 mm did not have a large influence on the results. By implementing the mesh sensitivity analysis, it was possible to keep the amount of time used on the analyses to a minimum with as accurate results as necessary.
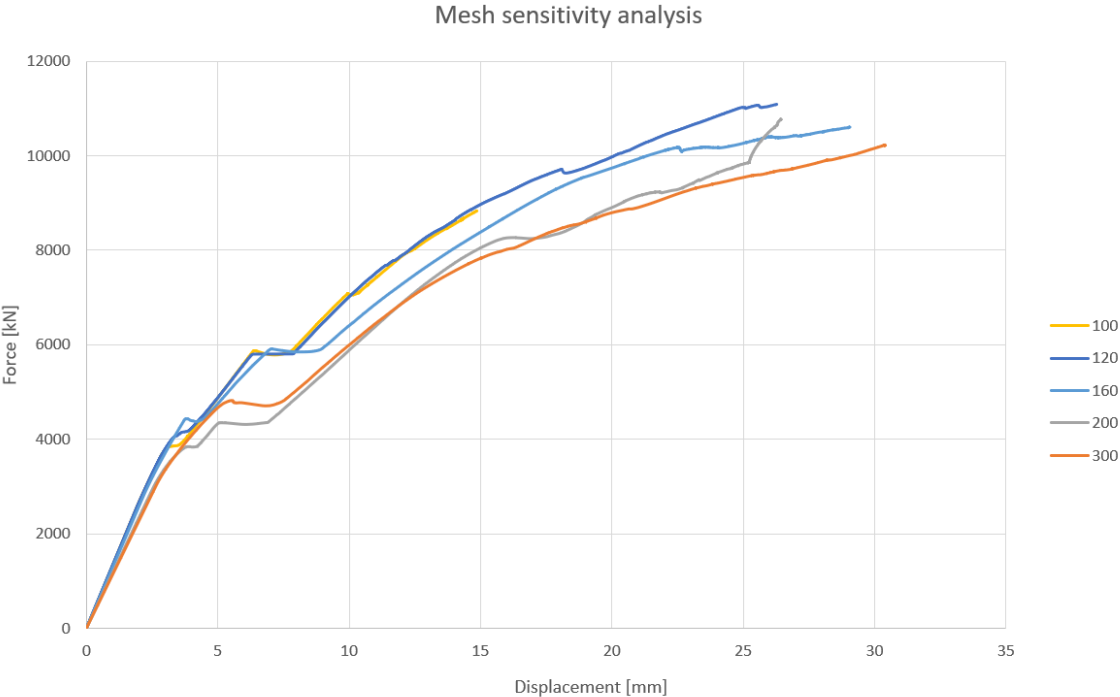


*Figure 41 - Mesh sensitivity analysis*

For the analysis, a static simulation was chosen as it was assumed to give sufficient accuracy in the results. There are also several other reasons why this type of analysis is suitable for this case particularly. A static analysis can be performed if the structure does not depend on time,

and the loads are constant. However, in a dynamic analysis, the load might change with time. It is not necessary to run a dynamic analysis since the research only addresses strengthening of the bridge, and that the problem can be solved through a static analysis. This implies that the program only assumes a stiffness matrix, while a dynamic analysis also includes a mass matrix and a damping matrix [62, 67].

The model incorporates the backward Euler method. In Abaqus, this is usually applied in combination with the damage plasticity model. For the equilibrium iterations, a material Jacobian that is consistent with this integration operator is applied [62].

## 7.7  Model updating

Modal updating is a process where the parameters of a finite element model is adjusted so that the predictions in terms of eigenvalues and eigenvectors correspond with measurements collected from modal testing [68]. Model updating results in having more optimal material properties, which validates the finite element model for further analysis.

### 7.7.1  Modal analysis

Modal analysis can be used to determine the natural frequencies and the corresponding mode shapes of a structure. It has become a major technique for improving and optimizing the dynamic characteristics of structures. The two main modal analysis techniques are experimental modal analysis (EMA) and operational modal analysis (OMA). A hammer or other vibration device is used in the EMA technique to collect the structure's reaction and excitation. However, the EMA approach has shown to be impractical when the costs of providing effective excitation to some major civil structures become too expensive [69].

### 7.7.2  Operational modal analysis (OMA)

Wind and traffic are dynamic loads that most civil engineering structures, such as bridges and buildings, are exposed to. The input of these impacts cannot be defined exactly because they are not directly measurable. Vibrating massive structures with a shaker or impact hammer, on the other hand, is an extremely expensive and complex procedure. For these reasons, researchers decided to determine the structure's properties by focusing only on the structural response of the system regardless of the input loads. Operational modal analysis (OMA) is therefore, a popular method among civil engineers for estimating the dynamic

characteristics of a structure based entirely on the output response [70]. OMA can therefore be used to find the natural frequencies, mode shapes and the damping ratio of a structure. The method can be divided into time domain and frequency domain approaches. The last one is utilized in this study.

Frequency domain decomposition (FDD) is categorized as one of the frequency domain approaches. The method was introduced by Brincker et al. [71] and includes determining a sequence of single degree of freedom systems as various responses for various structural modes.


### 7.7.3  Bridge assessment with Unquake OMAway sensors

To get the predicted material parameters in the FE-model to correspond with the real bridge, cyclographic sensors from Unquake were installed. Normally it is enough to assume the parameters based on theoretical research, and then predict the behavior in a FE-model with reliable results. However, several factors such as the age of the bridge, damages, existing cracks, and corrosion are often hard to predict. For older bridges it is especially difficult to know what mixtures, composition, and reinforcement are used. Therefore, it is very beneficial to install sensors on the bridges that can measure the natural frequencies. The sensors will provide information about the modal parameters, which later can be used to update the FE-model to make it correspond to the experimental behavior. This will lead to more realistic and reliable results and is a proper way to control the deformations, stresses, and strains in the bridge.

The sensors that are used are Unquake OMAway. These sensors perform Operational Modal Analysis for vibration and earthquake monitoring. Unquake OMAway (Earlier called Unquake Suite) is a type of software that allows the customer to conduct Operational Modal Analysis. This enables synchronization of the Unquake Accelerographs measurements. The program also performs frequency domain decomposition (FDD) for a specified session and calculate the modal characteristics of a structure under assessment. Furthermore, it also has the ability to determine the natural frequencies for single or multiple combined cyclograph measurements by fast Fourier transformation (FFT), providing Fourier transform amplitudes [72].

*Figure 42 - Unquake OMAway sensor mounted on the Vattedal bridge*

The sensors can be used with 12V connection or simply by using a powerful power bank. Figure 42 above, show an accelerograph sensor while being connected to a datalogger and a power bank. The sensor can be seen mounted on the roadway, while the datalogger is located at the top of the curb. The GPS is external and are placed on top of the datalogger.

The datalogger is where the configurations are saved and where the data is stored. It is made of stainless steel, is waterproof, and can therefore handle quite harsh environments. The datalogger must be mounted or placed on a flat surface to prevent distortion of the results. To store the data, it is used a SD card. To read the results, the software Unquake OMAway is needed. This belongs to the same manufacturer. The sensor, also called accelerometer, is a 3-axis MEMS digital accelerometer suitable for applications like Structural Health Monitoring application, where accurate results is required. When placing the sensor, the Z-axis should not be used as the main axis. This is due to disturbances and sensitivity to bad power quality in this direction [72].

Each sensor was connected to a GPS which later can be used to adjust the time period so that the results are obtained within the same time period. This is necessary because all the sensors

cannot start tracking at the same time. The time records obtained by GPS synchronization measurement can be used to coordinate several instruments and perform various modal data analyses [72]. Each system was also connected a 20 000 mAh power bank to make sure that they had enough power throughout the time they were installed. Figure 43 illustrates one of the sensors attached to the roadway.



*Figure 43 - Close-up illustration of one of the sensors attached to the steel plate*

It was essential to process the results using the associated software once the sensors had been removed. The measured frequencies from the accelerograph sensors were transferred and visualized using Unquake OMAway. Accelerograph session logs were merged into a single file and moved to a new directory location. The operational modal analysis took place in this new location. The OMA step only works properly for sampling rates of 250 Hz. It turned out that three out of six sensors had the wrong sampling rate during the measurements. At the time of the installation process, this was an unknown issue. Also, for one of the remaining sensors with the correct frequency the SD-card did not work properly, implying that the software only was able to read the data from 2 out of 6 sensors. Figure 44 illustrates sensor 4, 5 and 6 and all of these had issues and could not be used for further analysis. The two sensors that had the right sampling rate was sensor 2 and 3. Since sensor 2 was located at the mid-span of the bridge and sensor 3 was located at the support, there was still possible to get some frequencies out of the measurements. Therefore, the OMA was still conducted with an awareness that the results may not be as reliable as desired.
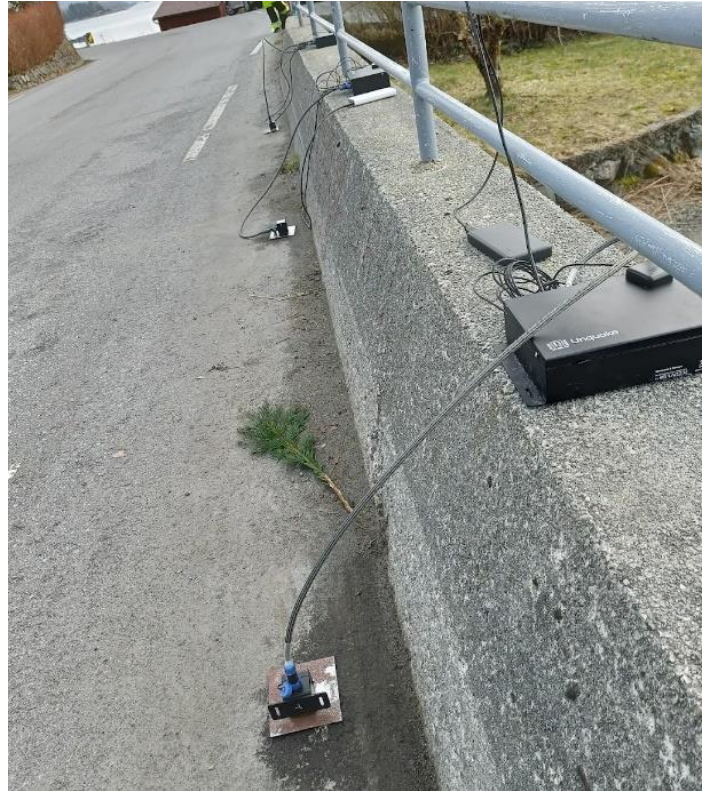
*Figure 44 - South-west illustration of three of the non-working sensors installed at the Vattedal bridge*

### 7.7.4 Sensor strategy

The sensors were intended as a supplement in order to validate the FE-model in Abaqus. However, the work required to get the most out of it, which included preparing the equipment, installing the sensors, and processing the result was a more complex procedure than what was first anticipated. Firstly, a thorough understanding of the mechanics and an accessory overview was conducted. All the equipment also had to be checked for defects and all the SD-cards had to be empty. After accounting for all of the equipment, the total number of sensors that could be used was 6. This was assumed to be a sufficient number of sensors for the bridge that would be assessed.

The OMAway sensors operate within a 3D-coordinate system consisting of global and local axis. Each sensor should, therefore, ideally be placed in different angles. The reason for this is that it is only focused on the sensors x and y direction, but angle variation is needed to cover all directions in the bridge's global axis. This implies both x, y, and z-axis for the bridge. Table 7 shows which direction each of the sensors cover in the global system. Take for instance sensor 1, this sensors x-axis covers the global z-axis, and the y-axis covers the global x-axis. It should be noted that the manufacturer does not recommend using the z-axis as a

complimentary axis in three-dimensional test instances, or as a major axis in two-dimensional measurements. This is due to the fact that it has a greater amount of electrical noise and is more sensitive to poor power quality.

| Sensor | Global X | Global Y | Global Z |
|--------|----------|----------|----------|
| 1 | Y | Z | X |
| 2 | Z | Y | X |
| 3 | X | Y | Z |
| 4 | Z | Y | X |
| 5 | Y | X | Z |
| 6 | Y | Z | X |

*Table 7 - Corresponding sensor axis to the global coordinate system*

The sensor is subsequently installed with a strong magnet on a specific steel plate and orientated appropriately according to the installer's judgment. Near the bridge curbs, the steel plates were installed directly on the asphalt as illustrated in Figure 44. To ensure appropriate adhesion between the asphalt and the plates, the asphalt was first moistened before a glue was applied beneath the plates. The steel plates already had some deformable caulks at one side and the glue was applied on top of this layer.

The sensors were mounted in a certain order to get the best possible results from the measurements. After recommendations from the manufacturer and other conducted experiments, the sensors are not installed equally on each side, specifically to cover most of the bridge. The sensors were installed like Figure 45 illustrates.

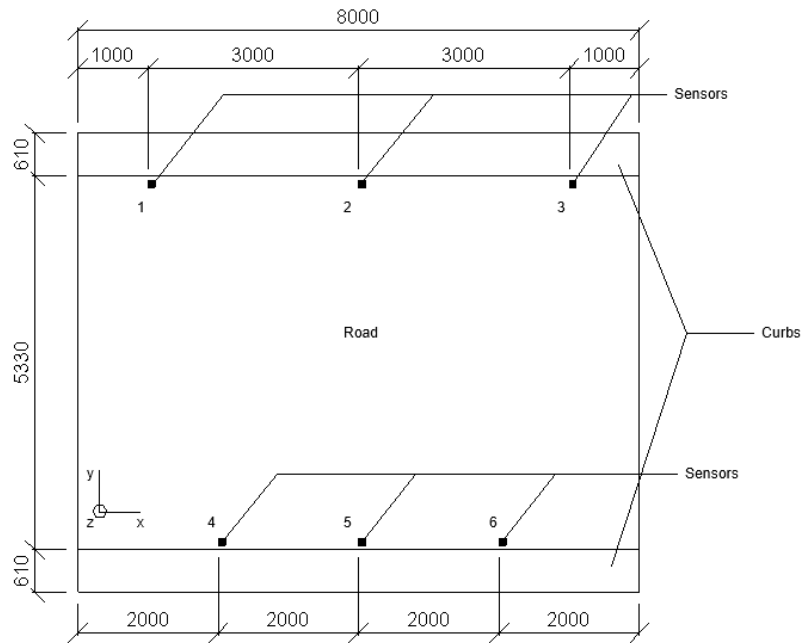*Figure 45 - Sensor placement developed in Revit*

After the manufacturer's advice, the sensors should be installed for at least 6-8 hours. Unfortunately, after about 4.5 hours of measuring it started to rain. Since some of the dataloggers and cables had damages and missing screws from earlier use, it was decided to dismantle the sensors at this point in order to avoid any additional complications.

# 8   Results and discussion

This thesis bases the results on the development and the comparison of force- displacement curves and cracks development. The section also presents the results from the OMA on the Vattedal bridge.

## 8.1   Results from model updating

The reference model was updated through operational modal analysis (OMA). Since some of the sensors were not working properly, the results were affected by this. Anyway, an adjustment in the modulus of elasticity was performed based on the obtained frequencies. After digging more into the results from the OMA it was observed that for sensor 2, which is located close to the mid-span of the bridge, there were some frequencies in the horizontal sensor axes, when traffic passed. The results from sensor 2 in the horizontal direction using the FFT method have been presented in Figure 46. Blue is local y (same as global y) and orange is local z (representing global x).
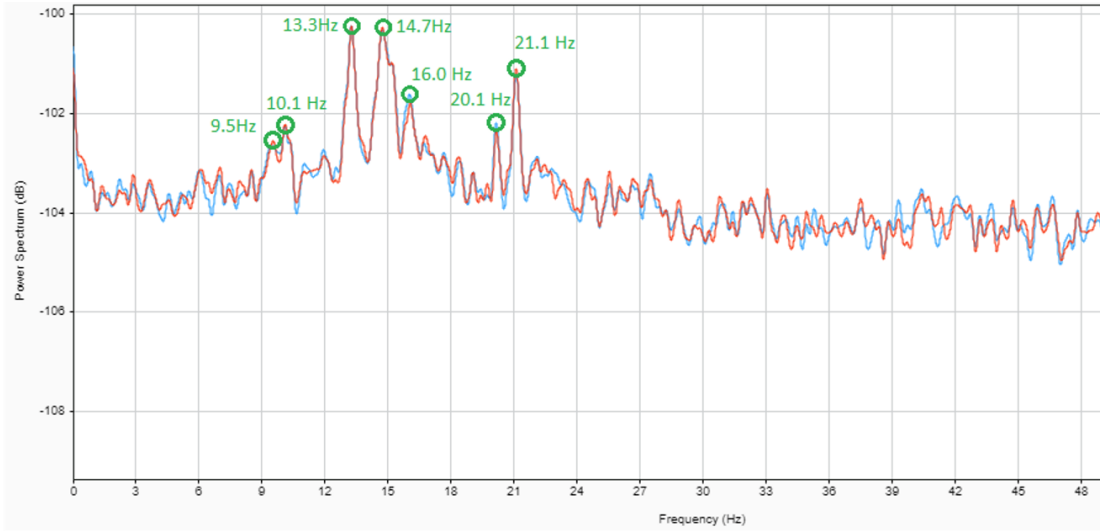


*Figure 46 - Results from FFT for sensor 2 in horizontal direction*

After the modal analysis was conducted, the first step was to compare and check if any of these frequencies existed in the Abaqus model. The best scenario would be to have a corresponding mode for each frequency in order to ensure that it is a validated model itself and what kind of DoF it activates. However, due to the misconfiguration of some sensors, there were only two sensors working satisfactorily. Regarding those two, only ~15Hz was derived through the OMA procedure. The other frequencies illustrated in Table 8 are

combined for both the working sensors and also include non-ambient vibrations like those coming from live loads as traffic and electricity noise.

| Mode | Eigenfrequency |
|------|---------------|
| Mode 1 | 14.7 |
| Mode 2 | 15.5 |
| Mode 3 | 16.03 |
| Mode 4 | 17.16 |
| Mode 5 | 17.6 |

*Table 8 - Modal frequencies obtained by OMA*

The results obtained from the FDD method of modal extraction have been presented in Figure 47. It must be noted that the program tries to keep the lowest amplitude vibrations to a minimum by restricting them to the ambient vibrations principle. High values to the left are noise coming from electrical equipment and traffic and cannot be considered within the frequency range.



*Figure 47 - Frequency domain composition (FDD) results from Unquake*

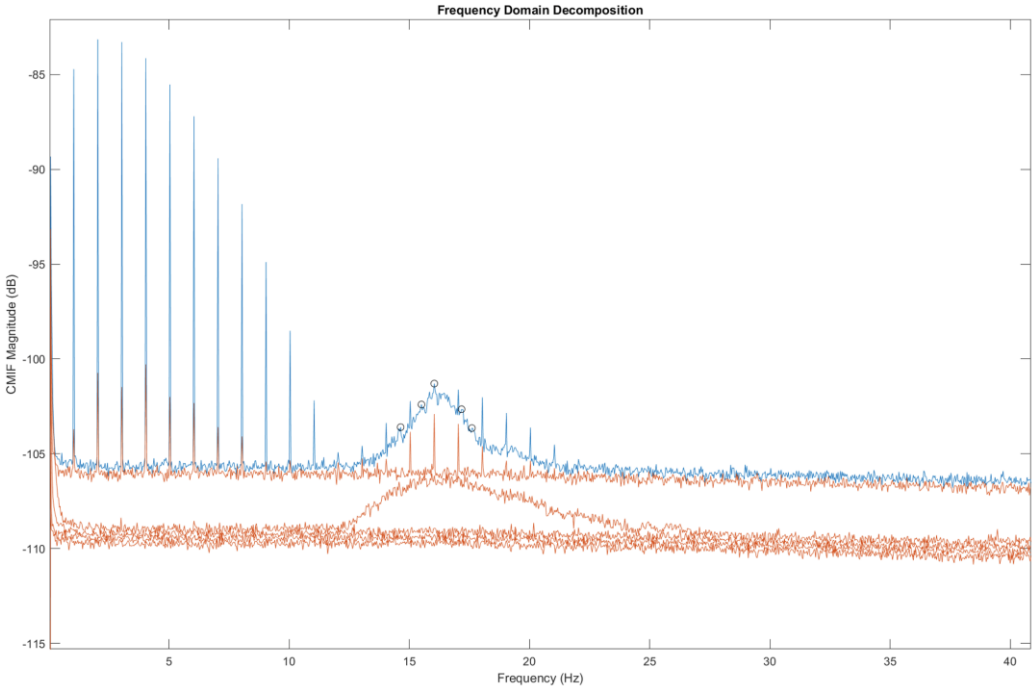It was discovered that the degrees of freedom that were active were parallel to gravity, except mode 3 (16.03 Hz), which also indicates a longitudinal DoF activation. The order of channels defined is the following: U1-x, U1-y, U1-z, U4-x, U4-y, U4-z. Before the Abaqus model was

updated, the existing frequencies were extracted by modal analysis in Abaqus. Those can be seen in Table 9.

| Mode | Eigenfrequency |
|---|---|
| Mode 1 | 10.725 |
| Mode 2 | 11.875 |
| Mode 3 | 13.239 |
| Mode 4 | 13.741 |
| Mode 5 | 14.124 |

*Table 9 - Modal frequencies for initial model, $E_c$ = 30000/$E_s$=200000*

The obtained natural frequencies obtained by modal analysis in Abaqus were low compared to those obtained from the experimental OMA. Therefore, the modulus of elasticity was gradually increased to move the model frequencies towards the experimental ones. Eurocode 2 suggests an E-module of 35 GPa for B40 concrete [66], so the values were moved toward this. By increasing the E-module to 37 GPa for the concrete ($E_c$) and to 210 GPa for the reinforcement ($E_s$), two of the same frequencies were achieved as obtained in the OMA. The 5 frequencies from the OMA varied between 14.7 and 17.6; therefore, this was the frequency rate chosen for the modal analysis in Abaqus. The resulting eigenfrequencies after changing the E-module can be seen in Table 10.

| Mode | Eigenfrequency |
|---|---|
| Mode 1 | 11.849 |
| Mode 2 | 13.150 |
| Mode 3 | 14.6 |
| Mode 4 | 15.202 |
| Mode 5 | 15.5 |

*Table 10 - Updated modal frequencies, $E_c$ = 37000/$E_s$=210000*

The mode shapes within the same frequency range as the OMA gave was plotted in Abaqus when the modulus of elasticity was updated. The two frequencies that corresponded with the ones in the OMA were, respectively mode 3 (14.6 Hz) and mode 5 (15.5 Hz). Although having the correct mode shape for each frequency would be ideal, increasing the elasticity of the materials, meaning a stiffer bridge, produces a more realistic model than what was initially designed. The 5 mode shapes corresponding to the eigenfrequencies in Table 10 can be seen in Figure 48 and 49.
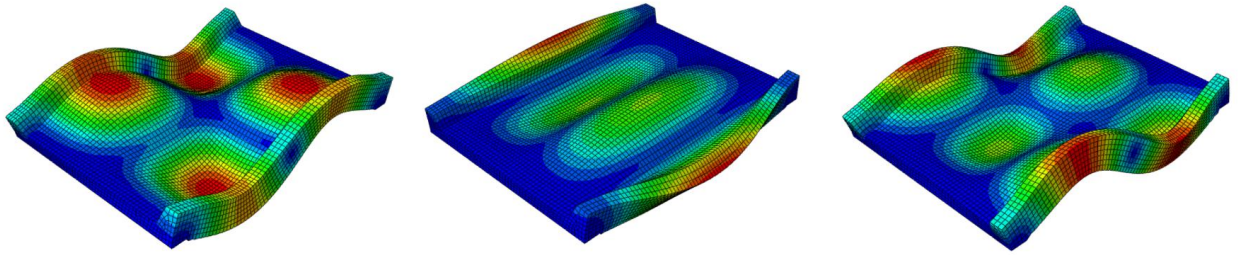
*Figure 48 - Mode shapes from Abaqus model. L: Mode 1, M: Mode 2, R: mode 4*

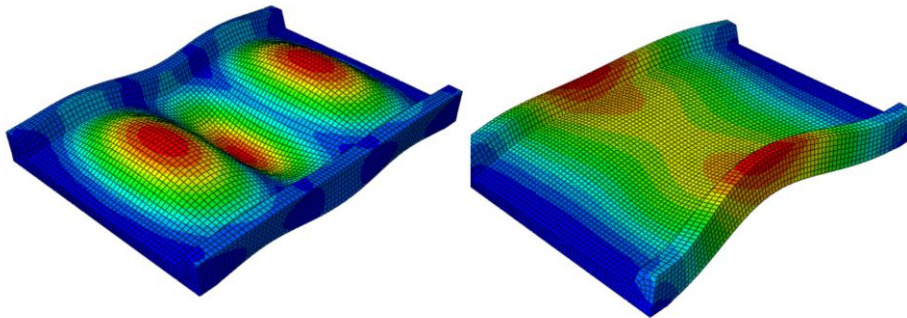Mode shape 3 and 5 corresponded to the experimental frequencies.



*Figure 49 - Corresponding mode shapes from experimental frequencies. L: Mode 3 and R: Mode 5*

## 8.2 Reference model

The reference model was analyzed and assessed several times to obtain the best possible results. After the process of model updating, the results obtained are presented underneath. The bridge acts as expected from a reinforced concrete bridge. The main purpose of these results is to be able to compare it to the strengthened bridge cases later on.

### 8.2.1 Force and displacement

The force-displacement curve for the reference model is illustrated in Figure 50. The graph illustrates the displacement at the mid-span and the total force applied on top of the bridge deck. Notice that this load is the total load on the top surface of the bridge, and not a distributed load pr $m^2$ or $mm^2$.
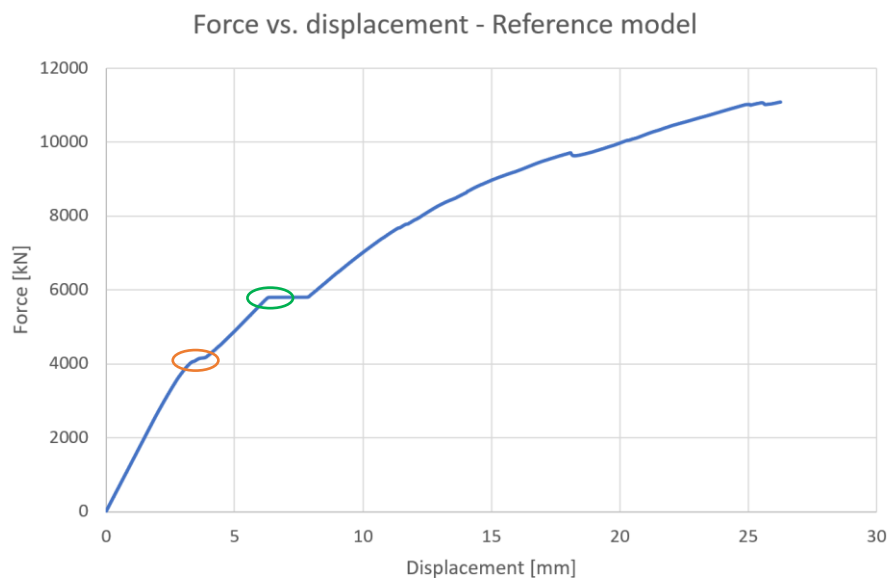


*Figure 50 - Force-displacement curve for the reference model*

It is observed from the figure that the bridge acts linear until 3,3 mm of displacement. At this point, marked by the orange circle, the first cracks appear on the upper side of the bridge. A resulting force of 4000 kN is applied before the first cracks appear on the upper side of the bridge deck. The green circle represents the first cracks on the underside of the bridge deck. This happens after a displacement of 6,3 mm and 5700 kN of the applied load. This crack can be seen in Figure 52 under crack development.

An illustration and visualization of the magnitude of the displacement are developed to be able to compare the results from the initial model to the strengthened cases. Figure 51

illustrates the displacement for the reference model. As expected, the largest deformation arises in the center of the bridge. The table to the left in the figure show that the deformation is 26,8 mm in the red circle. For this case the applied load is 11000 kN.
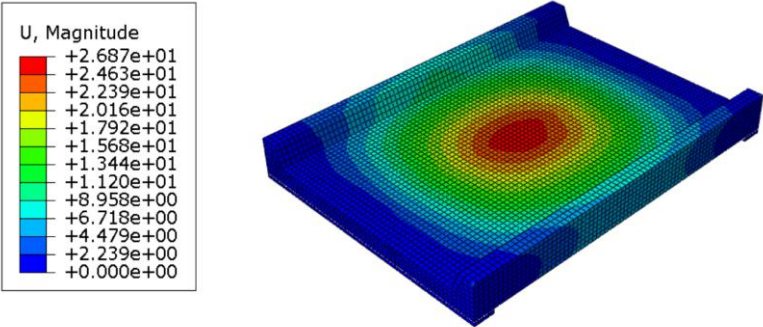


*Figure 51 - 3D illustration of max displacement for the reference model [mm]*

## 8.2.2  Crack development

To be able to compare the crack development with the strengthened cases, two different load instances are chosen, and these are the same for all the comparisons. Respectively at 7000 kN and 10500 kN. The reason for choosing these instances is because it gives a proper basis for the comparisons with the strengthened cases. At 7000 kN, crack propagation has started to develop on the tensile side. 10500 kN is near the maximum load applied to the reference model, and it is interesting to see the development of cracks for the strengthened cases at these instances. The results will be easily comparable by using these load instances. The crack propagation in the tensile zone is shown in Figure 52.
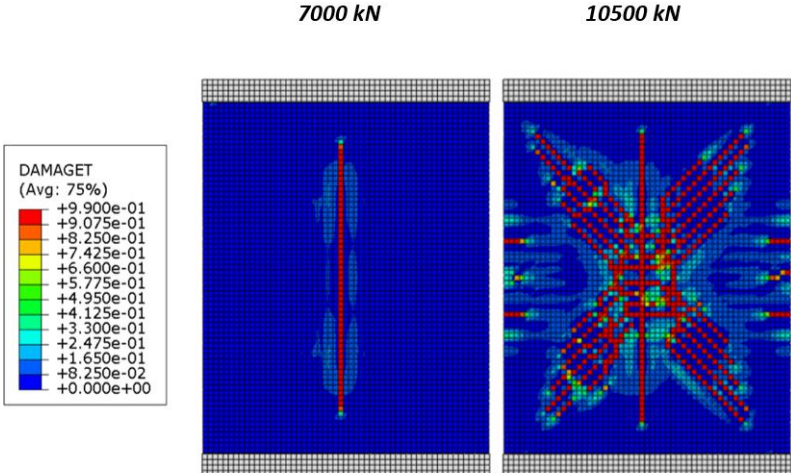


*Figure 52 - Crack development at two different load instances for the reference model*

As earlier presented in the theory, the concrete cracking is related to the stiffness damage factor, $d_t$. This represents the tensile damage factor and can vary between 0 and 1. A value of 0 means no damage at all, while 1 means fully damaged. This means that when a red dot or line appears in the model, it represents a crack or a damaged spot.

It is mainly focused on the crack propagation in the tension zone. The crack propagation in the tension zone for the two different load instances was extracted. The first load instance, 7000 kN, shows the reference model slightly after the first sign of cracking concrete on the tensile side. At this load, approximately 10 mm of displacement has occurred at the center of the bridge. It is visible at Figure 52 that the crack appears at the center of the bridge and moves in the longitudinal direction.

The last load instance, 10500 kN, show a massively increase in crack development. At this stage, the displacement has reached 22,3 mm at the middle. Multiple cracks appear near the mid-span of the bridge, with diagonal cracks towards the edges and corners. This occurs due to high principal stresses. With a closer look, it is possible to perceive the cracks near the center of each longitudinal side as well. What is not shown in the figures are the cracks on the upper side of the bridge. These cracks appear near the supports and develop along with the supports in the entire width of the bridge. With the max applied load of approximately 11000 kN, the deformation gets nearly 27 mm. With a longer and more accurate (finer mesh) analysis, the crack development could have been even more detailed, and a fully damaged bridge could have been visualized.

## 8.3   30 mm UHPC in the compression zone

This section presents the results from the 1$^{st}$ strengthening case where 30 mm UHPC was applied at the top of the bridge deck.

### 8.3.1   Force and displacement

The obtained force-displacement curve when 30 mm UHPC layer is applied at the top of the bridge deck is illustrated in Figure 53. The curve shows similar behavior to the reference model. It acts linear until 3,5 mm displacement, which occurs after 5100 kN of the applied load. At the first bend in the graph, cracks on the upper side of the bridge deck appear. At the second bend, the first cracks appear on the underside of the bridge deck. At this point the total load has reached 6900 kN. Due to some technical problems with Abaqus the analysis was aborted due to license/ inactivity after 4 days. Therefore, the graph does not reach as far as the reference model.
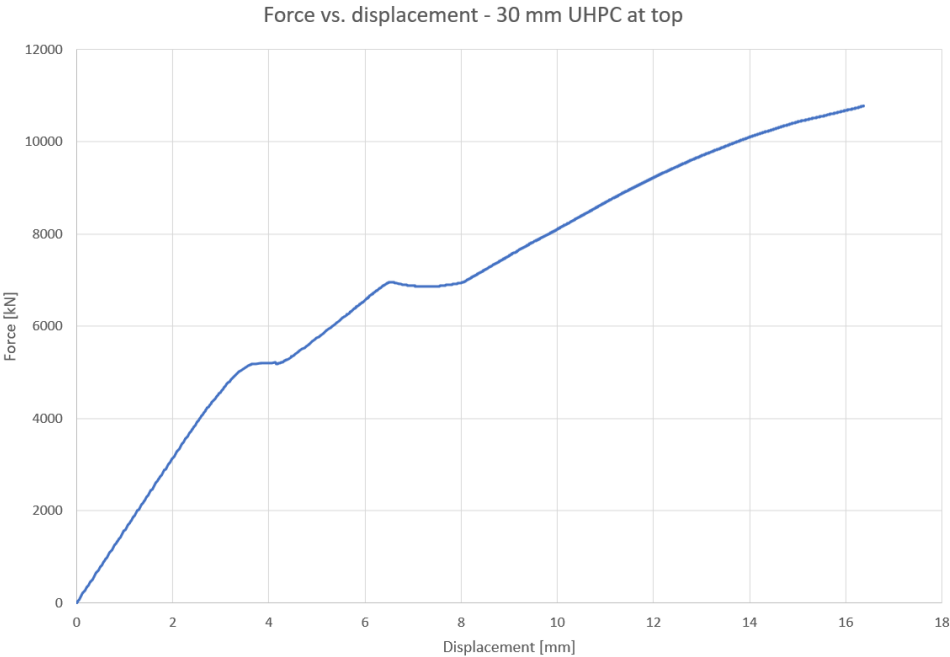


*Figure 53 - Force-displacement curve for the bridge strengthened with 30 mm UHPC on top*

An illustration and visualization of the displacement is shown in Figure 54. It illustrates the displacement for the 30 mm UHPC overlay in the compression zone model. As expected, the largest deformation arises in the center of the bridge. The color scheme presented to the left of the bridge deck show that the deformation is 16 mm in the center. At this instance, the applied load is 10700 kN.
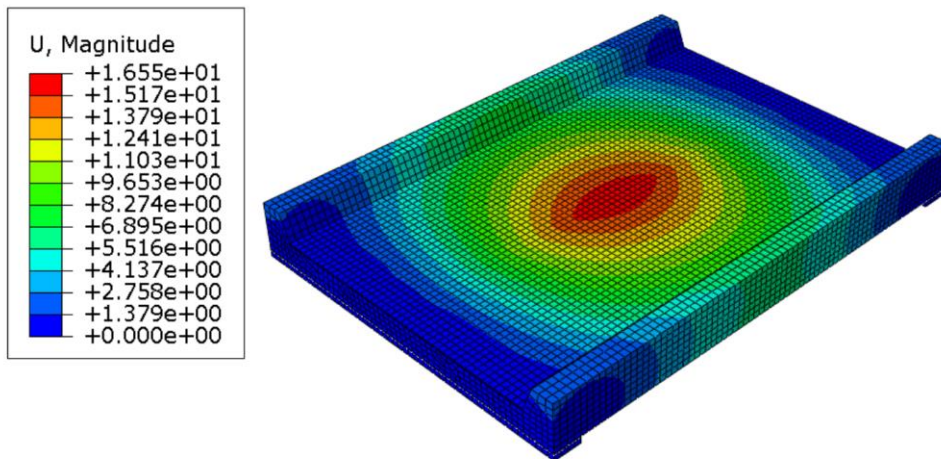
*Figure 54 - 3D illustration of max displacement for the bridge strengthened with 30 mm UHPC on top [mm]*

### 8.3.2 Crack development

The crack development in the tensile zone when a 30 mm UHPC layer is applied at the top of the bridge deck is illustrated in Figure 55. The first load instance, 7000 kN, shows the first sign of cracking concrete on the tensile side. This happens after 8,1 mm displacement at the center of the bridge. It is observed that the crack appears at the center of the bridge and moves in the longitudinal direction.
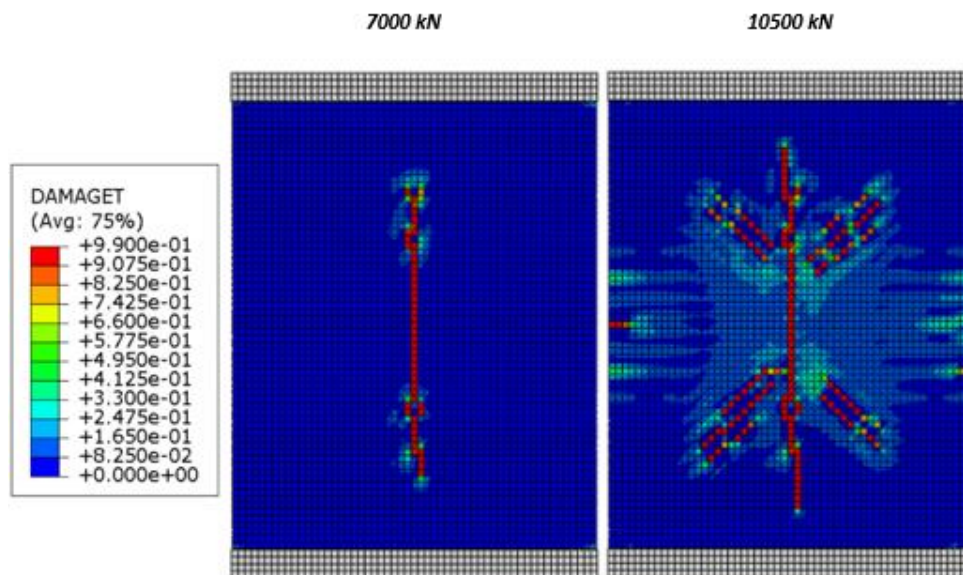


*Figure 55 - Crack development at two different load instances for the bridge strengthened with 30 mm UHPC on top*

The second load instance shows an increase in crack propagation. At this stage the applied load has reached 10500 kN, and the displacement are 15,3 mm at the middle. Multiple cracks appear near the mid-span of the bridge, with diagonal cracks towards the edges and corners. The diagonal cracks develop slightly unequal on each side of the center. This may be due to small asymmetries in the distribution of reinforcement. A slight development of cracks appears near the center of longitudinal sides. This can be seen as bright green cracks on the figure. The damage and cracks on the upper side of the bridge deck is not illustrated. These cracks appear near the supports, same as for the reference model.

## 8.4   30 mm UHPC in the tensile zone

This section presents the results from the FE-model where the bridge was strengthened with a 30 mm UHPC layer in the tension zone. Some problems occurred for this case when visualizing cracks as it didn't act symmetrical. It was discovered that by changing the mesh procedure, more symmetric crack propagation was obtained. The mesh size used for the visualization was 150 mm. However, since it was earlier discovered that a mesh size of 160 mm didn't gave as accurate results as wanted, the 150 mm meshed model was only used for visualizing cracks.

### 8.4.1   Force and displacement

The force-displacement curve is illustrated in Figure 56. The graph illustrates the displacement at the mid-span and the total force applied on top of the bridge deck.



*Figure 56 - Force-displacement curve for the bridge strengthened with 30 mm UHPC on the bottom*

The presented graph indicates that the bridge reaches out of its linear phase at 4150 kN. At this point, the first sign of damage occurs on the upper side near the supports and the displacement at the mid-span is 3 mm. The deformations are getting larger after this, and it starts acting more non-linear. The second peak indicates cracking in the tension zone and occurs when the force reaches 8150 kN and a displacement of 8,2 mm.

The analysis reaches a maximum force of 12850 kN. Figure 57 shows the deformations at this point. The color scheme to the left in the figure shows that the deformation is approximately 26,3 mm at the midspan of the bridge when the maximum load is reached.

*Figure 57 - 3D illustration of max displacement for 30 mm UHPC on the bottom [mm]*

## 8.4.2  Crack development

The development of cracks for the model strengthened with 30 mm UHPC in the tensile zone can be seen in Figure 58. The UHPC overlay in the tensile zone were hidden in the visualization to easier be able to compare the crack propagation with the reference model.
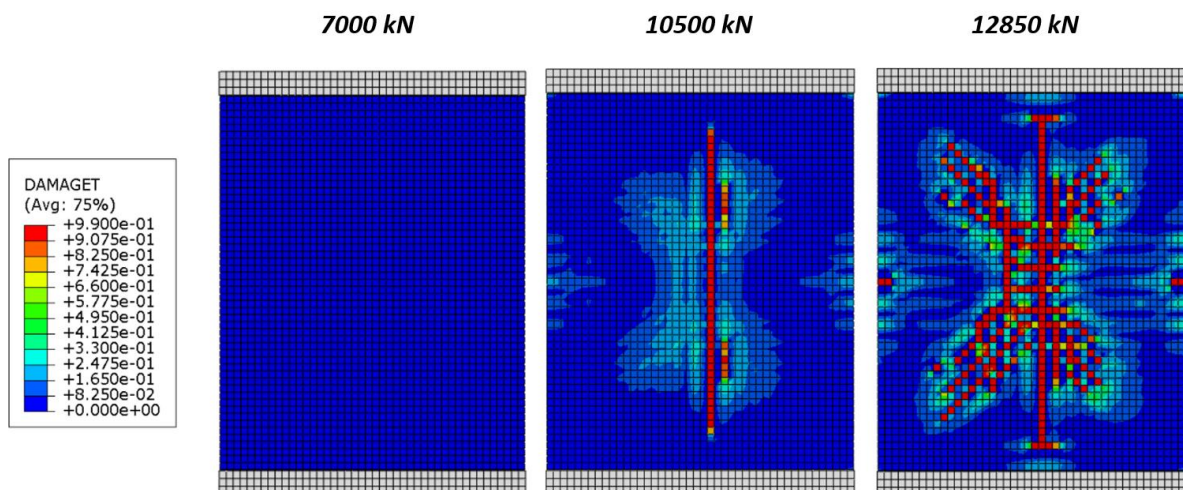


*Figure 58 - Crack development at three different load instances for 30 mm UHPC on the bottom*

The development of cracks in tension for three different load instances were extracted. No visible cracks are observed on the underside at 7000 kN. When the force reaches 10500 kN, there are visible signs of crack propagation in the longitudinal direction. At this point, cracks have also started to develop on the sides. The last load instance shows the cracks at maximum load, 12850 kN. When it reaches this load, the bridge has obtained a displacement of 26,3 mm and is the largest deformation for this analysis.  At this point, the high principal stresses cause oblique crack propagation. The visualization of the cracks is taken from the model with mesh size of 150. This is due to asymmetries in the crack propagation for the initial model.

## 8.5   50 mm UHPC in tensile zone

This section presents the results from the FE-model where the bridge was strengthened with a 50 mm UHPC layer in the tension zone.

### 8.5.1   Force and displacement

The force-displacement curve is illustrated in Figure 59. The graph illustrates the displacement at the mid-span and the total force applied on top of the bridge deck.
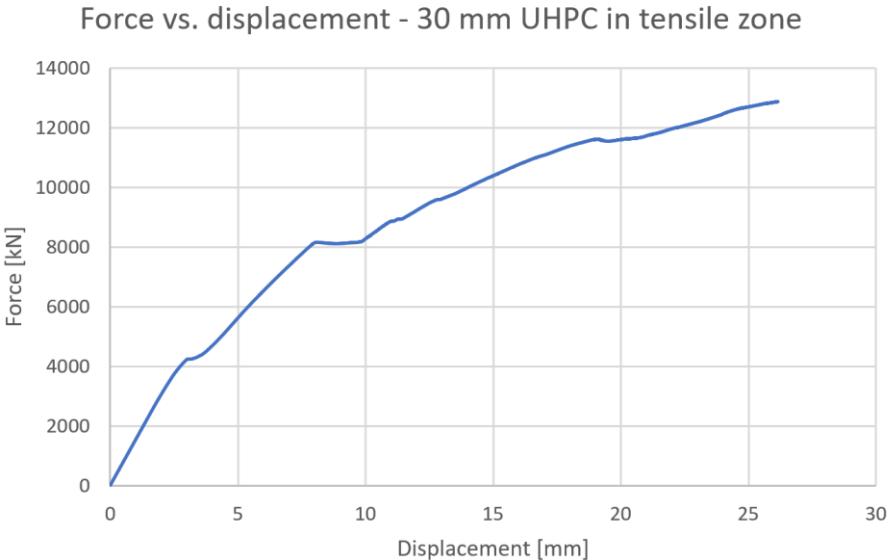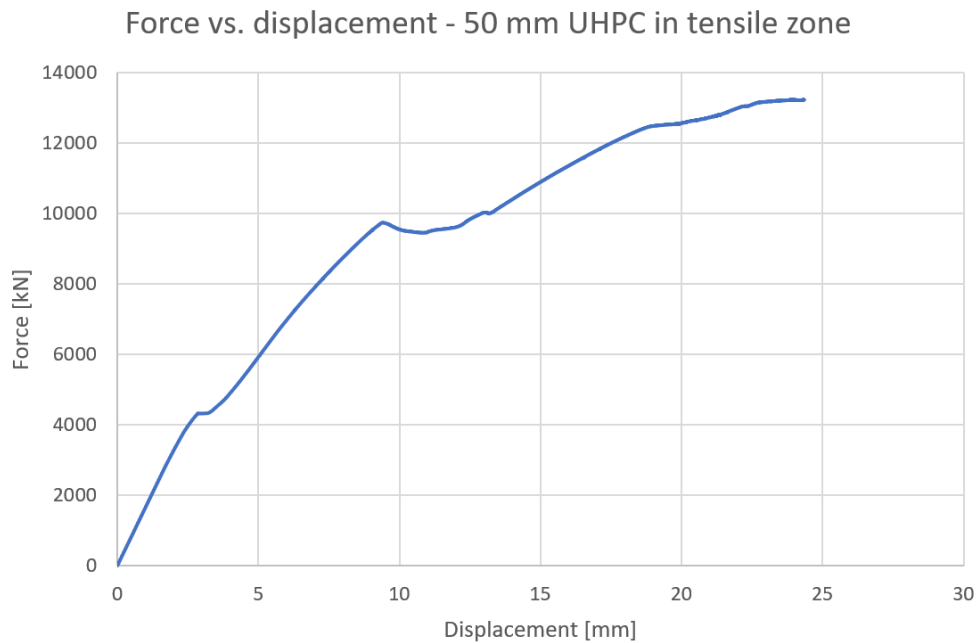


*Figure 59 - Force-displacement curve for the bridge strengthened with 50 mm UHPC on the bottom*

The graph shows that the first sign of damage occurs at 4200 mm when the displacement at the mid-span has reached 3 mm. The concrete starts acting non-linear at this point, and the deformations are increasing.

Same as for the other models, it was observed from the FE-model that the first peak indicates the first sign of cracks in the compression zone, while the second peak that occurs at 9700 kN indicates that the bridge cracks in the tensile zone. The bridge shows its first signs of cracking in the tensile zone at a displacement of 9,6 mm.

The analysis reaches a maximum force of around 13200 kN. Figure 60 shows the deformations at this point. The color scheme to the left in the figure shows that the deformation is approximately 24,6 mm at the midspan of the bridge at the maximum applied load.
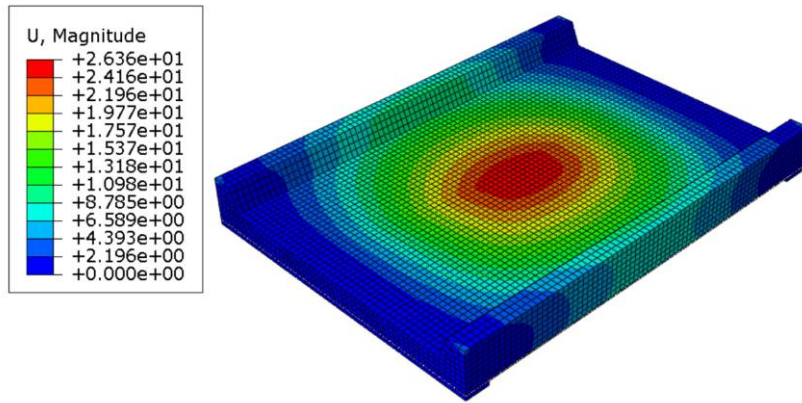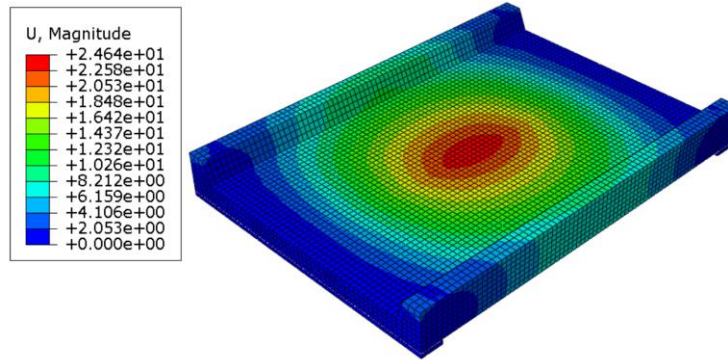
*Figure 60 - 3D illustration of max displacement for 50 mm UHPC on the bottom [mm]*

## 8.5.2 Crack development

The same procedure as previous cases were followed to obtain the results from the crack analysis for the beam bridge strengthened with 50 mm UHPC in the tension zone. The development of cracks for this model can be seen in Figure 61. Same as for the case with 30 mm UHPC in the tensile zone, the UHPC is hidden in the visualization.
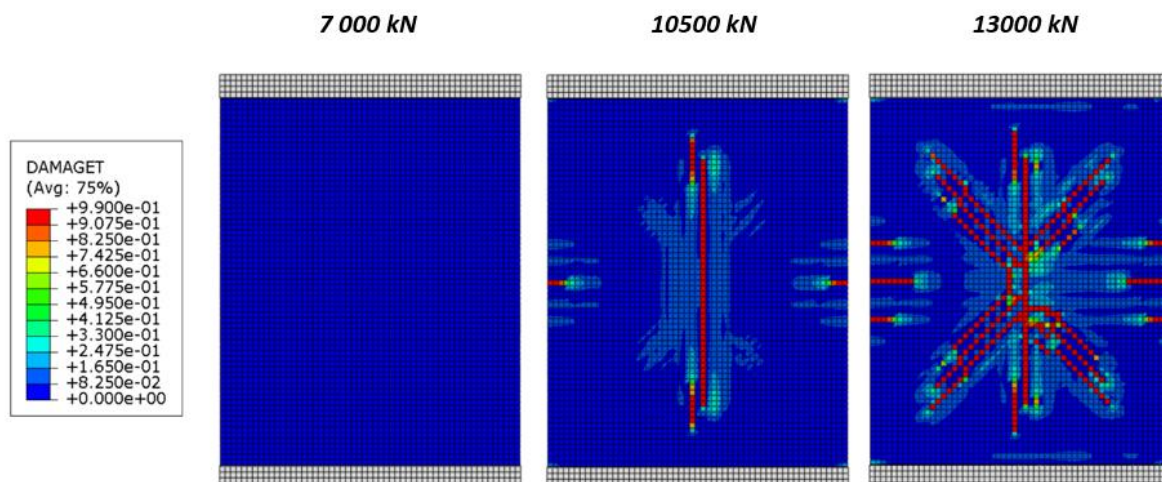


*Figure 61 - Crack development at three different load instances for 50 mm UHPC on the bottom*

The crack propagation in the tension zone for three different load instances was extracted. When the applied force has reached 7000 kN, there is still no signs of damage in the tension zone. When the force reaches 10500 kN, there are visible signs of crack propagation in the longitudinal direction and on the sides. The last load instance illustrates how the cracks have developed when it reaches 13000 kN. When it reaches this load, the bridge has obtained a displacement of 24,6 mm and is the largest deformation for this analysis. At this point, the high principal stresses cause oblique crack propagation towards the corners.

## 8.6 Comparison

Several UHPC configurations have been tested in order to find the most effective in terms of flexural strength. When comparing the force-displacement curves, it is observed that all the different models exhibit similar behavior until around 1500 kN. As expected, the reference model shows poor flexural behavior compared to the strengthened models. The comparison of force-displacement curves can be seen in Figure 62. All of the cases show somewhat similar behavior. The first peak at the force-displacement curves shows the initial cracks on the top of the bridge deck, while the second peak shows the initial cracks on the bottom. The two cases with 30 mm UHPC, on top and bottom, behave similarly after the initial cracks have occurred on the tensile side. The displacement is almost identical for the same load after the cracking.
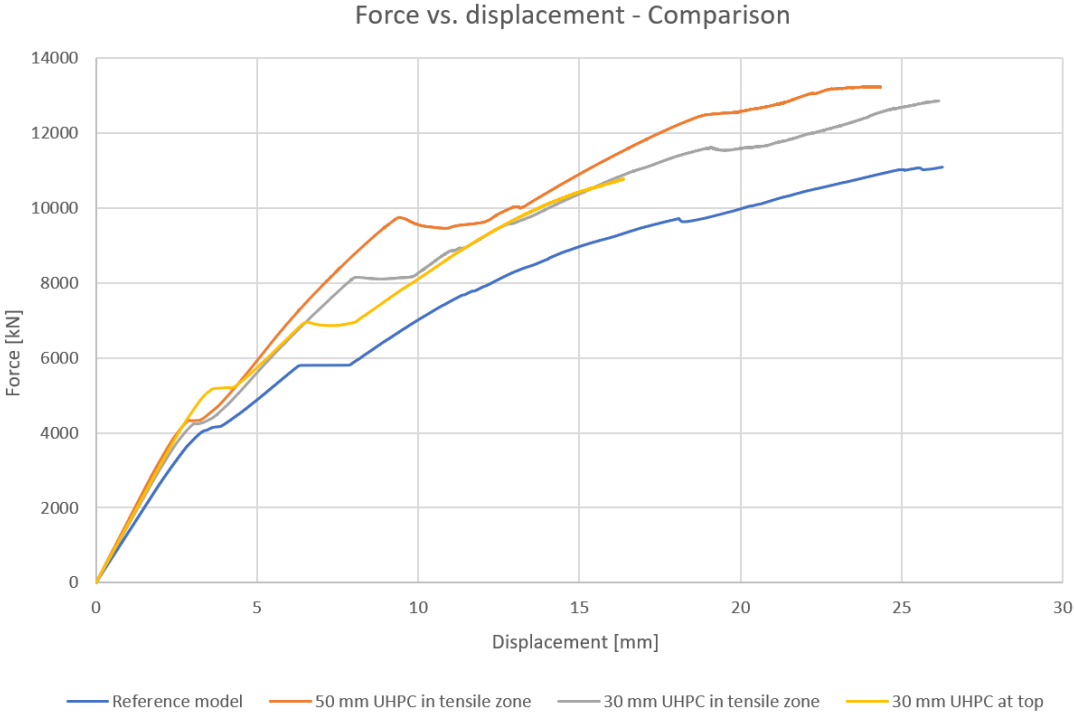


*Figure 62 - Comparison of force-displacement curves*

It was observed from the force-displacement curves that the bridge strengthened with 50 mm UHPC in the tensile zone shows the best improvement in terms of load capacity. However, when looking at the initial stage, the model strengthened with 30 mm at the top of the bridge deck has a longer linear phase than the other models. The UHPC layer at the top has as expected great influence on the cracking at the top. However, this model is the one that first takes damage in the tension zone.

Since all the models reach 10500 kN, it was chosen to compare the displacement at this point. It can be seen in Figure 62 that the model strengthened with 50 mm UHPC in the tensile zone has the smallest deformation at this point, while the reference model has the largest. The reason for this could be because it is more likely that the tensile capacity of the fibers in the UHPC are utilized, when UHPC is applied in the tensile zone.

The comparison of the different UHPC configurations is shown in Table 11. It is observed that the displacement of the bridge is a lot smaller for all the different strengthening cases. The top and bottom configurations with 30 mm improve the displacement very equally. At 10500 kN the displacements are exactly the same, 15,3 mm. However, the difference is in the cracking force at the top and bottom. The analysis has different max applied loads due to the duration. Some of the cases did not reach as far as the others.

| Comparison | Force [kN] | Displacement [mm] | Cracking Force top [kN] | Cracking Force bottom [kN] | Max load applied [kN] |
|---|---|---|---|---|---|
| Reference model | 10500 | 22.3 | 4000 | 5700 | 11000 |
| UHPC top (30mm) | 10500 | 15.3 | 5100 | 6900 | 10800 |
| UHPC bottom (30mm) | 10500 | 15.3 | 4150 | 8150 | 12850 |
| UHPC bottom (50mm) | 10500 | 14.2 | 4200 | 9700 | 13200 |

*Table 11 - Comparison of the different UHPC configurations*

Table 12 summarizes the improvements of the different UHPC configurations.

| Improvement | Displacement [mm] | Cracking Force top [kN] | Cracking Force bottom [kN] |
|---|---|---|---|
| Reference model | - | - | - |
| UHPC top (30mm) | 31.4% | 27.5% | 21% |
| UHPC bottom (30mm) | 31.4% | 3.75% | 43% |
| UHPC bottom (50mm) | 36.3% | 5% | 70.1% |

*Table 12 - Improvements of the different UHPC configurations*

As mentioned above, there are large differences in the improvement in crack development at the top and the bottom. The strengthening case with 30 mm UHPC at the top improves the crack distribution at the top drastically, with 27,5%. It also significantly improves the crack distribution at the bottom, with 21%. Compared to the configuration with 30 mm UHPC at the bottom, which has 3,75% and 43% improvement on the cracking force at top and bottom, respectively. The same trend can be seen when the UHPC layer is 50 mm. This indicates that the overall performance will be significantly improved by applying UHPC, either top or bottom. The biggest difference is that with UHPC on top it will be more evenly distributed improvement of the crack development on the top and bottom, while UHPC at the bottom will improve the crack development at the tensile side a lot more than the compression side.

## 8.7   Discussion

It was found time-consuming and difficult to model a whole bridge, and each element of it in 3D. Even though it's a relatively simple structure. For analysis of such bridges in Abaqus, more simplification should be made in order for the process to be beneficial in a real-case scenario. It is very hard to make the steel reinforcement correct when modelling it in 3D. A lot of time and investigation were spent making this correct. Other FEM software could also be considered where defining all material parameters manually is not necessary. This will make the modelling process a lot easier and time-saving. In Abaqus, all the material properties and plastic behavior have to be defined manually. As a result, a lot of effort was put into this part.

After the assessment that SVV did in Autumn 2021, the bridge was assumed reinforced with Ø22 instead of Ø20, and it was therefore concluded that the bridge did not need to be strengthened after all. However, for the purpose of the research, it was assumed that the bridge was reinforced with Ø20 and therefore had to be strengthened. It was anyway desirable from SVV that research regarding UHPC as strengthening was conducted, as it can be beneficial for future cases.

The availability of studies that investigates UHPC characteristics were found to be very limited. Therefore, the final sample of the research was small and a study with fairly conservative values had to be used. However, some changes were made in discussion with the supervisors

to get a more normal UHPC behavior. For instance, the modulus of elasticity for UHPC was changed from 35 GPa to 44 GPa, as the first value seems way too low.

The asphalt on top of the bridge is not considered in the model or the analysis. When the UHPC layer is applied to the top of the bridge deck, it is designed to be placed beneath the asphalt and in combination with the existing concrete. The asphalt may have some influence on the crack propagation on top.

Problems occurred during the modal assessment. The model could have been more accurate if more than two sensors worked properly with the right configurations. The existing cracks and conditions of the bridge were not accounted for in the analysis but should be conducted if applying UHPC. This is both too time and resource-consuming for this type of study but would be an interesting point of view in future work. The results from the frequency analysis in Abaqus gave eigenfrequencies and mode shapes. This resulted in modal parameters for the model updating.

Since there has been a problem with cracks on the underside of the bridge deck, it was chosen to investigate the effect of the UHPC overlay thickness in the tensile zone. It was first tested with 30 mm (same as at the top) and then 50 mm. It turned out that the effect of adding 20 mm extra UHPC on the underside had high influence on the cracking force in the tensile zone and also on the deflection at high loads. This was a surprising outcome since higher thickness also leads to higher dead weight on the bridge.

To be able to compare the crack development, it was necessary to apply unnaturally large loads, so that the deformation in the bridge was big enough to get crack development. The analysis does not consider environmental impact, such as chloride ingress, alkali-silica reactions, corrosion, or others. An evenly distributed load was applied on top of the bridge deck, while the most realistic load on the bridge will be from a moving vehicle. This will give dynamic point loads. The bridge will, therefore, most likely be able to handle less force with this type of loading. Due to time and resources, this was not looked into. The analysis with 30 mm UHPC on top did not exceed as far as the other cases. It stopped at an applied load of 10800 kN. However, the results were sufficient enough to use in this case.

The crack propagation from the strengthening case with 30 mm UHPC in the tensile zone with 120 mesh size were not symmetrical. Three different analyzes with this strengthening case

were attempted, all with the same result. The same model was used for the 50 mm UHPC case without this symmetry problem. One thing that was considered was to divide the bridge in half, and only simulate one side of the bridge, and assume symmetry from these results. Lack of time is the reason this was not conducted. Instead, it was chosen to break down the analysis and do it over again with a new mesh. Mesh size of 300 and 200 were first conducted to see if the results were getting symmetrical with the new approach. Due to time limitation, it was only possible to run the final analysis with mesh size of 150. That is the reason for the different mesh size in the visualization.

# 9 Conclusion and future work

Through FEM analysis in Abaqus and literature study, results regarding the structural response of the Vattedal bridge strengthened with different UHPC configurations are obtained. Same as for the Swiss study performed by Brühwiler et al. presented earlier, the Vattedal bridge will be significantly strengthened by applying UHPC overlays, both at top and bottom. In the presented results, the case with 50 mm UHPC on the underside of the bridge improved the structural performance of the bridge the most.

It has been observed that applying UHPC in the bridge's tensile zone has small influence on the crack propagation at the top of the bridge deck. This means that it will be essential what condition the bridge is in when applying UHPC. If the bridge needs strengthening and there are signs of crack development at the top of the bridge deck, UHPC should be applied at the top to prevent further crack development. By looking at displacement, the behavior of the case with UHPC on top and the case with UHPC on the bottom are almost identical after cracking has occurred on the tensile side. This indicates that the flexural improvement is very similar if the UHPC is applied at the top or the bottom.

The UHPC overlays improved the structural performance, but it also reduced the amount of crack propagation significantly. Since the development of cracks is reduced, it will protect the structure from environmental impacts such as alkali-silica reactions, corrosion, and chloride ingress. Because UHPC has nearly ten times as good resistance against corrosion than normal concrete, it will improve the corrosion resistance due to the unique properties of UHPC. As a result, damages due to environmental impact is significantly reduced compared to using conventional concrete.

To get the best possible result from the strengthening, a proper bonding between the existing concrete and the UHPC are crucial. Measures such as removal of damaged concrete, sandblasting, and bonding with epoxy can be important. The extent of these measures must be considered for each strengthening case. It is important that the bridge is well prepared so that the service life will be as long as possible. This will greatly impact the final results of the eventual physical strengthening.

The FEM model of the Vattedal bridge was validated through operational modal analysis and model updating. The results gathered from the bridge assessment gave the natural

frequencies that were used to validate the model through operational modal analysis. The natural frequencies in the original model were extracted and moved towards the experimental values. This gave the FE-model a more realistic behavior. Implementing this part in the analysis made the results more reliable and realistic.

Through the work with this thesis, knowledge about concrete bridges, and strengthening with ultra-high performance concrete has been conducted. The outcomes support the idea that UHPC might become the new standard for concrete structure rehabilitation and repair in the future. The construction industry is always improving, and new constructions are becoming highly advanced. Concrete might be a more desirable material for complex structures where UHPC can utilize its unique strength and durability features. Architects and consultants may therefore find it to be a highly recommended material for the future.

## 9.1   Future work

It would be interesting to invest more time and resources in this study in the future. There are lots of things that can be investigated further. The analysis in Abaqus could have been conducted with even finer mesh, different loading cases, and more UHPC configurations.  The finer mesh would make the results more detailed. More realistic results could have been obtained with dynamic loadings, such as vehicle loads. This would require a lot of time, since each analysis in this study lasted up to one week. By executing this, it would be possible to compare differences from this study and how much the bridge is strengthened even more detailed.

Another interesting investigation for future research would be to check whether UHPC can have the same strengthening on other structural elements. The structure investigated in the presented study is just a simple concrete bridge with a short span. For instance, it would be interesting to look at different bridge types, different materials, and load instances. Strengthening with the use of UHPC at loadbearing walls, floors, columns, and steel bridges would also be very relevant. It could also be relevant to address and compare different types of steel fibers.

As mentioned earlier, the bridge assessment with Unquake sensors was not optimally conducted. Therefore, it would be appropriate to conduct this type of assessment over again with more than only two working sensors. Therefore, this study can be a helpful tool for

further investigation in modal updating and learning from the mistakes made here and improving them. The equipment should be thoroughly checked; make sure that all the SD-cards are functioning, cables are working correctly, the sensors are operating within the right sampling rate, and that the glue on the steel plates has appropriately hardened before leaving. The assessment duration should also have been extended from 5 hours to approximately 10 hours to make sure that the results are sufficient.

To perform calculations regarding bridge classification upgrade from BkT8 to Bk10/60 could be a proper way to continue this research. It would be interesting to see if the bridge could be upgraded to Bk10/60 by executing this UHPC strengthening.

Experimental testing of a full or intermediate scale beam is also relevant for future research. This would give realistic results on how effective the different UHPC strengthening configurations analyzed in this thesis would be. It is then possible to compare the practical and theoretical results, and how closely related these results would be.

# References

[1]     E. Brühwiler, E. Denarié, and K. Habel, "Ultra-high performance fibre reinforced concrete for advanced rehabilitation of bridges," in *Proceedings (eds GL Balasz & A. Borosnyoi), fib-Symposium, Budapest*, 2005, pp. 951-956.

[2]     Y. Zhu, Y. Zhang, H. H. Hussein, and G. Chen, "Flexural strengthening of reinforced concrete beams or slabs using ultra-high performance concrete (UHPC): A state of the art review," *Engineering Structures,* vol. 205, p. 110035, 2020/02/15/ 2020, doi: https://doi.org/10.1016/j.engstruct.2019.110035.

[3]     I.-Y. Koo and S.-G. Hong, "Strengthening RC columns with ultra high performance concrete," in *2016 Structures Congress*, 2016.

[4]     M. Shafieifar, M. Farzad, and A. Azizinamini, "Experimental and numerical study on mechanical properties of Ultra High Performance Concrete (UHPC)," *Construction and Building Materials,* vol. 156, pp. 402-411, 2017/12/15/ 2017, doi: https://doi.org/10.1016/j.conbuildmat.2017.08.170.

[5]     M. Hafezolghorani Esfahani, F. Hejazi, R. Vaghei, M. Jaafar, and K. Karimzadeh, "Simplified Damage Plasticity Model for Concrete," *Structural Engineering International,* vol. 27, pp. 68-78, 02/01 2017, doi: 10.2749/101686616X1081.

[6]     D. T. Hashim, F. Hejazi, and V. Y. Lei, "Simplified Constitutive and Damage Plasticity Models for UHPFRC with Different Types of Fiber," *International Journal of Concrete Structures and Materials,* vol. 14, no. 1, pp. 1-21, 2020.

[7]     "What is UHPC? – Part 1: Birth of UHPC," ed: RDConcrete.

[8]     M. L. Bjørnar Degnes, "Numerical analysis of an existing concrete beam strengthened with UHPC overlays," Oslo, 2021.

[9]     M. A. Bajaber and I. Y. Hakeem, "UHPC evolution, development, and utilization in construction: a review," *Journal of Materials Research and Technology,* vol. 10, pp. 1058-1074, 2021/01/01/ 2021, doi: https://doi.org/10.1016/j.jmrt.2020.12.051.

[10]    PortlandCementAssociation, "Ultra High Performance Concrete," ed. Cement.org, 2019.

[11]    "The First North Amercian Broad Based Structural Design Guide on UHPC," ACI, 2016.

[12]    U. Solutions, "What is Ultra High performing concrete," ed, 2018.

[13]    J. Kozlowski, "e.construct.US LLC completed a peer review of a new sustainable EASSCM ultra-high-performance concrete (UHPC) mix from AEEE Capital Holding & Advisory Group," ed, 2021.

[14]    Cement.org, "Ultra-High Performance Concrete," ed.

[15]    S. Abbas, M. L. Nehdi, and M. A. Saleem, "Ultra-High Performance Concrete: Mechanical Performance, Durability, Sustainability and Implementation Challenges," *International Journal of Concrete Structures and Materials,* vol. 10, no. 3, pp. 271-295, 2016/09/01 2016, doi: 10.1007/s40069-016-0157-4.

[16]    G. ChunPing, "Ultrahigh performance concrete–properties, applications and perspectives," Science China, Nanjing, 2015.

[17] E. N. John Lawler, "Advances in Ultra-high Performance Concrete," ed: Wiss Janney Elstner Associates, 2019.

[18] M. Zhou, W. Lu, J. Song, and G. C. Lee, "Application of Ultra-High Performance Concrete in bridge engineering," *Construction and Building Materials,* vol. 186, pp. 1256-1267, 2018/10/20/ 2018, doi: https://doi.org/10.1016/j.conbuildmat.2018.08.036.

[19] A. Joshaghani, M. A. Moeini, M. Balapour, and A. Moazenian, "Effects of supplementary cementitious materials on mechanical and durability properties of high-performance non-shrinking grout (HPNSG)," *Journal of Sustainable Cement-Based Materials,* vol. 7, no. 1, pp. 38-56, 2018/01/02 2018, doi: 10.1080/21650373.2017.1372318.

[20] E. Fehling, H. Baltzer, and N. Janberg, *Ultra-high performance concrete UHPC : fundamentals, design, examples*, 5th ed. Berlin, Germany: Ernst & Sohn, 2014.

[21] O. Mishra and S. P. Singh, "An overview of microstructural and material properties of ultra-high-performance concrete," *Journal of Sustainable Cement-Based Materials,* vol. 8, no. 2, pp. 97-143, 2019/03/04 2019, doi: 10.1080/21650373.2018.1564398.

[22] Y. Shao, K. L. Tich, S. B. Boaro, and S. L. Billington, "Impact of fiber distribution and cyclic loading on the bond behavior of steel-reinforced UHPC," *Cement and Concrete Composites,* vol. 126, p. 104338, 2022/02/01/ 2022, doi: https://doi.org/10.1016/j.cemconcomp.2021.104338.

[23] B. A. Graybeal, "Material Property Characterization of Ultra-High Performance Concrete," (in English), Tech Report 2006. [Online]. Available: https://rosap.ntl.bts.gov/view/dot/38714.

[24] FHWA, "Ultra-High Performance Concrete: A State-Of-The-Art Report for The Bridge Community," ed. FHWA, 2013.

[25] J. Ma, M. Orgass, F. Dehn, D. Schmidt, and N. Tue, *Comparative Investigations on UltraHigh Performance Concrete with and without Coarse Aggregates*. 2004.

[26] A. Alsalman, C. N. Dang, G. S. Prinz, and W. M. Hale, "Evaluation of modulus of elasticity of ultra-high performance concrete," *Construction and Building Materials,* vol. 153, pp. 918-928, 2017/10/30/ 2017, doi: https://doi.org/10.1016/j.conbuildmat.2017.07.158.

[27] H. Belyadi, E. Fathi, and F. Belyadi, "Chapter Thirteen - Rock mechanical properties and in situ stresses," in *Hydraulic Fracturing in Unconventional Reservoirs (Second Edition)*: Gulf Professional Publishing, 2019, pp. 215-231.

[28] Z. B. Haber, I. De la Varga, B. A. Graybeal, B. Nakashoji, and R. El-Helou, "Properties and Behavior of UHPC-Class Materials," (in English), Tech Report 2018. [Online]. Available: https://rosap.ntl.bts.gov/view/dot/37528.

[29] T. A. Birkedal, V. P. Hovland, and V. V. Netland, "Bestandighetsstudie av Ultra-High Performance Concrete (UHPC) : En forskning om påvirkningen av rissvidde, overdekning og eksponeringsmiljø med hensyn på betongens beskyttelsesevne mot armeringskorrosjon," University of Agder, 2020.

[30] F. H. Administration, "UHPC: A Robust Solution for Highway Infrastructure," ed: United States Department of Transportation, 2019.

[31]    J. Walraven, "The development of high performance concrete: From an academic hobby to an appreciated component in the tool box of structural engineers," 2016.

[32]    NPCA, "UHPC: Performance on High," ed. precast.org, 2016.

[33]    FHWA, "Improving bridge preservation with UHPC," in *Public Roads - Winter 2021*, ed. Federal Higway Administration, 2021.

[34]    M. C. Pierre Y. Blais, "Precast, Prestressed Pedestrian Bridge World's First Reactive Powder Concrete Structure," *PCI,* vol. 44, no. 5, p. 71, 1999.

[35]    S. A. Paschalis, "Strengthening of existing reinforced concrete structures using ultra high performance fiber reinforced concrete," University of Brighton, 2017.

[36]    Y.-F. Wu, T. Liu, and D. J. Oehlers, "Fundamental principles that govern retrofitting of reinforced concrete columns by steel and FRP jacketing," *Advances in Structural Engineering,* vol. 9, no. 4, pp. 507-533, 2006.

[37]    N. Anwar and F. A. Najam, "Chapter Seven - Retrofitting of Cross-Sections," in *Structural Cross Sections*, N. Anwar and F. A. Najam Eds.: Butterworth-Heinemann, 2017, pp. 483-530.

[38]    S. Raza, K. Khan, S. Menegon, H.-H. Tsang, and J. Wilson, "Strengthening and Repair of Reinforced Concrete Columns by Jacketing: State-of-the-Art Review," *Sustainability,* vol. 11, p. 3208, 06/09 2019, doi: 10.3390/su11113208.

[39]    M. Esmaeilnia Omran and S. Mollaei, "Investigation of Axial Strengthened Reinforced Concrete Columns under Lateral Blast Loading," *Shock and Vibration,* vol. 2017, p. 3252543, 2017/10/16 2017, doi: 10.1155/2017/3252543.

[40]    E. Julio, F. Branco, and V. Silva, "Structural rehabilitation of columns with reinforced concrete jacketing," *Progress in Structural Engineering and Materials,* vol. 5, no. 1, pp. 29-37, 2003.

[41]    M. N. S. Hadi, A. H. M. Algburi, M. N. Sheikh, and A. T. Carrigan, "Axial and flexural behaviour of circular reinforced concrete columns strengthened with reactive powder concrete jacket and fibre reinforced polymer wrapping," *Construction and Building Materials,* vol. 172, pp. 717-727, 2018/05/30/ 2018, doi: https://doi.org/10.1016/j.conbuildmat.2018.03.196.

[42]    P. R. Prem and A. R. Murthy, "Acoustic emission and flexural behaviour of RC beams strengthened with UHPC overlay," *Construction and Building Materials,* vol. 123, pp. 481-492, 2016.

[43]    J. He, W. Chen, B. Zhang, J. Yu, and H. Liu, "The Mechanical Properties and Damage Evolution of UHPC Reinforced with Glass Fibers and High-Performance Polypropylene Fibers," *Materials,* vol. 14, no. 9, p. 2455, 2021.

[44]    H. Martín-Sanz *et al.*, "Getting more out of existing structures: Steel bridge strengthening via UHPFRC," *Frontiers in Built Environment,* vol. 5, p. 26, 2019.

[45]    M. Farzad, M. Shafieifar, and A. Azizinamini, "Experimental and numerical study on bond strength between conventional concrete and Ultra High-Performance Concrete (UHPC)," *Engineering Structures,* vol. 186, pp. 297-305, 2019.

[46]    S. Shann, "Application of ultra high performance concrete (UHPC) as a thin-bonded overlay for concrete bridge decks," 01/01 2012.

[47]    A. Valikhani, A. J. Jahromi, I. M. Mantawy, and A. Azizinamini, "Experimental evaluation of concrete-to-UHPC bond strength with correlation to surface roughness for repair application," *Construction and Building Materials,* vol. 238, p. 117753, 2020.

[48]    D. R. P. Authority, "Commodore Barry Bridge," ed. drpa.org.

[49]    J. Summers, "Use of Ultra-High Performance Concrete on the Commodore Barry Bridge," ed. Roads and bridges, 2020.

[50]    B. Graybeal, E. Brühwiler, B.-S. Kim, F. Toutlemonde, Y. L. Voo, and A. Zaghi, "International perspective on UHPC in bridge engineering," *Journal of Bridge Engineering,* vol. 25, no. 11, p. 04020094, 2020.

[51]    M. Lanner, "Strengthening of Structures Using Ultra-high Performance Concrete," 2021.

[52]    Sweco, "Karbonfiberbånforsterkning av 12-1185 Vattedal bru," 2021.

[53]    Z. Ahmad, "CHAPTER 2 - BASIC CONCEPTS IN CORROSION," in *Principles of Corrosion Engineering and Corrosion Control*, Z. Ahmad Ed. Oxford: Butterworth-Heinemann, 2006, pp. 9-56.

[54]    *Bruklassifisering - Håndbok R412*, S. Vegvesen, 2014.

[55]    D. I. Jacobsen, *Hvordan gjennomføre undersøkelser?* Norge: Cappelen Damm, 2015.

[56]    D. Cvetković *et al.*, *Numerical Modeling and Computer Simulation*. 2020.

[57]    F. Sirois and F. Grilli, "Potential and limits of numerical modelling for supporting the development of HTS devices," *Superconductor Science and Technology,* vol. 28, 12/06 2014, doi: 10.1088/0953-2048/28/4/043002.

[58]    M. Gigante, "What is Finite Element Analysis?," ed, 2019.

[59]    V. Plevris and G. Markeset, "Educational Challenges in Computer-based Finite Element Analysis and Design of Structures," *Journal of Computer Science,* vol. 14, no. 10, pp. 1351-1362, 2018. [Online]. Available: http://dx.doi.org/10.3844/jcssp.2018.1351.1362.

[60]    J. Lubliner, J. Oliver, S. Oller, and E. Oñate, "A plastic-damage model for concrete," *International Journal of Solids and Structures,* vol. 25, no. 3, pp. 299-326, 1989/01/01/ 1989, doi: https://doi.org/10.1016/0020-7683(89)90050-4.

[61]    J. J. Lee and G. Fenves, "Plastic-Damage Model for Cyclic Loading of Concrete Structures," *ASCE,* 1998.

[62]    Simulia, "Abaqus 6.11 Theory manual," ed.

[63]    Ø. Grøstad and E. Sandberg, "Analysing UHPFRC beams with the help of ANSYS," *University of Agder,* 2018.

[64]    G. Torelli, M. Gillie, P. Mandal, and V.-X. Tran, "A multiaxial load-induced thermal strain constitutive model for concrete," *International Journal of Solids and Structures,* vol. 108, 11/01 2016, doi: 10.1016/j.ijsolstr.2016.11.017.

[65]    S. Vegvesen, "12-1185 Vattedal gammel klassifiseringsrapport," 2004.

[66] *Eurokode 2: Prosjektering av betongkonstruksjoner - del 1-1: Allmenne regler og regler for bygninger*, 2008.

[67] F. Solutions, "Static vs Dynamic Analysis," ed.

[68] J. E. Mottershead, M. Link, M. I. Friswell, and C. Schedlinski, "Model Updating," in *Handbook of Experimental Structural Dynamics*, R. Allemang and P. Avitabile Eds. New York, NY: Springer New York, 2020, pp. 1-53.

[69] L. Wang, W. Ping, C. Zhao, J. Zhen, and Y. Zhao, "In situ evaluation of dynamic characteristics of prefabricated ballastless track slab using EMA and OMA techniques," *Measurement,* vol. 160, p. 107866, 2020/08/01/ 2020, doi: https://doi.org/10.1016/j.measurement.2020.107866.

[70] M. Ghalishooyan and A. Shooshtari, "Operational modal analysis techniques and their theoretical and practical aspects: A comprehensive review and introduction," *6th International Operational Modal Analysis Conference, IOMAC 2015,* 01/01 2015.

[71] R. Brincker, L. Zhang, and P. Andersen, "Modal identification from ambient responses using frequency domain decomposition," in *Proceedings of the 18th international modal analysis conference (IMAC)*, 2000, vol. 1: San Antonio, TX, USA, pp. 625-630.

[72] Unquake, "Unquake Accelerograph Theory manual," in "Structures and Sensors," Athens.

# Attachments

## Attachment content

A- 12-1185Vattedal – Initial drawings
B- Concrete damage plasticity parameters for normal concrete
C- Concrete damage plasticity parameters for UHPC
D- Rebar drawings from SVV

# Attachment A
## 12-1185Vattedal – Initial drawings

The initial drawings from 1966 is attached.

# Attachment B

Concrete damage plasticity parameters for normal concrete [5].

| Material parameters | B40 | Plasticity parameters | |
|---|---|---|---|
| | | Dilation angle | 31 |
| Concrete elasticity | | Eccentricity | 0.1 |
| E (GPa) | 30 | fb0/fc0 | 1.16 |
| v | 0.2 | K | 0.67 |
| | | Viscosity parameter | 0 |
| Concrete compressive behavior | | Concrete compression damage | |
| Yield stress | Inelastic strain | Damage parameter | Inelastic strain |
| 20.4 | 0 | 0 | 0 |
| 25.6 | 2.666667e-05 | 0 | 2.666667e-05 |
| 30 | 0.00008 | 0 | 0.00008 |
| 33.6 | 0.00016 | 0 | 0.00016 |
| 36.4 | 0.000266667 | 0 | 0.000266667 |
| 38.4 | 0.0004 | 0 | 0.0004 |
| 39.6 | 0.00056 | 0 | 0.00056 |
| 40 | 0.000746667 | 0 | 0.000746667 |
| 39.6 | 0.00096 | 0.01 | 0.00096 |
| 38.4 | 0.0012 | 0.04 | 0.0012 |
| 36.4 | 0.001466667 | 0.09 | 0.001466667 |
| 33.6 | 0.00176 | 0.16 | 0.00176 |
| 30 | 0.00208 | 0.25 | 0.00208 |
| 25.6 | 0.002426667 | 0.36 | 0.002426667 |
| 20.4 | 0.0028 | 0.49 | 0.0028 |
| 14.4 | 0.0032 | 0.64 | 0.0032 |
| 7.6 | 0.003626667 | 0.81 | 0.003626667 |
| Concrete tensile behavior | | Concrete tension damage | |
| Yield stress | Cracking strain | Damage parameter | Cracking strain |
| 4 | 0 | 0 | 0 |
| 0.04 | 0.001333333 | 0.99 | 0.001333333 |

# Attachment C

Concrete damage plasticity parameters for UHPC [6].

| Material parameters | UHPFRC 133,6MPa | Plasticity parameters | |
|---|---|---|---|
| Material parameters | UHPFRC 133,6MPa | Dilation angle | 33 |
| Concrete elasticity | | Eccentricity | 0.1 |
| E (GPa) | 35 | fb0/fc0 | 1.16 |
| v | 0.2 | K | 0.67 |
| v | 0.2 | Viscosity parameter | 0 |
| Concrete compressive behavior | | Concrete compression damage | |
| Yield stress | Inelastic strain | Damage parameter | Inelastic strain |
| 0 (15) | 0 | 0 | 0 |
| 20.9 | 0.000242 | 0 | 0.000242 |
| 40.8 | 0.000708 | 0 | 0.000708 |
| 61.9 | 0.000893 | 0 | 0.000893 |
| 71.9 | 0.00101 | 0 | 0.00101 |
| 80.9 | 0.001147 | 0 | 0.001147 |
| 90.9 | 0.001328 | 0 | 0.001328 |
| 109.8 | 0.00345 | 0 | 0.00345 |
| 133.6 | 0.0039 | 0 | 0.0039 |
| 35.1 | 0.00435 | 0.73728 | 0.00435 |
| 21.6 | 0.0046168 | 0.838421 | 0.0046168 |
| 16.2 | 0.0046255 | 0.878816 | 0.0046255 |
| 10.8 | 0.0046284 | 0.919211 | 0.0046284 |
| 5.4 | 0.0046371 | 0.959605 | 0.0046371 |
| 2.7 | 0.0046429 | 0.979803 | 0.0046429 |
| Concrete tensile behavior | | Concrete tension damage | |
| Yield stress | Cracking strain | Damage parameter | Cracking strain |
| 7.75 | 0 | 0 | 0 |
| 0.00601 | 0.004665 | 0.999224 | 0.004665 |

# Attachment D

## Rebar drawings from SVV

The following drawing of the rebars were used in the analysis. One change was done, and that is the center-center distance. It was changed from 100 mm to 158 mm because of the information in "Karbonfiberbåndforsterkning av 12-1185 Vattedal bru" [52].

Beregnet 19.02.2004 Kl.19:37:20
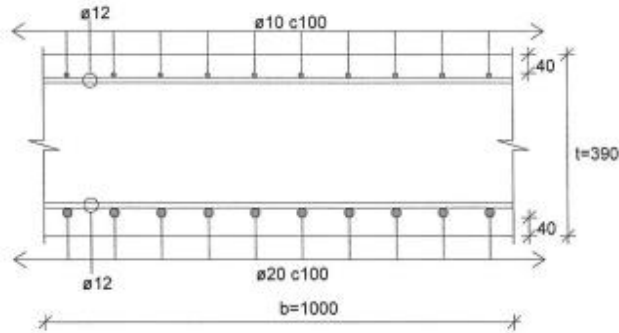


$M_f = 275,0$ kNm

Betongkvalitet : C25

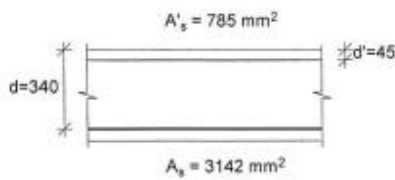$f_{cn} = 16,8$ MPa , $\gamma_c = 1,40 \Rightarrow f_{cd} = 12,0$ MPa
$f_{sk} = 400,0$ MPa , $\gamma_s = 1,25 \Rightarrow f_{sd} = 320,0$ MPa
$E_{cn} = 23313$ MPa
$\varepsilon_{cn} = -0,72 \cdot 10^{-3}$
$\varepsilon_{co} = -1,97 \cdot 10^{-3}$
$\varepsilon_{cu} = -3,84 \cdot 10^{-3}$

$A'_s = 785$ mm²

$d' = 45$

$d = 340$

$A_s = 3142$ mm²

$M = M_d = 304,4$ kNm :
$\alpha = 0,241 \Rightarrow \alpha d = 82$ mm
$\varepsilon_s = 10,00 \cdot 10^{-3}$ , $\sigma_s = 320,0$ MPa
$\varepsilon_c = -3,17 \cdot 10^{-3}$ , $\sigma_c = -12,0$ MPa
$\varepsilon_s' = -1,42 \cdot 10^{-3}$ , $\sigma_s' = -227,9$ MPa
$S = 1005,3$ kN
$T_c = 826,3$ kN
$T_s' = 179,0$ kN
$z = 305$ mm , $h' = 295$ mm

$M = M_f = 275,0$ kNm :
$\alpha = 0,362 \Rightarrow \alpha d = 123$ mm
$\varepsilon_s = 1,86 \cdot 10^{-3}$ , $\sigma_s = 297,5$ MPa
$\varepsilon_c = -1,05 \cdot 10^{-3}$ , $\sigma_c = -10,6$ MPa
$\varepsilon_s' = -0,67 \cdot 10^{-3}$ , $\sigma_s' = -106,9$ MPa
$S = 934,6$ kN
$T_c = 850,7$ kN
$T_s' = 84,0$ kN
$z = 294$ mm , $h' = 295$ mm